ON ACCURATE AND EFFICIENT VALUATION OF FINANCIAL CONTRACTS UNDER MODELS WITH JUMPS

by

Johannes Stolte

Department of Mathematics
Imperial College London
London SW7 2AZ
United Kingdom

Submitted to Imperial College London
for the degree of
Doctor of Philosophy

2013

Abstract

The aim of this thesis is to develop efficient valuation methods for financial contracts under models with jumps and stochastic volatility, and to present their rigorous mathematical underpinning. For efficient risk management, large books of exotic options need to be priced and hedged under models that are flexible enough to describe the observed option prices at speeds close to real time. To do so, hundreds of vanilla options, which are quoted in terms of implied volatility, need to be calibrated to market prices quickly and accurately on a regular basis. With this in mind we develop efficient methods for the evaluation of (i) vanilla options, (ii) implied volatility and (iii) common path-dependent options.

Firstly, we derive a new numerical method for the classical problem of pricing vanilla options quickly in time-changed Brownian motion models. The method is based on rational function approximations of the Black-Scholes formula. Detailed numerical results are given for a number of widely used models. In particular, we use the variance-gamma model, the CGMY model and the Heston model without correlation to illustrate our results. Comparison to the standard fast Fourier option pricing method with respect to speed appears to favour our newly developed method in the cases considered. Secondly, we use this method to derive a procedure to compute, for a given set of arbitrage-free European call option prices, the corresponding Black-Scholes implied volatility surface. In order to achieve this, rational function approximations of the inverse of the Black-Scholes formula are used. We are thus able to work out implied volatilities more efficiently than is possible using other common methods. Error estimates are presented for a wide range of parameters. Thirdly, we develop a new Monte Carlo variance reduction method to estimate the expectations of path-dependent functionals, such as first-passage times and occupation times, under a class of stochastic volatility models with jumps. The method is based on a recursive approximation of the first-passage time probabilities and expected occupation times of Lévy bridge processes that relies in part on a randomisation of the time-parameter. We derive the explicit form of the recursive approximation in the case of bridge processes corresponding to the class of Lévy processes with mixed-exponential jumps, and

present a highly accurate numerical realisation. This class includes the linear Brownian motion, Kou's double-exponential jump-diffusion model and the hyper-exponential jump-diffusion model, and it is dense in the class of all Lévy processes. We determine the rate of convergence of the randomisation method and confirm it numerically. Subsequently, we combine the randomisation method with a continuous Euler-Maruyama scheme to estimate path-functionals under stochastic volatility models with jumps. Compared with standard Monte Carlo methods, we find that the method is significantly more efficient. To illustrate the efficiency of the method, it is applied to the valuation of range accruals and barrier options.

Declaration

I the undersigned hereby declare that the work presented in this thesis is my own. When material from other authors has been used, these have been duly acknowledged. This thesis has not previously been presented for this or any other PhD examinations.

Johannes Stolte

Acknowledgements

First and foremost I would like to thank my supervisor, Dr Martijn Pistorius, for guiding me through this long journey and for teaching me a lot of (financial) mathematics. He has always been approachable and excited about my findings.

It was a great pleasure to spent one month as visiting scholar at the Fields Institute in Toronto in 2010. I would like to thank Professors Tom Hurd and Alexey Kuznetsov for inspiring discussions during my stay.

For the first project, presented in Chapter 2, I would like to thank Hélyette Geman, Felicity Pearce, Walter Schachermayer, William Shaw, and the participants of the LGS PhD Day at the London School of Economics (2011), the Young Researchers in Mathematics Conference at Warwick University (2011), and the Fourth International Conference on Mathematical Finance (2011) for their useful comments. I would also like to thank Mike Staunton for a critical read of the resulting paper and for dedicating his column in the March 2012 edition of the Wilmott Magazine to the published article. Pistorius & Stolte [112] is based on the results presented in Chapter 2.

For the second project, presented in Chapter 3, I would like to thank Rama Cont, Dan Crisan, Antoine Jacquier, Vladimir Piterbarg, Johannes Ruf, David Taylor, Josef Teichmann, and the participants of the ETH workshop at Imperial College (2013), the Maastricht Workshop on Advances in Quantitative Economics (2013), the Research in Options Conference (2012), the Global Derivatives Trading & Risk Management Conference (2012), the Seventh World Congress of the Bachelier Finance Society (2012), a satellite workshop at the University of the Witwatersrand (2011), and the Finance and Stochastics Seminar at Imperial College (2011) for useful comments. I would also like to thank Dr Aleksandar Mijatović for his valuable insight and comments. Mijatović *et al.* [107] is based on the results presented in Chapter 3.

During the entire period of my PhD studies, I was supported by a EPSRC Doctoral Training Account Scholarship covering full tuition fees and an allowance for research costs. In my third year I was supported by a doctoral grant (Ref. Nr. D/11/42213) from the German Academic Exchange Service (DAAD), for which I am very grateful.

I would like to thank Dr Harry Zheng and Dr Christopher Barnett for their useful comments during the transfer viva.

It is a great pleasure for me to have Professor Sergei Levendorskiĭ and Professor Mark Davis as examiners for my thesis, and I would like to thank them for accepting this.

Finally I want to thank my mother, Maria, and all my family for their support. This work would not have seen the light of day, were it not for Sofia's uncountable smiles, and Felicity's positivity and encouragement.

Contents

List of Figures

List of Tables

Introduction

It is by now well established that the classical Black-Scholes model, introduced in 1973, lacks the flexibility to fit accurately to observed option price data (see, *e.g.*, Gatheral [62] and the references therein). Still, four decades after its introduction, the model continues to be widely used, especially as a universal benchmark model, in part due to its tractability. In a frictionless market in which the asset price is modelled as a geometric Brownian motion (GBM) with constant drift and constant volatility, the price of a European call or put option has a closed form: the celebrated Black-Scholes formula. The Black-Scholes formula is employed by traders to convert prices into units of implied volatility and vice versa. However, the presence of an implied volatility smile in option markets contradicts the assumptions of the Black-Scholes model, and demonstrates that the returns are asymmetric and leptokurtic. At shorter maturities, the volatility smile becomes more pronounced, showing an increasing deviation from the GBM model. Additionally, real market asset prices typically exhibit jumps and volatility clustering, while price paths in the Black-Scholes model are continuous and have constant volatility. When assuming that asset prices are continuous, one neglects the abrupt price movements in which most of the risk seems to be concentrated. These observations are well known: we refer the reader to Cont & Tankov [43] and Gatheral [62] for relevant background and further references.

A variety of models has been proposed to provide an improved description of the price dynamics of the underlying that can more accurately describe the option surface. Most of these models incorporate jumps, where empirical data strongly suggests their presence. The incorporation of jumps is usually achieved by modelling the noise of the stochastic differential equation (SDE) by a Lévy process with stationary and independent increments, which can fit the volatility smile at a single maturity very well (see, *e.g.*, Schoutens [123] and the references therein). When the asset price is modelled as $S_t = S_0 \mathrm{e}^{X_t}$, where X_t is a Lévy process, it is common to refer to it as an *exponential Lévy model*. A variety of models in the exponential Lévy class have been proposed in the literature: KoBoL (also known as CGMY) model (Boyarchenko & Levendorskiĭ & Levendorskiĭ [23], Carr *et al.* [38]), variance-gamma (VG) model (Madan & Seneta [99], Madan *et al.* [98]), Normal-inverse Gaussian (NIG) model (Barndorff-Nielsen [14]), Merton model (Merton [105]), double-exponential jump-diffusion model (Kou [78]), hyper-exponential jump-diffusion model (Lipton [93], Mordecki [108]) and mixed-exponential jump-diffusion model (see, *e.g.*, Cai & Kou [34]), among others. All of these models are able to account for asymmetry and excess kurtosis in the returns while incorporating jumps, and therefore overcome most of the shortfalls of the Black-Scholes model.

Stochastic volatility models represent another important generalisation of the Black-Scholes model. In particular, the observed feature of volatility clustering is well handled by stochastic volatility models and cannot be handled by exponential Lévy models because of their independent increments. These models can generate smiles and skews similar to those observed in the market, but are not able to calibrate well to short-term implied volatility patterns. In order to overcome this issue, stochastic volatility models with jumps were introduced such as the Bates model (Bates [17]) and the Scott model (Scott [124]). Note that stochastic volatility Lévy models (Carr *et al.* [39]) also combine stochastic volatility and jumps.

For these more realistic and more suitable models, tractable closed-form solutions for vanilla options, barrier options and range accruals, which are amongst the most popular derivatives in the financial market, are rarely available. Barrier options form effective risk management tools and are liquidly traded in the Foreign Exchange markets. Range accruals, together with callable range accruals and accrual swaps, on the other hand, are occupation time derivatives, which are amongst the most popular exotic derivatives in the interest rates market (see Brigo & Mercurio [30], for example). The closely related corridor options have been considered in Fusai & Tagliani [60] for the Black-Scholes model and in Cai *et al.* [33] for the Kou model.

A financial institution active in the derivatives market will seek to evaluate large portfolios of vanilla options at speeds close to real time in order to control its risk positions. Additionally, the large portfolios of exotic options need to be efficiently priced and hedged in models that are flexible enough to describe the observed option prices (*i.e.*, calibrate to the vanilla market price quotes). It is therefore of paramount importance to price vanilla options, as well as exotic options, as quickly and accurately as possible. To account for this necessity, a particularly high emphasis of this thesis is put on the efficiency of the introduced valuation methods, so that this work can also be seen to lie in the area of computational finance.

Chapter 2 is devoted to the development of a new and efficient method for the pricing of vanilla options in the class of time-changed Brownian motion models, using rational approximations. Such approximations are known to offer an efficient and accurate method for computation of the cumulative normal distribution function (see Abramowitz & Stegun [3] for details) and could therefore be expected to perform well for approximations of the Black-Scholes formula, which is given in terms of the cumulative normal distribution function. Drawing on this theory, the value of a vanilla option in a time-changed model is approximated, taking the form of a linear combination of a number of *negative exponential moments* of the *clock*. The clock is an increasing stochastic process independent of the Brownian motion driving the asset price. This yields an explicit approximation for the value of a vanilla option in those time-changed models for which the Laplace transform (and hence any negative exponential moment) of the clock is available in tractable form. For many of the popular time-changed models the Laplace transform of the clock is known in closed-form, where stochastic volatility Lévy models can also be handled. The rational function approximation method is then applied to compute Black-Scholes implied volatilities more efficiently than with the use of other common methods. In the case of implied volatility, the method is not limited to time-changed models, but can be used for any given set of arbitrage-free vanilla option prices.

Especially for the path-dependent barrier options and the range accruals considered in Chapter 3, analytic expressions that can be evaluated efficiently rarely exist. Generally, one needs to utilise Monte Carlo, finite difference or Fourier-based methods for the numerical evaluation of these exotic options. It is worth noting that (semi-)analytical approaches have been developed for specific models (for parametric diffusion models see Davydov & Linetsky [50] and Lipton [92], and for particular subclasses of exponential Lévy models see Boyarchenko & Levendorskiĭ [21], Geman & Yor [65], Jeannin & Pistorius [77], Lipton [93], Kou & Wang [80], Rogers [117] and Sepp [125]). Kuznetsov *et al.* [82] recently introduced the so called Wiener-Hopf Monte Carlo method for general Lévy processes, which draws upon Carr's so-called 'Randomisation' technique. However, one needs to sample each path in the Monte Carlo method at a large number of exponential random times, which makes the algorithm rather slow. The method presented in Chapter 3 of this thesis is different since it enables one to sample the endpoint of the path, in the case of a Lévy process, in one big step and then utilises derived results of the corresponding bridge. For this reason, we refer to the method as *Lévy bridge Monte Carlo method*, which is based on a recursive approximation of path-dependent functionals that relies in part on a randomisation of the time-parameter. Combined with the continuous Euler-Maruyama scheme, the method can be used for a class of stochastic volatility models with jumps. For the class of mixed-exponential jump-diffusion (MEJD) models, the recursions are given in explicit form, which follow from the explicit Wiener-Hopf factorisation for this class of models. Employing the randomisation method, a recursive algorithm is built to quickly approximate these path-dependent quantities at a fixed maturity, T, where we use Richardson extrapolation to accelerate convergence. The resulting bridge sampling Monte Carlo method converges faster than the standard Euler-Maruyama method, while taking advantage of the generality and flexibility of Monte Carlo methods. We analyse the rate of convergence and run times for the recursive algorithm in detail, and perform a variety of Monte Carlo simulations for a number of exotic derivatives and models. By utilising the Lévy bridge Monte Carlo method we investigate the convergence rate of the discrete and continuous Euler scheme under a class of stochastic volatility models with jump. We find strong evidence for the rates to carry over from the diffusion setting, for which Gobet [68] rigorously proved the rates of convergence to be 0.5 and 1.0 for the discrete and continuous Euler scheme respectively.

The remainder of this thesis is organised as follows. In Chapter 1 we present preliminaries on options, models and methods that are relevant for the derivations in later chapters. Chapter 2 is devoted to the development of the rational function approximation for time-changed Brownian motion models and implied volatilities. Chapter 3 presents the Lévy bridge Monte Carlo method, and its application to the valuation of barrier options and range accruals. At the end of Sections 2 and 3 we give concluding remarks.

Chapter 1

Preliminaries on options, models and methods

In this chapter of the thesis we review preliminary topics needed for the discussion and derivations in Chapters 2 and 3. In all that follows, we assume frictionless markets and no arbitrage, and take as given an equivalent martingale measure (EMM) $\mathbb{Q}$ chosen by the market. All stochastic processes defined in the following are assumed to live on the complete filtered probability space $(\Omega, \mathcal{F}, \{\mathcal{F}_t, t \geq 0\}, \mathbb{Q})$. The underlying is defined as a stochastic process S_t, which usually refers to a stock process in the equity market, but can also refer to an interest rate, exchange rate, swap rate, default rate or a commodities price. The majority of this thesis is devoted to pricing (exotic) options, the three of which are discussed in Section 1.1, on exponential Lévy models and stochastic volatility models with jumps. Since we assume the risk-free interest rate $r \geq 0$ and the dividend yield $q \geq 0$ to be constant throughout this thesis, the only unknown after we have defined the payoff of the option is the law of $(S_t)_{t\geq 0}$ under $\mathbb{Q}$, where we assume that $S_t \mathrm{e}^{-(r-q)t}$ is a martingale (under the measure $\mathbb{Q}$ and with respect to its natural filtration). We present the most common models for (S_t) in Section 1.2. Tractable closed-form expressions for option pricing are not available for most of the discussed models, not even for vanilla options, and one needs to rely on numerical pricing methods to determine their value. Section 1.3 reviews the three main pricing methods used for the models and options discussed here. Mathematical tools and techniques that will be crucial to derive the valuation methods presented in the remainder of the thesis are summarised in Section 1.4.

1.1 Payoffs

In the following we define three types of European options by their payoff H_T. These are European because they must be exercised, if at all, on a specified date, and are therefore in contrast to American options where the time of exercise is at the holder's discretion. H_T represents the amount of money paid by the option writer to the option holder at maturity T. In our market setting, the value $\Pi_t(H_T)$ at time t of a financial instrument with payoff H_T and maturity T may then be computed as the discounted conditional expectation of its terminal payoff with respect to the EMM $\mathbb{Q}$ such that:

$$\Pi_t(H_T) = \mathrm{e}^{-r(T-t)}\mathbb{E}^{\mathbb{Q}}[H_T|\mathcal{F}_t], \tag{1.1.1}$$

where r denotes the deterministic and constant interest rate throughout this thesis. We will discuss plain vanilla call and put options in Section 1.1.1, barrier options in Section 1.1.2 and range accruals in Section 1.1.3.

1.1.1 Plain vanilla call and put options

The term *plain vanilla* refers to the simplest, most standard, and most widely traded options. Therefore, plain vanilla mainly refers to the European call and put options discussed in this section, which are traded on automated exchanges.

A European call option on an asset (S_t) with maturity date T and strike price K is a contingent claim that gives its holder the right, but not the obligation, to buy the asset at date T for a fixed price K. The payoff at maturity is therefore $H_T(K) = \max(S_T - K, 0)$. The arbitrage-free value of a call option at time zero can hence be expressed as the discounted expectation of this payoff:

$$C_0(K,T) = \mathrm{e}^{-rT}\mathbb{E}^{\mathbb{Q}}[(S_T - K)^+]. \tag{1.1.2}$$

Similarly, we define the arbitrage-free value of a European put option as

$$P_0(K,T) = \mathrm{e}^{-rT}\mathbb{E}^{\mathbb{Q}}[(K - S_T)^+], \tag{1.1.3}$$

where the two can be linked through the put-call parity, which holds independently of the chosen model for the underlying S_t. The put-call parity for a stock with continuous dividend yield q, for example, is given by

$$C_t(K,T) + P_t(K,T) = S_t\mathrm{e}^{-q(T-t)} - K\mathrm{e}^{-r(T-t)}.$$

In this framework, one could therefore deduce the put value from that of the call, or vice versa, when the other parameters are given. We use this parity in Chapter 2, so that we only need to focus on the valuation of call options.

1.1.2 Barrier options

Barrier options belong to the class of most widely-used instruments in derivative markets. One of the main reasons for their popularity is the fact that they are cheaper than standard (vanilla) options, but can offer a similar kind of payoff. Single barrier options, that are barrier options with only one barrier level, are so common in the FX market, for example, that they are sometimes included in broader definitions of the vanilla class. A natural extension is formed by the class of double barrier options.

Single barrier options are available in eight different types, which is any possible combination of down or up, knock-in or knock-out and put or call. An up-and-out call option with strike K, for example, has the same payoff profile as a European call option with strike K as long as the underlying has not reached or exceeded the barrier level H. As soon as the underlying is quoted at or above the barrier, the up-and-out call becomes worthless. The payoff profiles of all other barrier options follow logically. It should be noted that any barrier option is therefore a path dependent exotic option.

To further illustrate, the general expression for the payoff, H_T, of a knock-out option at expiry can be summed by Equation (1.1.4).

$$H_T^{out}(K,H) = [\phi(S_T - K)]^+ I_{\{\eta S_t > \eta H, 0 \le t \le T\}}, \tag{1.1.4}$$

where $\phi = 1$ for a call and $\phi = -1$ for a put. In addition, $\eta = 1$ if a down-and-out is considered and $\eta = -1$ if an up-and-out is considered. The indicator function I has a value of 1 as long as $\eta S_t > \eta H$ holds for all t between 0 and T and a value of 0 otherwise. A similar functional form can be given for all knock-in options, which also follows from a more instructive result however. Equation (1.1.5) gives the payoff of a knock-in option as the difference of the corresponding knock-out option and the underlying plain vanilla call or put with same strike as the barrier options (see Carr & Chou [37]).

$$H_T^{in}(K,H) = H_T^{vanilla}(K) - H_T^{out}(K,H). \tag{1.1.5}$$

By no arbitrage and since the two sides of the previous equation deliver the same payoff at maturity, their value should also be the same at every time t before maturity. This identity is usually referred to as *in-out-parity* and is very useful if valuing the *in* option is substantially easier than valuing the *out* option, or vice versa.

Another way to define barrier options is via the upper hitting time ($\tau_U = \inf\{t : S_t \geq U\}$) or lower hitting time ($\tau_L = \inf\{t : S_t \leq L\}$), so that the payoff of an up-and-out call, for example, can be defined as $H_T^{out}(K, U) = [S_T - K]^+ I_{(\tau_U > T)}$. If, in addition, we define $\tau_{LU} = \min(\tau_L, \tau_U)$, the payoff of a double-out barrier call option can be expressed as $H_T^{out}(K, L, U) = [S_T - K]^+ I_{(\tau_{LU} > T)}$. In the celebrated Black-Scholes model, there are analytic formulas for single-barrier options, based on the reflection principle for Brownian motion and a quickly converging infinite series for double-barrier options. Valuation formulas for single barrier options in the Black-Scholes model go back as far as the papers by Goldman *et al.* [69] and Merton [104]. For early work on double barrier options see Kunitomo & Ikeda [81], Geman & Yor [65] and Pelsser [110]. For barrier options under universal volatility models, we refer to Lipton & McGhee [95]. The special case of the zero correlation Heston model is treated in Lipton [92]. However, when pricing barrier options in exponential Lévy models or stochastic volatility models, one usually needs to resort to numerical methods. We reference more recent work in Section 1.3 when discussing the particular numerical method. Also the static hedging of single barrier options is by now well understood. Pioneering work in this direction include the articles by Derman *et al.* [52] and Carr & Chou [36]. For an overview of more recent static hedges and an analysis of their performance under realistic market conditions see Stolte [128].

1.1.3 Range accruals

Range accruals are a subclass of occupation time derivatives, where the payoff depends on the time spent by the underlying asset (most commonly the Libor rate) in a predetermined range. Like barrier options, range accruals are usually traded at a discount when compared to standard products, like floating rate notes, since no interest is paid for the time the range is left. Usually range accruals are written on interest rates, stock indices or swap rates. Range accruals essentially come in two different forms, where the accruing time is either discrete or continuous. The discrete version can be priced as a sum of digital options, since the payoff depends on a finite number of discrete time points (*e.g.* for every trading day at 12:00am, one needs to check whether the 3-month Libor rate is in some predefined range over the lifetime of the option). See Fusai & Tagliani [60] for work in this direction. The continuous version, which we consider in Chapter 3, has the following time-zero value;

$$RN_0(a_1, a_2) = \mathrm{e}^{-rT}\mathbb{E}\left[\frac{C}{T}\int_0^T I_{\{a_1 \leq S_s \leq a_2\}}\mathrm{d}s\right],$$

where a_1 and a_2 are the lower and upper bounds respectively, and C is the nominal. The integral term measures the time the underlying spends in the range $[a_1, a_2]$, and the payoff is the ratio of this integral and the total time to maturity multiplied by the nominal amount.

Occupation time options are sometimes defined to be slightly more general in that a minimum coupon clause is included in the payoff

$$H_T^{CO} = \max\left[\frac{C}{T}\int_0^T I_{\{a_1 \leq S_s \leq a_2\}}\mathrm{d}s, K\right],$$

or that these interest payments are made every three month, for example, over a two year maturity, where we refer to these options as corridor options (CO).

Akahori [4] obtains a pricing formula for $RN_0(a_1, a_2)$ for the case that the underlying follows a geometric Brownian motion and $a_1 = -\infty$ (or $a_2 = \infty$). Fusai [59] derives the Laplace transform when both a_1 and a_2 are finite (also for corridor options). This work was extended by Cai *et al.* [33] for Kou's double-exponential jump-diffusion model (see Section 1.2.3) by deriving double Laplace transforms for the option value. Two related derivatives are the step options introduced by Linetsky [91] and the Parisian options introduced by Chesney *et al.* [41]. In both of these articles, the authors use inverse Laplace transforms to calculate the option price in the geometric Brownian motion setting. These two options can be seen as hybrids between barrier options and occupation time options, where the knock-out/knock-in only occurs if the underlying spends a predefined time above/below the barrier. The option value and delta are therefore continuous functions of the underlying price at the barrier (contrary to the standard barrier option), which enables continuous hedging.

1.2 An overview of models for the underlying process

We recall that the time t value of an option is equal to the discounted expectation of its terminal payoff with respect to the EMM $\mathbb{Q}$ as defined in Equation (1.1.1). After defining the payoff of an option, the only ingredient missing is specifying the model for the underlying process $(S_t)_{t\geq 0}$. In the general setup outlined above, specifying an option pricing model is then equivalent to specifying the law of $(S_t)_{t\geq 0}$ under $\mathbb{Q}$, which is also referred to as the 'risk-neutral' or 'risk-adjusted' dynamics of S. Here we will concentrate on some of the most popular risk-neutral dynamics of S that will all be utilised in the remainder of this thesis. Many of the models utilised here are exponential Lévy models, where Lévy processes are introduced next. We will then discuss three subclasses of Lévy processes: time-changed Brownian motions, jump-diffusion processes and infinite active processes in Section 1.2.2, 1.2.3 and 1.2.4 respectively. In Section 1.2.5 we review stochastic volatility models (with jumps). All models reviewed in this section can be written as $S_t = S_0\mathrm{e}^{Y_t}$, where Y_t is a stochastic process. We review below some of the most popular models S_t together with the dynamics for the corresponding stochastic process Y_t.

1.2.1 Lévy processes

A Lévy process $(X_t)_{t\geq 0}$ is a stochastic process with independent stationary increments that is stochastically continuous with $X_0 = 0$. It has marginal distributions that are infinitely divisible. A probability distribution F on $\mathbb{R}$ is said to be infinitely divisible if for any integer $m \geq 2$, there exists m i.i.d. random variables $Y_1, ..., Y_m$ such that $Y_1 + ... + Y_m$ has distribution F. Well-known examples of infinitely divisible laws are the Gaussian and the gamma distributions. Lévy processes provide key examples of stochastic processes in continuous time and are used widely in mathematical finance to model the risk-neutral price dynamics.

The characteristic function of a random variable is the Fourier transform (see Section 1.3.2) of its distribution. This transform is very useful in the current context as many probabilistic properties of a random variable correspond to analytical properties of its characteristic function. Given a Lévy process $(X_t)_{t\geq 0}$, define the corresponding characteristic function as follows:

$$\Phi_{X_t}(z) \equiv \mathbb{E}[\mathrm{e}^{\mathrm{i}zX_t}] = \int_{-\infty}^{\infty} \mathrm{e}^{\mathrm{i}zx}\mathrm{d}\mu_{X_t}(x) = \mathrm{e}^{-t\phi(z)}, \quad z \in \mathbb{R}, \tag{1.2.1}$$

where $\phi : \mathbb{R} \to \mathbb{C}$ is called the characteristic exponent and μ_{X_t} is the distribution of X_t (note that the associated density may not exist - indeed, the distribution of a compound Poisson process has an atom at zero for all t). Note that the characteristic exponent is the cumulant generating function of X_1 and that the only degree of freedom we have in specifying a Lévy process is to specify its distribution at a single point in time (*e.g.* at $t = 1$). A characteristic function is always continuous and satisfies $\Phi_X(0) = 1$. The characteristic exponent can be shown to exist and shown to be a continuous function. By the Lévy-Khintchine representation it is also known that the characteristic exponent can be written as

$$\phi(z) = -\mathtt{i}\gamma z + \frac{1}{2}Az^2 + \int_{-\infty}^{\infty} \left(1 - \mathrm{e}^{\mathtt{i}zx} + \mathtt{i}zxI_{|x|\leq 1}\right)\nu(\mathrm{d}x),$$

with characteristic triplet (A, ν, γ), where $\gamma \in \mathbb{R}$ represents a linear drift, A represents the diffusion component and ν is named the Lévy measure, which is a measure on $(\mathbb{R}, \mathcal{B}(\mathbb{R}))$ satisfying the conditions:

$$\int_{|x|\leq 1} |x|^2 \nu(\mathrm{d}x) < \infty, \qquad \int_{|x|\geq 1} \nu(\mathrm{d}x) < \infty.$$

For any set $B \in \mathcal{B}(\mathbb{R})$, for which $\nu(B)$ is finite, $\nu(B)$ is equal to the expected number, per unit time, of jumps whose size belongs to B.

In addition it is known that any Lévy process can be decomposed into the sum of a Brownian motion, a linear drift and a purely discontinuous process composed by superposing independent compound Poisson processes. This important result is known as the Lévy-Itô decomposition (for more details see Sato [121]).

Lévy models can be broadly divided into two categories: (a) jump-diffusion or finite activity models (discussed in Section 1.2.3), and (b) infinite activity models (discussed in Section 1.2.4). Many of the models in the second category can be written as Brownian motions time-changed by an increasing stochastic process. We will discuss time-changed Brownian motion models in Section 1.2.2. The idea of stochastic time-changes was first discussed in a financial context by Clark [42], who modelled the observed price process as a Brownian motion run on an independent second process called the clock.

A research direction that obtained a lot of attention in recent years is the investigation of the asymptotic behaviour for the short-term or long-term volatility smile of Lévy processes. For a recent survey and new results see Andersen & Lipton [8] and references within. For background on the application of Lévy processes in option pricing see Cont & Tankov [44] and Schoutens [123]. Sato [121] and Bertoin [18] are general treatments of the theory of Lévy processes.

1.2.2 Time-changed Brownian motions

A time-changed Brownian motion with drift is defined as

$$X_t = \theta Z_t + \sigma W_{Z_t}, \tag{1.2.2}$$

where $(W_t)_{t\geq 0}$ is a Brownian motion and (Z_t) is an independent stochastic process called the clock. The clock $(Z_t)_{t\geq 0}$ is required to be an increasing process for which the Laplace transform at time t should be available in tractable form. Typically, the process (Z_t) is modelled by either a Lévy subordinator or as a time integral of a positive diffusion; we discuss both of these approaches below in more detail. Note that suitable models for the clock can also be constructed by combining these two ingredients and therefore include time-changes of the form $Z_t = Z_t^1 + Z_t^2$ or $Z_t = Z^1_{Z_t^2}$, where both (Z_t^1) and (Z_t^2) can be (i) a Lévy subordinator, (ii) an integral of a non-negative process, or (iii) any other increasing process. It is worth noting that the three stochastic volatility Lévy processes discussed by Carr *et al.* [39] are of this form. This follows since the processes considered in [39] are three Lévy processes time-changed by a mean-reverting square root process, where each of the Lévy processes itself (the processes corresponding to the normal inverse Gaussian model, the VG model and the CGMY model) can be written as a time-changed Brownian process.

Time-changing with an independent Lévy subordinator. A Lévy subordinator $(Z_t)_{t\geq 0}$ is a Lévy process that takes values in $\mathbb{R}_+$ with characteristic triplet $(0, \rho, \beta)$ satisfying $\rho((-\infty, 0]) = 0$, $\int_0^\infty (x \wedge 1)\rho(dx) < \infty$, and $\beta \geq 0$; that is, $(Z_t)_{t\geq 0}$ has no diffusion component, only non-negative jumps of finite variation, and a non-negative drift. As a consequence, the trajectories of Z are almost surely increasing. Since (Z_t) is a positive random variable for all t, it is natural to describe its distribution using the Laplace transform:

$$\mathbb{E}[\mathrm{e}^{-uZ_t}] = \mathrm{e}^{-t\psi(u)} = \mathrm{e}^{-t\left(\beta u + \int_0^\infty \left(1-\mathrm{e}^{-ux}\right)\rho(dx)\right)}, \qquad \forall u \geq 0, \tag{1.2.3}$$

where $\psi(u)$ is called the Laplace exponent of Z (see Section 1.3.2 for details on Laplace transforms). Since $(Z_t)_{t\geq 0}$ is an increasing process, it can be interpreted as a 'time deformation' and be used as a stochastic clock. Subordinating any Lévy process (in particular, a Brownian motion) by another independent Lévy process will yield a new Lévy process with known Lévy triplet:

Theorem 1.2.1 (Theorem 30.1 in Sato [121]). *Let $\{Z_t : t \geq 0\}$ be a subordinator (an increasing Lévy process on $\mathbb{R}$) with Lévy measure ρ, drift β_0, and $P_{Z_1} = \lambda$. That is,*

$$\mathbb{E}\left[\mathrm{e}^{-uZ_t}\right] = \int_{[0,\infty)} \mathrm{e}^{-us}\lambda^t(\mathrm{d}s) = \mathrm{e}^{t\phi(-u)}, \qquad u \geq 0,$$

where, for any complex w with Re $w \leq 0$,

$$\phi(w) = \beta_0 w + \int_{(0,\infty)} (\mathrm{e}^{ws} - 1)\,\rho(\mathrm{d}s)$$

with

$$\beta_0 \geq 0 \quad \textit{and} \quad \int_{(0,\infty)} (1 \wedge s)\,\rho(\mathrm{d}s) < \infty.$$

Let $\{X_t : t \geq 0\}$ be a Lévy process on $\mathbb{R}^d$ with generating triplet (A, ν, γ) and let $\mu = P_{X_1}$. Suppose that $\{X_t\}$ and $\{Z_t\}$ are independent. Define

$$Y_t(w) = X_{Z_t(w)}(w), \qquad t \geq 0.$$

Then $\{Y_t\}$ is a Lévy process on $\mathbb{R}^d$ and

$$\begin{aligned}
\mathbb{P}\left[Y_t \in B\right] &= \int_{[0,\infty)} \mu^s(B)\lambda^t(\mathrm{d}s), \qquad B \in \mathcal{B}(\mathbb{R}^d),\\
\mathbb{E}\left[\mathrm{e}^{\mathrm{i}\langle z, Y_t\rangle}\right] &= \mathrm{e}^{t\phi(\log\hat{\mu}(z))}, \qquad z \in \mathbb{R}^d.
\end{aligned}$$

The generating triplet $(A^{\#}, \nu^{\#}, \gamma^{\#})$ of $\{Y_t\}$ is a follows:

$$\begin{aligned}
A^{\#} &= \beta_0 A,\\
\nu^{\#}(B) &= \beta_0\nu(B) + \int_{(0,\infty)} \mu^s(B)\rho(\mathrm{d}s), \qquad B \in \mathcal{B}(\mathbb{R}^d \backslash \{0\}),\\
\gamma^{\#} &= \beta_0\gamma + \int_{(0,\infty)} \rho(\mathrm{d}s) \int_{|x|\leq 1} x\mu^s(\mathrm{d}x).
\end{aligned}$$

If $\beta_0 = 0$ and $\int_{(0,1]} s^{1/2}\rho(\mathrm{d}s) < \infty$, then $\{Y_t\}$ is a type A or B and has drift 0.

Subordinating a Brownian motion leads to another Brownian motion if it is observed on a new time scale, that is, the stochastic time scale given by Z_t. The financial interpretation of this new time scale is business time, which is faster when more information arrives at the market and slower when less information arrives. This makes models derived by Brownian subordination easier to interpret than general Lévy models. In particular, all models discussed in Section 1.2.4 can be represented as time-changed Brownian motion models, where (Z_t) is modelled by a Lévy subordinator. For each of the three models discussed in that section, we give details about the Laplace transform of the clock. Standard references on Lévy subordination include Bertoin [18] (Chapter 3) and Sato [121]. Also see Geman *et al.* [64] for background on the role of subordination in financial applications.

Time-changing with a time integral of a positive Markov process. In this case the stochastic clock $(Z_t)_{t\geq 0}$ is defined as follows:

$$Z_t = \int_0^t V_s ds, \tag{1.2.4}$$

where $(V_t)_{t\geq 0}$ is a mean-reverting non-negative Markov process. The mean-reversion is required to guarantee that the random time-change persists. As an example of this class of models, we refer to the Heston model without correlation discussed in Section 1.2.5. Another example are the so-called quadratic models (see Leippold & Wu [85]), which arise by taking $(V_t)_{t\geq 0}$ to be a mean-reverting affine jump-diffusion process.

1.2.3 Jump diffusion processes

A Lévy process of jump-diffusion type has the following form:

$$X_t = \mu t + \sigma W_t + \sum_{i=1}^{N_t} J_i, \qquad \mu \in \mathbb{R}, \sigma > 0, \tag{1.2.5}$$

where W_t is a standard Brownian motion, σ the volatility, N is a Poisson process with intensity λ and J_i are jump sizes (i.i.d. variables). All sources of randomness are assumed to be independent of each other. To define a jump diffusion model completely, one needs to specify the distribution of the jumps and this is where the four models discussed in the sequel of this section differ from each other. In this category of models, a finite number of jumps occurs at random times before a finite time-horizon and these can be interpreted as rare events, crashes or large drawdowns. In all of these models, the distribution of the jump sizes is known, which makes them easy to simulate. These models also perform quite well for the purposes of implied volatility interpolation and are particularly useful in pricing options with short maturities, which is one of the reasons they are among the most popular alternatives to the classical Black-Scholes model. However, they rarely lead to closed-form densities, so that statistical estimation and calculation of moments or quantiles become computationally more involved. We proceed by presenting the Merton model, Kou's double-exponential jump-diffusion model, the hyper-exponential jump-diffusion model and the mixed-exponential jump-diffusion model in more detail.

Gaussian jumps (Merton model). The Merton model was introduced by Merton in 1976 [105] and he was the first to explore jump-diffusion models in a financial context. In this model, the jumps J_i in Equation (1.2.5) are assumed to have a Gaussian distribution with mean γ and standard deviation δ: $J_i \sim \mathcal{N}(\gamma, \delta^2)$. In this model, it can be shown that the probability density of X_t is a quickly converging series. Indeed,

$$\mathbb{P}(X_t \in A) \;=\; \sum_{k=0}^{\infty} \mathbb{P}(X_t \in A | N_t = k)\mathbb{P}(N_t = k)$$

entails that the probability density is

$$p_t(x) \;=\; \mathrm{e}^{-\lambda t} \sum_{k=0}^{\infty} \frac{(\lambda t)^k \exp\left(-\frac{(x-\mu t - k\gamma)^2}{2(\sigma^2 t + k\delta^2)}\right)}{k!\sqrt{2\pi(\sigma^2 t + k\delta^2)}}$$

and that similarly, arbitrage-free values of European options follow as an infinite series of terms involving the Black-Scholes formula (see Equation 2.1.5):

$$C_0(K,T) \;=\; \sum_{k=0}^{\infty} \frac{(\lambda' T)^k \mathrm{e}^{-\lambda' T}}{k!} C_{BS}(S_0, K, T, r_n, 0, \sigma_n),$$

where $\lambda' = \lambda \mathrm{e}^{\gamma + \delta^2/2}$, $\sigma_n^2 T = \sigma^2 T + n\delta^2$, $r_n T = (r + \mu_J)T + n(\gamma + \delta^2/2)$, and μ_J is the jump compensator. The Lévy density is given by

$$\nu(x) = \frac{\lambda}{\sqrt{2\pi}\delta} \exp\left(-\frac{(x-\gamma)^2}{2\delta^2}\right)$$

and it follows that the characteristic function of X_T is be explicitly stated as

$$\Phi_{X_T}(z) = \exp\left(\mathtt{i} z\omega T - \frac{1}{2}z^2\sigma^2 T + \lambda T(\mathrm{e}^{\mathtt{i}z\gamma - z^2\delta^2/2} - 1)\right),$$

where $\omega = -\frac{1}{2}\sigma^2 - \lambda(\mathrm{e}^{\gamma+\delta^2/2} - 1)$. We refer to Merton [105] for more details and derivations.

Double-exponential jumps (Kou model). In the Kou model [78] the jumps are distributed according to a double-exponential density

$$f(x) := p^+\alpha^+\mathrm{e}^{-\alpha^+ x} I_{(0,\infty)}(x) + p^-\alpha^-\mathrm{e}^{-\alpha^-|x|} I_{(-\infty,0)}(x),$$

where $p^+ + p^- = 1$ and $p^\pm \in [0,1]$. In addition we restrict to $\alpha^+ > 1$ and $\alpha^- > 0$ to ensure that the stock price has a finite expectation. It follows that the characteristic function is given by

$$\Phi_{X_T}(z) = \exp\left(\mathtt{i}z\omega T - \frac{1}{2}z^2\sigma^2 T + \lambda T\left(\frac{p^+}{\alpha^+ - \mathtt{i}z} - \frac{p^-}{\alpha^- + \mathtt{i}z}\right)\right),$$

where $\omega = -\frac{1}{2}\sigma^2 - \lambda\left(\frac{p^+}{\alpha^+ + 1} - \frac{p^-}{\alpha^- - 1}\right)$. Although the probability density is not available in closed form, Kou derives tractable expressions for plain vanilla options, which depend on special functions that can be time consuming and delicate to compute. Kou & Wang [79] give analytic expressions for the Laplace transforms of barrier and lookback options, and derive an iterative procedure to solve these, which again depend on the special function.

Hyper-exponential jumps (HEJD model). The hyper-exponential jump-diffusion (HEJD) model was first used in a finance context by Lipton [93] and Mordecki [108], and is a special case of the wider class of mixed-exponential jump-diffusions, which we discuss below. It can be seen as a generalisation of Kou's double-exponential jump-diffusion model replacing the double-exponential distribution by a hyper-exponential distribution, which is given by:

$$f(x) := \sum_{i=1}^{m^+} p_i^+ \alpha_i^+ \mathrm{e}^{-\alpha_i^+ x} I_{(0,\infty)}(x) + \sum_{j=1}^{m^-} p_j^- \alpha_j^- \mathrm{e}^{-\alpha_j^- |x|} I_{(-\infty,0)}(x),$$

where

$$p_k^\pm \in [0,1], \ \sum_{k=1}^{m^\pm} p_k^\pm = q^\pm, \quad q^+ + q^- = 1 \quad \text{and} \quad -\alpha_{m^-}^- < \cdots < -\alpha_1^- < 0 < \alpha_1^+ < \cdots < \alpha_{m^+}^+.$$

For this model the Laplace exponent $\psi(s) = \log \mathbb{E}[\mathrm{e}^{sX_1}]$ for $s \in (-\alpha_1^-, \alpha_1^+)$ can be shown to take the following form

$$\psi(s) = \mu s + \sigma^2 s^2/2 + \lambda\left(\sum_{i=1}^{m^+} p_i^+ \frac{\alpha_i^+}{\alpha_i^+ - s} + \sum_{j=1}^{m^-} p_j^- \frac{\alpha_j^-}{\alpha_j^- + s} - 1\right). \tag{1.2.6}$$

If in addition $\alpha_i^+ > 1$ for all i, then $\mathbb{E}[S_t] < \infty$. When defining $\rho_k^\pm(q)$ as the roots of the Cramér-Lundberg equation

$$\psi(s) = q, \quad q > 0, \tag{1.2.7}$$

the roots satisfy

$$\rho_{m^-+1}^-(q) < -\alpha_{m^-}^- < \rho_{m^-}^-(q) < -\alpha_{m^--1}^- < \cdots < \rho_2^-(q) < -\alpha_1^- < \rho_1^-(q) < 0$$

$$0 < \rho_1^+(q) < \alpha_1^+ < \rho_2^+(q) < \cdots < \rho_{m^+}^+(q) < \alpha_{m^+}^+ < \rho_{m^++1}^+(q),$$

if q is real. Note that this encapsulating structure makes it easy to find them numerically. It is also worth mentioning that the hyper-exponential distribution can approximate any jump diffusion models with completely monotone jump size distributions arbitrarily closely. For further background on the HEJD process, which is a special case of a phase-type Lévy process, see Asmussen *et al.* [10].

Mixed-exponential jumps (MEJD model). The mixed-exponential jump diffusion (MEJD) model has been used in applied probability for many years (see Asmussen [9] and references therein, for example) and was first used in finance by Cai & Kou [34]. The jumps in the MEJD model have a mixed-exponential distribution, which is a weighted average of exponential distributions with possibly negative weights. It therefore generalises the hyper-exponential distribution, where all weights need to be positive, as well as the double-exponential distribution, which is a weighted average of only two exponential distributions. Compared to the hyper-exponential distribution, one loses the encapsulating structure for the roots of the Cramér-Lundberg equation so that it takes longer to find these numerically, but gains that this distribution is dense with respect to the class of all distributions in the sense of weak convergence (see Botta & Harris [19]). For example included are discrete distributions, the normal distribution and various exponential-, power- and heavy-tail distributions.

The jumps J_i are distributed according to the mixed-exponential density

$$f(x) := \sum_{i=1}^{m^+} p_i^+ \alpha_i^+ \mathrm{e}^{-\alpha_i^+ x} I_{(0,\infty)}(x) + \sum_{j=1}^{m^-} p_j^- \alpha_j^- \mathrm{e}^{-\alpha_j^- |x|} I_{(-\infty,0)}(x),$$

where

$$\sum_{k=1}^{m^\pm} p_k^\pm = q^\pm, \quad q^+ + q^- = 1 \quad \text{and} \quad -\alpha_{m^-}^- < \cdots < -\alpha_1^- < 0 < \alpha_1^+ < \cdots < \alpha_{m^+}^+.$$

Since the weights, $p_k^\pm$, are allowed to be negative in the MEJD model, one needs to restrict the model parameters to guarantee that $f(x)$ remains a probability density function (PDF). A necessary condition for it to be a PDF is $p_1^\pm > 0$, $\sum_{k=1}^{m^\pm} p_k^\pm \alpha_k^\pm \geq 0$. A sufficient condition is $\sum_{k=1}^{l} p_k^\pm \alpha_k^\pm \geq 0 \quad \forall l = 1, ..., m^\pm$ (for alternative conditions see Bartholomew [16]). We impose the additional condition that $\alpha_i^+ > 1$ to ensure that the stock price S_t has a finite expectation. Contrary to the models before, here the roots can (and mostly will) be complex. The Laplace exponent is of the same form as for the HEJD model and we restate it here for convenience

$$\psi(s) = \mu s + \sigma^2 s^2/2 + \lambda \left(\sum_{i=1}^{m^+} p_i^+ \frac{\alpha_i^+}{\alpha_i^+ - s} + \sum_{j=1}^{m^-} p_j^- \frac{\alpha_j^-}{\alpha_j^- + s} - 1 \right) \tag{1.2.8}$$

for $s \in (-\alpha_1^-, \alpha_1^+)$.

1.2.4 Infinite activity models

The second category comprises models with infinitely many jumps in every time interval. It has been argued that such models give a more realistic description of the price process at various time scales (see Madan [97], Carr *et al.* [38] and Geman [63]). These models are capable of generating non-trivial small-time behaviour and, as shown in [38], the Brownian component is no longer needed. As mentioned above, many of the models in this category can be constructed via Brownian subordination, which adds analytical tractability. We now discuss three infinite active models in more detail.

Variance-gamma model. The variance-gamma (VG) process was first introduced to finance by Madan & Seneta [99] in its symmetric version, and later extended to its asymmetric version by Madan, Carr & Chang [98]. In the asymmetric version discussed here, the VG process has three parameters: $\theta \in \mathbb{R}$, $\sigma > 0$, $\nu > 0$. It is defined by evaluating a Brownian motion with drift θ and volatility σ, as given in Equation (1.2.2), at an independent gamma time. Specifically, the time-change (Z_t) is now given by a gamma process independent of (W_t) with marginal distribution at time t following a gamma distribution $G(\frac{t}{\nu}, \nu)$ with shape parameter $\frac{t}{\nu}$ and scale parameter ν. The probability density function, conditional on $Z_0 = 0$, is given by

$$f_{Z_t}(x) = \frac{x^{\frac{t}{\nu}-1}\mathrm{e}^{-\frac{x}{\nu}}}{\nu^{\frac{t}{\nu}}\Gamma(\frac{t}{\nu})}. \tag{1.2.9}$$

The Laplace transform of the value (Z_t) of the corresponding clock at time t therefore has the following form:

$$\mathbb{E}[\mathrm{e}^{-uZ_t}] = (1+\nu u)^{-\frac{t}{\nu}}. \tag{1.2.10}$$

CGMY model. The eponymous CGMY model is named after Carr, Geman, Madan & Yor [38] and can be seen as a generalisation of the VG model discussed above. It is also referred to as the KoBoL model as it was first used in finance by Boyarchenko & Levendorskiĭ [23] and is based on Koponen processes. In particular, the class of tempered stable processes that can be represented as time-changed Brownian motion coincides with this model. The characteristic function of (X_t) in this model can be shown to equal:

$$\mathbb{E}[\mathrm{e}^{\mathrm{i}zX_t}] \quad = \quad \mathrm{e}^{tC\Gamma(-Y)[(M-\mathrm{i}z)^Y+(G+\mathrm{i}z)^Y-M^Y-G^Y]}. \tag{1.2.11}$$

The Laplace transform of the corresponding clock (Z_t) at time t (see Madan & Yor [100] for details) is given by

$$\begin{aligned}
\mathbb{E}[\mathrm{e}^{-uZ_t}] &= \mathrm{e}^{tC\Gamma(-Y)[2r^Y\cos(\eta Y)-M^Y-G^Y]} \qquad (1.2.12)\\
r &= \sqrt{2u+GM}\\
\eta &= \arctan\left(\frac{\sqrt{2u-((G-M)/2)^2}}{(G+M)/2}\right).
\end{aligned}$$

For this model we set the drift in Equation (1.2.2) equal to $\theta = \frac{G-M}{2}$ and the volatility to $\sigma = 1$.

NIG model. The normal inverse Gaussian (NIG) model was introduced by Barndorff-Nielsen [13]. In this model, the log returns of the risky asset $\log(S_{t+s}/S_t)$ are assumed to follow a $NIG(\alpha, \beta, \delta s)$ distribution (where s represents the length of the increment). The NIG distribution with parameters $\alpha > 0, -\alpha < \beta < \alpha,$ and $\delta > 0$ is infinitely divisible and defined as the normal variance-mean mixture of a normal distribution where the mixing density is the inverse Gaussian distribution. The probability density function is defined on the whole real line and given by

$$f(x;\alpha,\beta,\delta) = \frac{\alpha\delta}{\pi}\frac{K_1(\alpha\sqrt{\delta^2-x^2})}{\sqrt{\delta^2+x^2}}\mathrm{e}^{\left(\delta\sqrt{\alpha^2+\beta^2}+\beta x\right)}, \quad x\in\mathbb{R},$$

where K_1 is the modified Bessel function of third order and index 1. The corresponding characteristic function is

$$\Phi(u;\alpha,\beta,\delta) = \exp\left(-\delta\left(\sqrt{\alpha^2-(\beta+iu)^2}-\sqrt{\alpha^2-\beta^2}\right)\right).$$

The NIG distribution is a special case of generalised hyperbolic distributions and can approximate most hyperbolic distributions very closely. If we define the NIG process as a Lévy process with stationary and independent NIG-distributed increments, where $X_0 = 0$ with probability 1, then this process has no Brownian component, a Lévy measure of $\nu(\mathrm{d}x) = \alpha\delta\pi^{-1}\exp(\beta x)K_1(\alpha|x|)(|x|)^{-1}\mathrm{d}x$ and a drift component of $\gamma = 2\delta\alpha\pi^{-1}\int_0^1 \sinh(\beta x)K_1(\alpha x)\mathrm{d}x$. Alternatively, the NIG process can be written as a time changed Brownian motion – in the setting of (1.2.2) it follows that $\sigma = \delta$, $\theta = \beta\delta^2$, and the clock follows an inverse Gaussian process with parameters $\mu = 1$ and $\lambda = \delta\sqrt{\alpha^2-\beta^2}$. This model was later extended to the generalised hyperbolic class by Eberlein, Keller & Prause [55].

1.2.5 Stochastic volatility models

In a stochastic volatility model, a second random process (σ_t) is introduced, such that

$$\frac{\mathrm{d}S_t}{S_t} = \mu \mathrm{d}t + \sigma_t \mathrm{d}W_t, \tag{1.2.13}$$

where $(\sigma_t)_{t\geq 0}$ is a positive stochastic process interpreted as the instantaneous volatility of the underlying and chosen to be mean-reverting in most models. Contrary to the exponential-Lévy models, the price process S_t is no longer Markovian, since it now also depends on the level of volatility. Well known stochastic volatility models are the Hull-White model [74], the Stein-Stein model [127] and the Heston model [72]. In all three of these models, $(\sigma_t)_{t\geq 0}$ is a diffusion driven by a Brownian motion, so that (S_t, σ_t) becomes a two-dimensional Markovian diffusion. These models can generate smiles and skews similar to those observed in the market, but are not able to calibrate to short-term implied volatility patterns well. The Bates model [17] overcomes this issue by introducing jumps in the price process. In general, jumps can be added to either the price process or the volatility process, or both. In addition, the Brownian motion in the volatility process can be correlated to the Brownian motion in the price process. If the characteristic functions for the log-price exists in closed form, European options can be priced quickly using the Fourier inversion method reviewed in Section 1.3.2. For path-dependent options the Fourier transforms are not available in closed form though and one must turn to other numerical methods. Andersen [6] and more recently Glasserman & Kim [67] develop efficient simulation methods for the Heston model that can be used in a Monte Carlo method (see Section 1.3.1). The Heston model is one of the most popular stochastic volatility model, which is the reason we discuss it in more detail below (we discuss the general case first and then restrict to the zero-correlation case). The stochastic volatility model with jumps introduced by Bates is discussed at the end of this section. Two further stochastic volatility models that are widely used are the SABR model [70] and the Barndorff-Nielsen & Shephard model [15].

Heston model with correlation

In the Heston model [72], the volatility process σ_t in Equation (1.2.13) is equal to the square root of a positive CIR rate process as introduced by Cox, Ingersoll & Ross [47].

The stochastic differential equation for this square root process $(V_t)_{t\geq 0}$ is given by

$$dV_t = \kappa(\delta - V_t)\mathrm{d}t + \xi\sqrt{V_t}\mathrm{d}B_t, \qquad t \geq 0, \tag{1.2.14}$$

where B_t is another standard Brownian motion. The correlation between W_t and B_t is given by $\rho \in [-1, 1]$. Additionally, the CIR activity rate process starts at $V_0 > 0$, $\kappa > 0$ is the rate of mean reversion, $\delta > 0$ is the long-run activity rate level and $\xi > 0$ is the active rate volatility. It is further assumed that the Feller condition ($2\kappa\delta \geq \xi^2$) is satisfied to ensure that the process never hits zero. The transition law of the variance process $(V_t)_{t\geq 0}$ is a scaled non-central chi-square distribution so that V_t can be simulated exactly given V_0:

$$V_t = \frac{\xi^2(1-\mathrm{e}^{-\kappa t})}{4\kappa}\chi_\theta'^2\left(\frac{4\kappa\mathrm{e}^{-\kappa t}}{\xi^2(1-\mathrm{e}^{-\kappa t})}V_0\right), \quad t > 0, \quad \theta = \frac{4\kappa\delta}{\xi^2}, \tag{1.2.15}$$

where $\chi_\gamma'^2(\lambda)$ denotes a non-central chi-square random variable with γ degrees of freedom and non-centrality parameter λ.

Following the Broadie-Kaya method [31], the Heston model can then be described by the following pair of stochastic differential equations

$$\begin{aligned}
\frac{\mathrm{d}S_t}{S_t} &= \mu\mathrm{d}t + \sqrt{V_t}(\rho\mathrm{d}B_t + \sqrt{1-\rho^2}\mathrm{d}W_t) \\
dV_t &= \kappa(\delta - V_t)\mathrm{d}t + \xi\sqrt{V_t}\mathrm{d}B_t, \qquad t \geq 0,
\end{aligned}$$

so that one can write

$$S_t = S_0 \exp\left(\mu t - \frac{1}{2}\int_0^t V_s\mathrm{d}s + \rho\int_0^t \sqrt{V_s}\mathrm{d}B_s + \sqrt{1-\rho^2}\int_0^t \sqrt{V_s}\mathrm{d}W_s\right),$$

where the two Brownian motions W_t and B_t are now independent. Notice that it also follows from (1.2.14) that

$$\int_0^t \sqrt{V_s}\mathrm{d}B_s = \frac{1}{\xi}\left(V_t - V_0 - \kappa\delta t + \kappa\int_0^t V_s\mathrm{d}s\right). \tag{1.2.16}$$

Broadie and Kaya then observe that $\log(S_t/S_0)$ is conditionally normal, given $\int_0^t V_s\mathrm{d}s$:

$$\log(S_t/S_0) \sim \mathcal{N}\left(\mu t - \frac{1}{2}\int_0^t V_s\mathrm{d}s + \frac{\rho}{\xi}\left(V_t - V_0 - \kappa\delta t + \kappa\int_0^t V_s\mathrm{d}s\right), \sqrt{1-\rho^2}\int_0^t V_s\mathrm{d}s\right).$$

It therefore follows, that simulating S_t in the Heston model, given (S_0, V_0), reduces to sampling from

$$\left(\int_0^t V_s\mathrm{d}s \,\middle|\, V_0, V_t\right). \tag{1.2.17}$$

Broadie and Kaya sample from Equation (1.2.17), the conditional distribution of the integrated variance over $[0,t]$, given the level of the variance at the endpoints, through numerical inversion of its characteristic function. However, this method is rather time-consuming, and Glasserman & Kim [67] develop a very efficient method to sample from (1.2.17) using properties of squared Bessel bridges.

Heston model without correlation

The Heston model without correlation is obtained by setting $\rho = 0$ in the above and can be written as a time-changed Brownian motion model. To do so, define $(V_t)_{t\geq 0}$ in Equation (1.2.4) to be equal to the positive CIR rate process defined in (1.2.14) where B_t is now independent of the Brownian motion (W_t) in Equation (1.2.2).

The characteristic function of (Z_t) is well known from the work of Cox, Ingersoll & Ross [47]. We recall that the Laplace transform of (Z_t) in this setting is given by

$$\begin{aligned}\mathbb{E}[\mathrm{e}^{-uZ_t}] &= A(t,u)\mathrm{e}^{-B(t,u)V_0} \\ &= \left(\frac{2\eta \mathrm{e}^{\frac{(\eta+\kappa)t}{2}}}{(\eta+\kappa)(\mathrm{e}^{\eta t}-1)+2\eta}\right)^{\frac{2\kappa\delta}{\xi^2}} \exp\left[\frac{-2u(\mathrm{e}^{\eta t}-1)V_0}{(\eta+\kappa)(\mathrm{e}^{\eta t}-1)+2\eta}\right], \quad (1.2.18)\end{aligned}$$

where $\eta = \sqrt{2\xi^2 u + \kappa^2}$. In the setting of (1.2.2), the Heston model without correlation corresponds to the parameter values $\sigma = 1$ and $\theta = -\frac{\sigma^2}{2} = -\frac{1}{2}$.

Bates model

The Bates model [17] is a combination of the Heston model with correlation and the Merton model. The only difference to the Heston model is that proportional log-normal jumps are added to the price equation. As mentioned above, this seemingly small change overcomes the difficulty that stochastic volatility models without jumps have when calibrating short maturities. The model can be described by the following pair of stochastic differential equations

$$\begin{aligned}\frac{\mathrm{d}S_t}{S_t} &= \mu \mathrm{d}t + \sqrt{V_t}(\rho \mathrm{d}B_t + \sqrt{1-\rho^2}\mathrm{d}W_t) + c\mathrm{d}Z_t \\ dV_t &= \kappa(\delta - V_t)\mathrm{d}t + \xi\sqrt{V_t}\mathrm{d}B_t, \qquad t \geq 0,\end{aligned}$$

where everything is defined as above, and Z_t is a compound Poisson process with intensity λ and log-normal distributed jump sizes as in the Merton model. Scott [124] generalises this model by modelling the interest rate by another independent mean-reverting stochastic process. One can also generalise the Bates model by replacing the Gaussian distribution for the jumps by any other distribution - we will refer to this model as the *generalised Bates model* from here onwards.

1.3 Pricing methods

For most of the models discussed in the previous section even plain vanilla options are not available in 'truly' tractable closed-form and one needs to resort to numerical methods for their valuation. One might argue that two exceptions are the Heston model, for which semi-closed-form Fourier transformations are available, and the Kou model, for which vanilla options can be explicitly expressed in terms of special functions. In the Merton model vanilla options follow as a quickly converging infinite series of Black-Scholes prices. Computationally more complicated are exotic options however, for which no tractable closed-form formulas are available for any of the discussed models. One is hence left with the question of which numerical pricing method to choose. In mathematical finance, the Monte Carlo method, Laplace/Fourier inversion method and finite difference methods are the most widely used methods. Note that there are more tailored methods that might be more efficient for a particular class of models/options.

Laplace/Fourier inversion methods are usually very efficient if the Laplace/Fourier transformation of the quantity of interest can be derived in closed form. Additionally, the Fast Fourier Transform (FFT) method can be used to perform the transform for many options with same maturity but different strike in one go. Finite Difference methods are very fast and efficient in low dimensions, but become less feasible for higher dimensions because computational complexity grows exponentially with dimension (for a fixed precision). Monte Carlo methods, on the other hand, grow linearly with dimension and are therefore more efficient in these cases. The basic Monte Carlo method, the Euler-Maruyama method defined below, converges rather slowly however, and one is therefore fostered to use and develop efficient variance reduction techniques.

We discuss Monte Carlo methods in Section 1.3.1 and Laplace/Fourier inversion methods in Section 1.3.2. In the latter section, we also discuss the standard FFT method, as presented by Carr & Madan [40], in detail. In both sections we review the main properties of the particular method, but put most emphasis on how to use them in order to price (exotic) options for the models discussed in Section 1.2. The third method, the finite difference method, is a numerical method for approximating the solution of a differential equation using finite difference equations to approximate derivatives. For the class of Lévy models, the option value solves a second-order partial integro-differential equation. We refer the interested reader to the papers by Andersen & Andreasen [7] and Cont & Voltchkova [44] for more details. Note that other methods have been proposed to solve these differential equation – see Amin [5], who uses multinomial trees, Boyarchenko & Levendorskiĭ [25] and Matache *et al.* [103], who use a wavelet Galerkin method. Since we do not use the finite difference method in the remainder of this thesis, we will not discuss it in more detail here.

1.3.1 Monte Carlo method

The well-known Monte Carlo method is one of the most widely used methods in science and engineering due to its flexibility and generality. It is easy to implement, requires only a few lines of coding (in its basic form) and is intuitive to understand. Already in the 18^{th} century people were using Monte Carlo simulations, without calling it that, to estimate the value of π by experiment. For that they counted the number of throws that landed inside a square compared to those ending up in an inscribed circle. However, it was also used before to estimate the chances of a biased die for example. In the last century the Monte Carlo approach pervaded a number of scientific fields including engineering, experimental psychology, astronomy, biology, physics, economics and demography. Phelim Boyle (see Boyle [27]) introduced the concept to finance in order to price options on stocks with discrete dividend payments. Nowadays the method is heavily used in quantitative finance to value exotic options (possibly depending on multiple underlyings) for which no analytic expressions exist. The method is appealing for financial applications, since most derivative securities can be priced in a coherent way and correlations are easy to handle. In its basic form the method can be implemented directly from a contract's term sheet without the need for any further mathematics other than a model for the dynamics of the financial underlyings.

In our context, we are interested in approximating an expectation of a given function $\mathbb{E}[f(X)]$ by drawing N 'random' numbers x_i and evaluating the equally weighted

N-iteration estimator:

$$\hat{\mathbb{E}}_N[f(X)] := \frac{1}{N}\sum_{i=1}^{N} f(x_i).$$

The core principle of the Monte Carlo method is the strong law of large numbers, which establishes that the empirical average of N i.i.d. random samples $X_1, X_2, ..., X_N$ with $\mathbb{E}[|X_i|] < \infty$ for $i = 1, 2, ..., N$ converges to the expectation μ $(= \mathbb{E}[X_1])$ almost surely as N goes to infinity. By the central limit theorem, if $X_1, X_2, ..., X_N$ are i.i.d. random variables with finite second moment that have expectation μ and standard deviation $0 < \sigma < \infty$, then the sample mean

$$\hat{X}_N = \frac{1}{N}\sum_{i=1}^{N} X_i$$

satisfies

$$\frac{\hat{X}_N - \mu}{\sigma/\sqrt{N}} \xrightarrow{d} \mathcal{N}(0,1),$$

as $N \to \infty$. The central limit theorem states that the error is asymptotically Gaussian, with a standard deviation of the order of one over the square root of the number of samples. From the above it follows that the probability that an interval of the form

$$\left(\hat{X}_N - z_{\delta/2}\frac{\sigma}{\sqrt{N}},\ \hat{X}_N + z_{\delta/2}\frac{\sigma}{\sqrt{N}}\right)$$

covers μ approaches $1-\delta$ as $N \to \infty$, where $1 - \Phi(z_{\delta/2}) = \delta/2$ and Φ denotes the standard cumulative normal distribution. Note that the above should really be understood as an *asymptotically valid confidence interval* for μ. Because σ is typically unknown, one usually approximates it by the sample standard deviation of the random variables $X_1, X_2, ..., X_N$:

$$s_N = \sqrt{\frac{1}{N-1}\sum_{i=1}^{N}(X_i - \hat{X}_N)^2},$$

where $s_N \to \sigma$ as $N \to \infty$ and we refer to

$$\hat{X}_N \pm z_{\delta/2}\frac{s_N}{\sqrt{N}} \tag{1.3.1}$$

as the $1-\delta$ confidence interval in Chapter 3. For more details on Monte Carlo methods in finance, see Jäckel [75] and Glasserman [66], and references therein. See the latter in particular for variance reduction techniques, which we review next.

Variance reduction techniques

The Euler-Maruyama method approximates the solution of a stochastic differential equation by discretisation. To be specific, assume that the process $X = \{X_t, t \in \mathbb{R}^+\}$ satisfies the Itō stochastic differential equation

$$\mathrm{d}X_t = a(X_t)\mathrm{d}t + b(X_t)\mathrm{d}W_t, \qquad t > 0,$$

with initial condition $X_0 = x_0$. Then the Euler-Maruyama approximation to the true solution X on the finite interval $[0, T]$ is the Markov chain Y' defined on the equidistant grid $\mathbb{T}_N = \{0 = \tau_0 < \tau_1 < \ldots < \tau_N = T\}$ as:

$$Y'_{\tau_{n+1}} = Y'_{\tau_n} + a(Y'_{\tau_n})\Delta_n + b(Y'_{\tau_n})\Delta W_n, \qquad n = 0, ..., N-1,$$

where $Y_0 = x_0$, $\Delta_n = T/N$ and $\Delta W_n = W_{\tau_{n+1}} - W_{\tau_n}$.

This basic method is known to converge extremely slowly, especially for path-dependent quantities (see Boyle *et al.* [28] for example). As can be seen, the standard deviation of the above classical method is $s_N/\sqrt{N}$. Note that to reduce the standard deviation by a factor of ten the number of simulations N has to be increased one hundredfold. Even with the on-going technological progress, developing efficient variance reduction techniques (so to reduce s_N) to make the Monte Carlo method converge quicker is therefore of paramount importance. The most common techniques, which all reduce the variance to increase the accuracy of the computation, are the antithetic sampling, control variate, importance sampling and stratification technique. In general, variance reduction techniques amount to rewriting the quantity to be computed as the expectation of a random variable that has a smaller variance.

When samples are drawn from a symmetric law, like the Gaussian law, antithetic sampling requires that the antithetic (symmetric) of each sample is also used. This assures that the sample mean is always 0, as it should be, and has the advantage that one gets two samples for the computational costs of one. We use this variance reduction technique for all Monte Carlo methods utilised in Chapter 3.

In addition, it can be very beneficial to use a control variate, which is one of the most widely used variance reduction techniques. The technique is particularly useful when pricing barrier option or range notes in the models discussed above. The principle behind the control variate variance reduction technique is to exploit information about the errors in estimates of known quantities to reduce the error in an estimate of an unknown quantity. The variance of the Monte Carlo method is reduced, because rather than simulating the unknown quantity, one simulates the difference between the known and unknown quantity, which should have a lower variance if the two are strongly correlated. Assume that unknown quantity X and control variate Y are two square integrable random variables. Here we want to estimate $\mathbb{E}[X]$, which can be written as

$$\mathbb{E}[X] = \mathbb{E}[X - Y] + \mathbb{E}[Y],$$

where $\mathbb{E}[Y]$ is known and $Var(X - Y) < Var(X)$. Then, rather than simulating $\mathbb{E}[X]$ directly, one can simulate $\mathbb{E}[X - Y]$ in the Monte Carlo method and add the known value $\mathbb{E}[Y]$ for every sample. In particular, for all models discussed in Section 1.2, one can use the quickly calculated price of a vanilla option (computed using a Fourier inversion method or the rational approximation method discussed in Chapter 2) as a control variate to price an exotic option. By the same argument, one could also use the price of the particular exotic option in the Black-Scholes model as a control variate in a model where the exotic option price is unknown. One should keep in mind however that the effectiveness of the control variate variance reduction technique reduces rapidly with a decreasing correlation (in absolute terms) between the two random variables, and one should always try to find a control variate that is correlated as much as possible with the unknown quantity.

Importance sampling methods proceed by changing the law of the samples to reduce the variance and stratified sampling constraints the fraction of samples drawn from specific subsets (called strata) of the sample space (for more details on variance reduction techniques also see Dagpunar [49] and references therein). Both of these methods should be used when applying the bridge sampling Monte Carlo method introduced in Chapter 3 in practice. We have not done so here in order to concentrate on the newly developed method separately.

Simulating a Lévy process

When simulating a jump-diffusion process, it is important to note that the jump component and the diffusion component are independent of each other, and can therefore be simulated independently. The number of jumps N_T of a Poisson process on the interval $[0, T]$ is a Poisson random variable with parameter λT. The jump times can be obtained by sampling N_T independent uniform random variables (on the interval $[0, T]$), rearranged in increasing order. The jump sizes are again independent, so that one needs to sample a total of N_T jumps according to the specific jump size distribution. A number of algorithms have been developed for jump diffusions based on the observation that between two jumps, the process simply follows a Brownian motion.

Lévy processes with infinite activity can usually not be simulated as described above, since the law of increments is not known in closed-form. However, one way to proceed is to approximate the jumps smaller than some $\epsilon > 0$ by a properly renormalised Brownian motion and therefore arrive at an approximating jump-diffusion (see Asmussen & Rosiński [11], where they give necessary and sufficient conditions on the Lévy measure under which the normalised error process resulting from the deletion of small jumps converges to a Brownian motion).

As we discussed above, many of these models can be represented as time-changed Brownian motion models. If it is easy to simulate the subordinator, simulation of paths is equally straightforward.

Acceptance-Rejection method

The acceptance-rejection method, often used in Monte Carlo simulations, is an efficient way to simulate from a known probability density function $f(x)$, which is difficult or impossible to sample. That is, we wish to generate a random variable X from $F(x) = \mathbb{P}(X \leq x)$ where an explicit formula for $F^{-1}(y)$ is not available or this inverse transform method (and any other method that is available to us) is not efficient. The idea of this method is to find an alternative probability distribution G, with density function $g(x)$, from which we can simulate efficiently and which is 'close' to $f(x)$. In particular, we assume that the ratio $f(x)/g(x)$ is bounded by a constant c ($\sup_x (f(x)/g(x)) \leq c$), which we want to be as close as possible to 1. The algorithm can then be quickly described as follows:

- Generate a random variable Y from the distribution of G.
- Generate a uniform random variable U (independent of Y).
- If $U \leq \frac{f(Y)}{cg(Y)}$ set $X = Y$ (accept), otherwise start over (reject).

In the following, we would like to show that the conditional distribution of Y given that $U \leq \frac{f(Y)}{cg(Y)}$ is indeed F, that is: $\mathbb{P}\left(Y \leq y \middle| U \leq \frac{f(Y)}{cg(Y)}\right) = F(y)$. First note that the ratio

$\frac{f(Y)}{cg(Y)}$ is a random variable, because $f(Y)$ and $g(Y)$ are. The ratio is also independent of U and $0 < \frac{f(Y)}{cg(Y)} \leq 1$. The number of iterations, N, needed to successfully generate X is itself a random variable following a geometric distribution ($\mathbb{P}(N = n) = (1-p)^{n-1}p$ for $n \geq 1$) with probability

$$p = \mathbb{P}\left(U \leq \frac{f(Y)}{cg(Y)}\right) = \frac{1}{c}.$$

The last equality can be shown to hold by first conditioning on Y

$$\mathbb{P}\left(U \leq \frac{f(Y)}{cg(Y)}\middle| Y = y\right) = \frac{f(y)}{cg(y)},$$

and then using the tower property and recalling that Y has density $g(y)$:

$$p = \int_{-\infty}^{\infty} \frac{f(y)}{cg(y)} g(y)\mathrm{d}y = \frac{1}{c}\int_{-\infty}^{\infty} f(y)\mathrm{d}y = \frac{1}{c}.$$

Next, note that

$$\begin{aligned}
\mathbb{P}\left(U \leq \frac{f(Y)}{cg(Y)}\middle| Y \leq y\right) &= \frac{\mathbb{P}\left(U \leq \frac{f(Y)}{cg(Y)}, Y \leq y\right)}{G(y)} \\
&= \int_{-\infty}^{y} \frac{\mathbb{P}\left(U \leq \frac{f(Y)}{cg(Y)}\middle| Y = w\right)}{G(y)} g(w)\mathrm{d}w \\
&= \frac{1}{G(y)}\int_{-\infty}^{y} \frac{f(w)}{cg(w)} g(w)\mathrm{d}w \\
&= \frac{1}{cG(y)}\int_{-\infty}^{y} f(w)\mathrm{d}w \\
&= \frac{F(y)}{cG(y)}.
\end{aligned}$$

Finally,

$$\mathbb{P}\left(Y \leq y \middle| U \leq \frac{f(Y)}{cg(Y)}\right) = \mathbb{P}\left(U \leq \frac{f(Y)}{cg(Y)}\middle| Y \leq y\right)\frac{G(y)}{1/c} = \frac{F(y)}{cG(y)} cG(y) = F(y),$$

where we used the basic fact that $\mathbb{P}(A|B) = \mathbb{P}(B|A)\frac{\mathbb{P}(A)}{\mathbb{P}(B)}$. For more details on this method we refer to Press *et al.* [113]. We will use the acceptance-rejection method in Chapter 3 to draw from the MEJD distribution (F) and use the HEJD distribution as the auxiliary distribution (G).

1.3.2 Laplace/Fourier inversion methods

A very natural and powerful method for solving boundary problems for partial differential equations, and more generally for integro-differential and pseudo-differential equations, is the Laplace or Fourier transform method. The method is heavily used in mathematical finance to derive plain vanilla option prices in the class of exponential Lévy models. For a few of the models discussed in the previous section, even Laplace transforms of barrier and lookback options are explicitly known. To obtain the option price, one therefore needs to perform a Laplace or Fourier inversion. This standard mathematical tool was first used in finance by Heston ([72]) for Gaussian models, and by Boyarchenko & Levendorskiĭ ([22]) and Carr & Madan ([40]) for Lévy models. We discuss Laplace transforms, inverse Laplace transforms and their application to mathematical finance below. We then discuss Fourier transforms, inverse Fourier transforms and their application to mathematical finance. In many practical cases, the inverse Fourier transforms are obtained by the Fast Fourier Transform method, which we present at the end of this section.

The Laplace transform

The Laplace transform, named after the French mathematician and astronomer Pierre-Simon Laplace, is a linear operator and integral transform of a function $f(t)$ with real argument $t \geq 0$ to a function $\mathcal{L}\{f(t)\}(s)$ with a real argument s. The Laplace transform $\mathcal{L}\{f(t)\}$ for a Borel measurable function $f(t)$ on $\mathbb{R}^+$ that satisfies $|f(t)| \leq M\mathrm{e}^{\alpha t}$ for some $\alpha > 0$, (we will refer to this as 'f is of exponential order') is defined by the improper integral:

$$F(s) = \mathcal{L}\{f(t)\}(s) = \int_0^\infty f(t)\mathrm{e}^{-st}\mathrm{d}t. \tag{1.3.2}$$

A necessary condition for existence of the integral is that f must be locally integrable on $[0, \infty)$. If the locally integrable function decays at infinity or is of exponential type, the integral can be understood as a (proper) Lebesgue integral. Following from the definition, the Laplace transform has many useful properties. Two of the most fundamental ones are the convolution integral and the fact that the Laplace transform of $f^{(n)}(t)$ can be expressed in terms of $F(s)$ and $f^{(m)}(0)$ for $m = 1, 2, ..., n-1$, where $f^{(n)}(t)$ is the n^{th} derivative of function $f(t)$. In general, many relationships and operations over the original $f(t)$ correspond to simpler relationships and operations over the images $F(s)$. In probability theory, for example, if X is a random variable with PDF f, then the Laplace transform of f is given by an expected value:

$$\mathcal{L}\{f\}(s) = \mathbb{E}\left[\mathrm{e}^{-sX}\right]. \tag{1.3.3}$$

Replacing s by $-t$ yields the moment generating function of X.

The Inverse Laplace transform will be denote as

$$\mathcal{L}^{-1}\{F(s)\}(t) = f(t). \tag{1.3.4}$$

Like the Laplace transform, also the inverse is linear and unique apart from the possible addition of null functions. In many cases it may not be possible to find $\mathcal{L}\{f(t)\}$ explicitly since it is an integral, but there is no guarantee at all of being able to find $\mathcal{L}^{-1}\{F(s)\}$, which is given by a complex integral. A formal definition of the inverse is provided in the following theorem.

Theorem 1.3.1. *(Inverse Laplace transform) If the Laplace transform of $f(t)$ is of exponential order and*

$$F(s) = \int_0^\infty \mathrm{e}^{-st} f(t)\mathrm{d}t,$$

then

$$f(s) = \lim_{k\to\infty} \left\{ \frac{1}{2\pi\mathtt{i}} \int_{\sigma-\mathtt{i}k}^{\sigma+\mathtt{i}k} F(s)\mathrm{e}^{st}\mathrm{d}s \right\}, \qquad t > 0,$$

where $|f(t)| \leq \mathrm{e}^{Mt}$ for some positive real number M and σ is another real number such that $\sigma > M$ (here $\mathtt{i} = \sqrt{-1}$ represents the imaginary unit).

Laplace transforms find a variety of applications in mathematical finance. We use it in Chapter 2 to represent the stochastic clock Z_T in a tractable form. In Chapter 3 we indirectly derive Laplace transforms of the one-sided first passage and the occupation time of a MEJD bridge at an exponential random time, although we don't refer to it as such. The motivation in both cases is that one is only able to derive explicit expressions in terms of the Laplace transforms and that these could be inverted numerically to obtain the quantity of interest (for more details on numerical inversion of the Laplace transform we refer to the algorithms presented in Abate & Whitt [2], and Petrella [111], and point to a survey by Abate *et al.* [1] and references therein). Based on the idea of numerically inverting Laplace transforms, there is a whole range of research articles that derive option prices (even those of (double) barrier or lookback options) for a variety of Lévy models in terms of their Laplace transform. Here we only name a few of the most prominent ones. Lipton [93] derives Laplace transforms for single barrier options, lookbacks and reverse knock-outs relying on fluctuation identities for the hyper-exponential jump-diffusion process. Kou & Wang [79] work out Laplace transforms of single barrier and lookback options for the Kou model using the memoryless property of the exponential distribution, Boyarchenko & Levendorskiĭ [24] develop Laplace transforms for single barrier and touch options under a wide class of Lévy processes, Sepp [125] derives Laplace transforms for double barrier and touch options with time-depending rebates, and Jeannin & Pistorius [77] propose Laplace transforms for single barrier options and sensitivities in the class of HEJD models. Most recently, Cai & Kou [34] develop double Laplace transforms for barrier options and sensitivities in the class of MEJD models. For a general treatment of Laplace transforms, we refer to Schiff [122].

The Fourier transform

The Fourier transform, named after the French mathematician Joseph Fourier, is another integral transform, which is defined as follows:

Definition 1.3.1. *Let h be an integrable function defined for all $x \in \mathbb{R}$ with values in $\mathbb{C}$. The Fourier transform of h is a mapping $\mathcal{F} : L^1 \to L^\infty$ defined by*

$$\mathcal{F}(h)(\omega) = \int_{-\infty}^{\infty} h(x)\mathrm{e}^{\mathrm{i}\omega x}\mathrm{d}x. \tag{1.3.5}$$

Usually ω is real, but it can also be taken to be a complex number under suitable integrability conditions on h. The Fourier transform is related to the Laplace transform, but whereas the Laplace transform resolves a function into its moments, the Fourier transform expresses a function as a series of modes of vibration (frequencies). Generalised functions need to be introduced to calculate the Fourier transform of a constant or a polynomial, for example. Under suitable conditions on h and $\mathcal{F}(h)$, following from Definition 1.3.1, the Fourier inverse theorem states:

$$h(x) = \mathcal{F}^{-1}\{\mathcal{F}\}(x) = \frac{1}{2\pi}\int_{-\infty}^{\infty} \mathcal{F}(h)(\omega)\mathrm{e}^{-\mathrm{i}\omega x}\mathrm{d}\omega. \tag{1.3.6}$$

The Fourier inversion theorem holds for all continuous functions that are absolutely integrable (*i.e.* $L^1(\mathbb{R}^n)$) with absolutely integrable Fourier transform. The Fourier transform can also be derived as a Fourier series expressed in its complex form when the period of the represented function is lengthened and allowed to approach infinity. When performed correctly, this integral leads to the Fourier transform as defined above. Properties like the shift theorems, transforming derivatives, etc. also exist for the Fourier transform, which makes it similarly useful for solving differential and integral equations.

In mathematical finance, Fourier transform methods have been mostly motivated by the move from the classical Black-Scholes model to exponential Lévy models. As mentioned before, for these models there are no explicit formulas (even for vanilla options in most cases), because the probability density of a Lévy process is typically not known in closed form. Since the characteristic function of this density can be expressed in terms of elementary functions for a majority of Lévy processes however, Fourier-based option pricing has been utilised successfully. We will see below that to evaluate a vanilla option for exponential Lévy models in this framework, one needs to perform one Fourier inversion numerically. The overall complexity of this computation per option price is not much higher than in the Black-Scholes framework, since one Fourier transform can simultaneously give option prices for a whole range of strikes and the procedure can be efficiently performed with the FFT method (see below).

Before the utilisation of the FFT method in mathematical finance, Heston [72] was one of the first to apply Fourier analysis to determine option prices. Heston numerically solved for the delta and the risk-neutral probability of finishing in the money, which combined with the stock price and the strike price generates option values. However, although the decomposition of an option price into probabilistic elements is theoretically attractive, it is numerically undesirable owing to discontinuity of the payoffs (see Bakshi & Madan [12]). In addition, this approach was unable to harness the considerable computational power of the FFT method. For a rigorous treatment on complex analysis and Fourier transforms we refer to Rudin [119].

Fast Fourier Transform (FFT) method

The most commonly used FFT method is the Cooley-Tukey method (Cooley & Tukey [45]), which was used in computer sciences for many years before applied to derivatives pricing. Carr & Madan [40] are the first to utilise the FFT method in a financial context. They derive the Fourier transforms of an option price and its time value for any model in which the characteristic function of the risk neutral density is known analytically. The FFT method allows them to perform the option pricing very efficiently. Both of the derived Fourier transforms in [40] are expressed in terms of the characteristic function of the log price - we will concentrate on the Fourier transform of the option price here.

Let $k = \log(K)$ and let $C_T(k)$ be the value of a T-maturity call option with strike e^k. If we let the risk-neutral density of the log price s_T be $q_T(s)$, then the characteristic function as defined in (1.2.1) can also be written as the Fourier transform of its density,

$$\Phi_T(u) \equiv \int_{-\infty}^{\infty} \mathrm{e}^{\mathtt{i}us} q_T(s)\mathrm{d}s.$$

The call option value $C_T(k)$ can then be expressed in terms of the risk-neutral density by

$$C_T(k) \equiv \int_{k}^{\infty} \mathrm{e}^{-rT}(\mathrm{e}^s - \mathrm{e}^k) q_T(s)\mathrm{d}s.$$

However, since the call option value $C_T(k)$ tends to S_0 as k tends to $-\infty$, the call option function is not square-integrable. Carr and Madan therefore introduce the modified call price $c_T(k)$ defined as

$$c_T(k) \equiv \mathrm{e}^{\alpha k} C_T(k)$$

for $\alpha > 0$. One should now expect the modified call option function to be square-integrable in k over the entire real line for a range of positive values of α. We define by Ψ_T the Fourier transform of $c_T(k)$:

$$\begin{aligned}
\Psi_T(v) &= \int_{-\infty}^{\infty} \mathrm{e}^{\mathtt{i}vk} c_T(k)\mathrm{d}k \\
&= \int_{-\infty}^{\infty} \mathrm{e}^{\mathtt{i}vk} \int_{k}^{\infty} \mathrm{e}^{\alpha k}\mathrm{e}^{-rT}(\mathrm{e}^s - \mathrm{e}^k) q_T(s)\mathrm{d}s\ \mathrm{d}k \\
&= \int_{-\infty}^{\infty} \mathrm{e}^{-rT} q_T(s) \int_{-\infty}^{s} (\mathrm{e}^{s+\alpha k} - \mathrm{e}^{k+\alpha k})\mathrm{e}^{\mathtt{i}vk}\mathrm{d}k\ \mathrm{d}s \\
&= \int_{-\infty}^{\infty} \mathrm{e}^{-rT} q_T(s) \int_{-\infty}^{s} \left(\mathrm{e}^{s+(\alpha+\mathtt{i}v)k} - \mathrm{e}^{(1+\alpha+\mathtt{i}v)k}\right) \mathrm{d}k\ \mathrm{d}s \\
&= \int_{-\infty}^{\infty} \mathrm{e}^{-rT} q_T(s) \left(\frac{\mathrm{e}^{(\alpha+1+\mathtt{i}v)s}}{\alpha+\mathtt{i}v} - \frac{\mathrm{e}^{(\alpha+1+\mathtt{i}v)s}}{\alpha+1+\mathtt{i}v}\right) \mathrm{d}s \\
&= \frac{\mathrm{e}^{-rT}\Phi_T(v-(\alpha+1)\mathtt{i})}{\alpha^2+\alpha-v^2+\mathtt{i}(2\alpha+1)v}. \qquad (1.3.7)
\end{aligned}$$

Note that the inverse Fourier transform of $c_T(k)$ follows from the first equation of the above and is equal to

$$c_T(k) = \frac{1}{2\pi}\int_{-\infty}^{\infty} \mathrm{e}^{-\mathtt{i}vk}\Psi_T(v)\mathrm{d}v.$$

One is now able to express the call option value in terms of the characteristic function

$$\begin{aligned}
C_T(k) &= \frac{\mathrm{e}^{-\alpha k}}{2\pi}\int_{-\infty}^{\infty} \mathrm{e}^{-\mathtt{i}vk}\Psi_T(v)\mathrm{d}v = \frac{\mathrm{e}^{-\alpha k}}{\pi}\int_{0}^{\infty} \mathrm{e}^{-\mathtt{i}vk}\Psi_T(v)\mathrm{d}v \\
&= \frac{\mathrm{e}^{-\alpha k}}{\pi}\int_{0}^{\infty} \mathrm{e}^{-\mathtt{i}vk}\frac{\mathrm{e}^{-rT}\Phi_T(v-(\alpha+1)\mathtt{i})}{\alpha^2+\alpha-v^2+\mathtt{i}(2\alpha+1)v}\mathrm{d}v, \qquad (1.3.8)
\end{aligned}$$

where the second equation holds because $C_T(k)$ is real and therefore function $\Psi_T(v)$ is odd in its imaginary part and even in its real part. The final expression for $C_T(k)$ lends itself for an application of the FFT, which we discuss next. For details on restrictions on α and a derivation of the Fourier transform of the time value of an option, we refer to the original paper.

The FFT is an efficient algorithm due to Cooley & Tukey [45] for computing the following discrete transformation of a vector $(x_n,\ n = 1, ..., N)$ into a vector $(w_n,\ n = 1, ..., N)$:

$$w_n = \sum_{j=1}^{N} \mathrm{e}^{\frac{-\mathrm{i}2\pi(j-1)(n-1)}{N}} x_j \text{ for } n = 1, ..., N. \tag{1.3.9}$$

Typically N is a power of 2. The number of multiplications of the FFT algorithm is of order $\mathcal{O}(NlogN)$ and is in contrast to the straightforward evaluation of the above sums which gives rise to $\mathcal{O}(N^2)$ numbers of multiplications. Note that the difference between $NlogN$ and N^2 is immense when N gets large. Using the FFT on the N point-grid $(0, \eta, 2\eta, 3\eta, ..., (N-1)\eta)$ gives the following approximation of (1.3.8):

$$C_T(k) \approx \frac{\mathrm{e}^{-\alpha k}}{\pi} \sum_{j=1}^{N} \mathrm{e}^{-\mathrm{i}v_j k} \Psi_T(v_j)\eta, \tag{1.3.10}$$

where $v_j = \eta(j-1)$. The FFT returns N values of k, where we employ a regular spacing of $\lambda = \frac{2b}{N}$ for log-strikes ranging from $-b$ to b, so that $k_n = -b + \lambda(n-1)$ for $n = 1, ..., N$. Substituting this into (1.3.10) yields:

$$\begin{aligned} C_T(k_n) &\approx \frac{\mathrm{e}^{-\alpha k}}{\pi} \sum_{j=1}^{N} \mathrm{e}^{-\mathrm{i}v_j(-b+\lambda(n-1))} \Psi_T(v_j)\eta \\ &= \frac{\mathrm{e}^{-\alpha k}}{\pi} \sum_{j=1}^{N} \mathrm{e}^{-\mathrm{i}\lambda\eta(j-1)(n-1)} \mathrm{e}^{\mathrm{i}v_j b} \Psi_T(v_j)\eta, \end{aligned}$$

for $n = 1, ..., N$, noting that $v_j = (j-1)\eta$. With the choice of $\lambda\eta = \frac{2\pi}{N}$, the above is an exact application of the FFT on the vector $\mathrm{e}^{\mathrm{i}v_j b}\Psi_T(v_j)\eta$. The final step in applying the FFT to the call option value, Carr & Madan [40] choose a more refined weighting (Simpson's rule) leading to the following approximation

$$C_T(k_n) \approx \frac{\mathrm{e}^{-\alpha k}}{\pi} \sum_{j=1}^{N} \mathrm{e}^{\frac{-\mathrm{i}2\pi(j-1)(n-1)}{N}} \mathrm{e}^{\mathrm{i}v_j b} \Psi_T(v_j)\eta \left(\frac{3 + (-1)^j - \delta_{j-1}}{3}\right),$$

where δ_n is the Kronecker delta function that is unity for $n = 0$ and zero otherwise.

Carr and Madan choose η to be 0.25 and α to be 1.5, which are the values we use in

Chapter 2. As can be seen, if we now choose a value for N, one can first calculate the corresponding values for λ and b, then generate the vectors v and k, before calculating the vector $A_j = \mathrm{e}^{\mathrm{i}v_j b}\Psi_T(v_j)\eta\left(\frac{3+(-1)^j-\delta_{j-1}}{3}\right)$ and passing it into a FFT engine (Matlab, for example, has a build-in FFT method). After that we multiply the resulting vector point-wise with $\frac{\mathrm{e}^{-\alpha k}}{\pi}$ to obtain option values for a wide range of strikes (see Press *et al.* [113] for more details).

We use the method, as presented here, as a benchmark to our newly developed method in Chapter 2 and refer to it as *standard FFT method* throughout the thesis. The standard FFT method was generalised and improved by a number of authors (*e.g.* Boyarchenko & Levendorskiĭ [26], Eberlein *et al.* [54], Lee [84], Lewis [89], Lipton [94] and Raible [114]). Other developments have taken place to make the FFT method faster. In particular, the Lewis-Lipton formula (see Lewis [89] and Lipton [93]) utilises the fact that payoff functions have their own representations in Fourier space. The approach expresses the option price as a convolution of generalised Fourier transforms using the Plancherel identity and can be up to 5 times faster than the original method by Carr and Madan. When one only needs the value of a single option, Boyarchenko & Levendorskiĭ [25] suggest to transform the contour of integration in the complex plane to achieve improved convergence. The alternative to these FFT methods that we present in Chapter 2, the rational approximation method, works without the need of inverse Fourier transforms. Note however that the rational approximation method is only applicable for the class of time changed Brownian motion models, which represents a subclass of the models the Fourier inversion approach can handle.

1.4 Mathematical tools and techniques

We review rational function approximation in Section 1.4.1, Richardson extrapolation in Section 1.4.2 and the Wiener-Hopf factorisation in Section 1.4.3.

1.4.1 Rational approximation

A rational function, $R_{n,m}(x)$, is any function that can be written as the ratio of two polynomial functions, $P_n(x)$ and $Q_m(x)$, which are of degree n and m, respectively. With this notation it follows that

$$R_{n,m}(x) = \frac{P_n(x)}{Q_m(x)},$$

where we defined $P_n(x) = \sum_{i=0}^{n} p_i x^i$ and $Q_m(x) = 1 + \sum_{i=1}^{m} q_i x^i$. Rational approximations generally outperform polynomial approximations in terms of computational efficiency, where we define computational efficiency as the maximum errors that can be achieved for a given computational effort (see Morris [109]). For some functions, the optimal rational function approximation is known further to be able to achieve substantially higher accuracy than the optimal polynomial approximation with the same number of coefficients. Rational function approximations have been extensively used in theoretical physics, engineering, statistics and economics. For background on rational approximations and applications, we refer to Ralston & Rabinowitz [115] (Chapter 7).

The ideal *minimax* solution would be that choice of p's and q's that minimises

$$\epsilon = \max_{a \le x \le b} \left| R_{n,m}(x) - \frac{P_n(x)}{Q_m(x)} \right|.$$

Since ϵ is bounded below by zero, some minimax solution is guaranteed to exist. Finding this minimax solution for a rational approximation (as well as for a polynomial approximation) is difficult and involves iterative procedures that can be computationally time consuming. For rational approximations these iterative procedures lead to the so-called Remes algorithms (Ralston & Wilf [116]). Chebyshev approximations can be obtained more quickly as these do not involve iterations, while leading to errors very close to those of the minimax solution. Therefore, when interested in obtaining rational approximations in Chapter 2, we employ rational Chebyshev approximations because of their computational efficiency. We will first review the general theory of Chebyshev approximations and then discuss rational Chebyshev approximations in more detail.

Chebyshev approximations

The Chebyshev polynomial of degree n is defined as

$$T_n(x) = \cos(n \ \arccos(x)) \quad \text{for } -1 \le x \le 1. \tag{1.4.1}$$

Even though these terms may look trigonometric, it should be noted that explicit expressions for $T_n(x)$ can be found by the following recursion

$$\begin{aligned} T_0(x) &= 1 \\ T_1(x) &= x \\ T_2(x) &= 2x^2 - 1 \\ T_3(x) &= 4x^3 - 3x \\ &\cdots \\ T_{n+1}(x) &= 2xT_n(x) - T_{n-1}(x) \quad n \geq 1, \end{aligned} \tag{1.4.2}$$

which was derived using the well-known formula for the sum of two cosines

$$\cos[(n+1)\theta] + \cos[(n-1)\theta] = 2\cos(n\theta)\cos(\theta)$$

with $x = \cos(\theta)$. Each Chebyshev polynomial $T_n(x)$ is continuous and has n zeros on the interval $[-1, 1]$. Each of the zeros is located at

$$x_k = \cos\left(\frac{\pi(k-0.5)}{n}\right) \qquad \text{k = 1,2,...,n,}$$

whereas the $n+1$ extrema are located at

$$x_k^* = \cos\left(\frac{\pi k}{n}\right) \qquad \text{k = 0,1,...,n.}$$

At its maxima $T_n(x) = 1$ and at its minima $T_n(x) = -1$ for all n. In addition, the Chebyshev polynomials satisfy a discrete orthogonality relation on $[-1, 1]$.

Under Dini-Lipschitz continuity of the interpolated function f, the Chebyshev interpolation converges as the number of nodes tends to infinity. This leads to a representation of f in terms of an infinite series of Chebyshev polynomials:

$$f(x) = \frac{c_0}{2} + \sum_{j=1}^{\infty} c_j T_j(x), \quad -1 \leq x \leq 1.$$

With this, and using the orthogonality of the Chebyshev polynomials, we obtain

$$c_j = \frac{2}{\pi}\int_{-1}^{1} \frac{f(x)T_j(x)}{\sqrt{1-x^2}}\mathrm{d}x = \frac{2}{\pi}\int_0^{\pi} f(\cos\theta)\cos(j\theta)\mathrm{d}\theta. \tag{1.4.3}$$

To compute these coefficients, fast algorithms can be used for this cosine transform. A discretisation of Equation (1.4.3) using the trapezoidal rule leads to a discrete cosine transform:

$$c_j = \frac{2}{N}\sum_{k=1}^{N} f(x_k)T_j(x_k) = \frac{2}{N}\sum_{k=1}^{N} f\left(\cos\left(\frac{\pi(k-0.5)}{N}\right)\right)\cos\left(\frac{\pi j(k-0.5)}{N}\right). \tag{1.4.4}$$

When setting

$$f_{Cheb}(x) = \frac{c_0}{2} + \sum_{j=1}^{N-1} c_j T_j(x), \tag{1.4.5}$$

it can be shown that this approximation is exactly equal to $f(x)$ at all N zeros of $T_N(x)$, and the approximation converges as $N \to \infty$. If the coefficients c_j decrease sufficiently rapidly in magnitude, the error of this approximation is

$$E_N(x) = \sum_{j=N+1}^{\infty} c_j T_j(x) \approx c_{N+1} T_{N+1}(x). \tag{1.4.6}$$

That is, the error can be approximated by the next term in the sum. How fast the coefficients c_j decrease depends on continuity and differentiability properties of the function to be expanded.

If one inserts the expressions given for $T_n(x)$ in (1.4.2) into Equation (1.4.5), one obtains a polynomial in x, which approximates the function $f(x)$ on the interval $[-1, 1]$. Even though this Chebyshev approximating polynomial is not equal to the minimax polynomial, which among all polynomials of the same degree has the smallest maximum deviation from the true function, it comes very close (Morris [109], Chapter 6). The minimax polynomial is very difficult and time consuming to calculate, whereas the Chebyshev approximating polynomial is almost identical and is extremely easy to compute.

Finally, if one is interested in approximating a variable $y \in [a, b]$, one should use the following change of variable to map it onto $x \in [-1, 1]$ and proceed as before

$$x = \frac{2y - (b + a)}{b - a}. \tag{1.4.7}$$

Rational Chebyshev approximations

Rather than approximating an arbitrary function $f(x)$ by a linear combination of Chebyshev polynomials, one can approximate $f(x)$ by a ratio of linear combinations of these polynomials as follows:

$$f(x) \approx \frac{\sum_{j=0}^{m} a_j T_j(x)}{\sum_{j=0}^{k} b_j T_j(x)} = T_{m,k}(x).$$

For simplicity and for all rational function approximations used here, set $m = k$, and define

$$f(x) \approx \frac{\sum_{j=0}^{m} a_j T_j(x)}{\sum_{j=0}^{m} b_j T_j(x)} = f_{RA}^{m}(x), \tag{1.4.8}$$

where $T_n(x)$ are the Chebyshev polynomials defined in (1.4.1) and $b_0 = 1$.

The error of the rational function approximation can be expressed as (see Morris [109] p.184 for more details)

$$f(x) - f_{RA}^m(x) = \frac{c_0}{2} + \sum_{j=1}^{\infty} c_j T_j(x) - \frac{\sum_{j=0}^m a_j T_j(x)}{\sum_{j=0}^m b_j T_j(x)}.$$

This equation can be rewritten as

$$\begin{aligned} f(x) \quad - \quad f_{RA}^m(x) &= \frac{\left[\frac{c_0}{2} + \sum_{j=1}^{\infty} c_j T_j(x)\right]\left[\sum_{j=0}^m b_j T_j(x)\right] - \sum_{j=0}^m a_j T_j(x)}{\sum_{j=0}^m b_j T_j(x)} \\ &= \frac{\frac{c_0}{2}\sum_{j=0}^m b_j T_j(x) + \sum_{j=1}^{\infty}\sum_{i=0}^m \frac{b_i c_j}{2}[T_{i+j}(x) + T_{|i-j|}(x)] - \sum_{j=0}^m a_j T_j(x)}{\sum_{j=0}^m b_j T_j(x)}, \end{aligned}$$

where we have used the fact that $2T_n(\theta)T_m(\theta) = T_{n+m}(\theta) + T_{|n-m|}(\theta)$. Collecting coefficients of like terms (in T_j) and setting the resulting coefficients to zero, one gets

$$a_0 = \sum_{i=0}^m \frac{b_i c_i}{2},$$

and

$$a_r = \frac{1}{2}\sum_{i=0}^m b_i(c_{i+r} + c_{|i-r|}) \qquad r = 1, 2, ..., 2m,$$

where $a_r = 0$ if $r > m$ and b_0 is chosen to be 1 (c_j is defined as in Equation (1.4.4)). This leads to a linear system of equations for any m, which can be solved easily for the parameters a_j and b_j of Equation (1.4.8). To illustrate, the following is the resulting system of equations for a 4×4 rational function approximation:

$$\begin{aligned} 2a_0 &= c_0 + b_1 c_1 + b_2 c_2 + b_3 c_3 + b_4 c_4 \\ 2a_1 &= 2c_1 + b_1(c_0 + c_2) + b_2(c_1 + c_3) + b_3(c_2 + c_4) + b_4(c_3 + c_5) \\ 2a_2 &= 2c_2 + b_1(c_1 + c_3) + b_2(c_0 + c_4) + b_3(c_1 + c_5) + b_4(c_2 + c_6) \\ 2a_3 &= 2c_3 + b_1(c_2 + c_4) + b_2(c_1 + c_5) + b_3(c_0 + c_6) + b_4(c_1 + c_7) \\ 2a_4 &= 2c_4 + b_1(c_3 + c_5) + b_2(c_2 + c_6) + b_3(c_1 + c_7) + b_4(c_0 + c_8) \\ 0 &= 2c_5 + b_1(c_4 + c_6) + b_2(c_3 + c_7) + b_3(c_2 + c_8) + b_4(c_1 + c_9) \\ 0 &= 2c_6 + b_1(c_5 + c_7) + b_2(c_4 + c_8) + b_3(c_3 + c_9) + b_4(c_2 + c_{10}) \\ 0 &= 2c_7 + b_1(c_6 + c_8) + b_2(c_5 + c_9) + b_3(c_4 + c_{10}) + b_4(c_3 + c_{11}) \\ 0 &= 2c_8 + b_1(c_7 + c_9) + b_2(c_6 + c_{10}) + b_3(c_5 + c_{11}) + b_4(c_4 + c_{12}). \end{aligned}$$

This system of equations can be written in matrix form as follows:

$$\begin{pmatrix} c_0 \\ c_1 \\ c_2 \\ c_3 \\ c_4 \\ c_5 \\ c_6 \\ c_7 \\ c_8 \end{pmatrix} = -\frac{1}{2} \begin{pmatrix} -4 & 0 & 0 & 0 & 0 & 2c_1 & 2c_2 & 2c_3 & 2c_4 \\ 0 & -2 & 0 & 0 & 0 & c_2+c_0 & c_3+c_1 & c_4+c_2 & c_5+c_3 \\ 0 & 0 & -2 & 0 & 0 & c_3+c_1 & c_4+c_0 & c_5+c_1 & c_6+c_2 \\ 0 & 0 & 0 & -2 & 0 & c_4+c_2 & c_5+c_1 & c_6+c_0 & c_7+c_1 \\ 0 & 0 & 0 & 0 & -2 & c_5+c_3 & c_6+c_2 & c_7+c_1 & c_8+c_0 \\ 0 & 0 & 0 & 0 & 0 & c_6+c_4 & c_7+c_3 & c_8+c_2 & c_9+c_1 \\ 0 & 0 & 0 & 0 & 0 & c_7+c_5 & c_8+c_4 & c_9+c_3 & c_{10}+c_2 \\ 0 & 0 & 0 & 0 & 0 & c_8+c_6 & c_9+c_5 & c_{10}+c_4 & c_{11}+c_3 \\ 0 & 0 & 0 & 0 & 0 & c_9+c_7 & c_{10}+c_6 & c_{11}+c_5 & c_{12}+c_4 \end{pmatrix} \begin{pmatrix} a_0 \\ a_1 \\ a_2 \\ a_3 \\ a_4 \\ b_1 \\ b_2 \\ b_3 \\ b_4 \end{pmatrix}.$$

Substituting the resulting coefficients of a_j and b_j into Equation (1.4.8) gives a rational Chebyshev approximation of function $f(x)$.

1.4.2 Richardson extrapolation

An important problem that arises in many scientific and engineering applications is that of approximating the limit of a slowly converging infinite sequences $\{P_n\}$. Rather than approximating the limit by calculating $\{P_n\}$ for a large value of n, which can be computationally very expensive to obtain, many of these limits can be approximated by extrapolation with a few number of terms for which n is small. The Richardson extrapolation, reviewed in this section, is one such extrapolation method and is named after Lewis Fry Richardson, who introduced the technique in the early 20th century. Most of the material reviewed in this section can also be found in a standard reference by Sidi [126].

In the cases of interest in this thesis, a given infinite sequence $\{P_n\}$ can be related to a function $P(y)$, such that $P_n = P(y_n), n = 0, 1, ...,$ for some monotonically decreasing sequence $y_n \subset (0, b]$, where $P(y)$ is known and therefore computable for $0 < y \leq b$. We further assume that $\lim_{n\to\infty} y_n = 0$, so that it follows from $\lim_{y\to 0+} P(y) = P$ that $\lim_{n\to\infty} P_n = P$ as well. If one further assumes that for some positive integer s, $P(y)$ is of the form

$$P(y) \quad = \quad P + \sum_{k=1}^{s} \alpha_k y^{\sigma_k} + \mathcal{O}(y^{\sigma_{s+1}}) \text{ as } y \to 0+, \tag{1.4.9}$$

where $0 < \sigma_1 < \sigma_2 < ... < \sigma_{s+1}$ and α_k are constants independent of y, then $\lim_{y\to 0+} P(y) = P$. It follows that one can approximate P by $P(y)$ for sufficiently small values of y - the error being $P(y) - P = \mathcal{O}(y^{\sigma_1})$ as $y \to 0+$. If σ_1 is sufficiently large, $P(y)$ can approximate

P well, even for values of y that are not so small. Otherwise, we have to calculate $P(y)$ for very small values of y, which is not always applicable however.

The sequences of interest in Chapter 3, for example, are of the form $\lim_{n\to\infty} \mathbb{P}(T/n)$, where T is the maturity of a financial derivative and $n = 1, 2, 3, ...$ is the number of recursive steps. If T is large, also n needs to be large in order to make $y_n = T/n$ feasibly small - calculations for large values of n are computationally very expensive however and would require High Precision Arithmetics to deal with round-off errors as detailed in Chapter 3.

The idea behind Richardson extrapolation on the other hand is to eliminate the y^{σ_1} term in (1.4.9) and derive a new approximation whose error is $\mathcal{O}(y^{\sigma_2})$ by taking a weighted average between $P(y)$ and $P(\omega y)$. To illustrate this technique, we now show how to first eliminate the term y^{σ_1} and then the term y^{σ_2} from Equation (1.4.9). Define a constant $\omega \in (0, 1)$ and set $y' = \omega y$, so that from (1.4.9) it follows

$$P(y') \quad = \quad P + \sum_{k=1}^{s} \alpha_k \omega^{\sigma_k} y^{\sigma_k} + \mathcal{O}(y^{\sigma_{s+1}}) \text{ as } y \to 0+ \, .$$

Define a weighted average of $P(y)$ and $P(\omega y)$ as $P(y, y')$ and verify that

$$P(y, y') = \frac{P(y') - \omega^{\sigma_1} P(y)}{1 - \omega^{\sigma_1}} \quad = \quad P + \sum_{k=2}^{s} \frac{\omega^{\sigma_k} - \omega^{\sigma_1}}{1 - \omega^{\sigma_1}} \alpha_k y^{\sigma_k} + \mathcal{O}(y^{\sigma_{s+1}}) \text{ as } y \to 0+ \, .$$

Note that $P(y, y') - P = \mathcal{O}(y^{\sigma_2})$ for $y \to 0+$, as we intended. To proceed, define a term $P(y', y'')$ analogous to $P(y, y')$, where $y'' = \omega^2 y$. One is then able to define a new approximation by

$$P(y, y', y'') = \frac{P(y', y'') - \omega^{\sigma_2} P(y, y')}{1 - \omega^{\sigma_2}} \quad = \quad P + \sum_{k=3}^{s} \frac{\omega^{\sigma_k} - \omega^{\sigma_1}}{1 - \omega^{\sigma_1}} \frac{\omega^{\sigma_k} - \omega^{\sigma_2}}{1 - \omega^{\sigma_2}} \alpha_k y^{\sigma_k} + \mathcal{O}(y^{\sigma_{s+1}})$$

as $y \to 0+$, which is a weighted average of $P(y, y')$ and $P(y', y'')$. Note further that the approximations $P(y)$, $P(y, y')$ and $P(y, y', y'')$ are of a similar form and that we have now successfully deleted the y^{σ_2} term in approximation $P(y, y', y'')$. The error between $P(y, y', y'')$ and P is $\mathcal{O}(y^{\sigma_3})$ as $y \to 0+$. It should be obvious that one can proceed in the same manner to eliminate more error terms in every step and therefore obtain yet better approximations. Note however, that to calculate $P(y, y', y'')$ one requires $P(y)$, $P(\omega y)$ and $P(\omega^2 y)$. For the sequences considered in this thesis, the easiest choice would be $\omega = \frac{1}{2}$, because n has to be discrete and the recursion $n + 1$ is computationally notably more expensive than recursion n. We therefore require $\mathbb{P}(T)$, $\mathbb{P}(T/2)$ and $\mathbb{P}(T/4)$ to calculate the approximation $P(y, y', y'')$ and we would require $\mathbb{P}(T/8)$ and $\mathbb{P}(T/16)$ in addition for approximation $P(y, y', y'', y''', y'''')$ if we were to continue in the same fashion. It is possible however to use the entire sequence of $\mathbb{P}(T/n)$ for $n = 1, 2, 3, 4, ...$ by varying the ω from step to step. The resulting formulas become more involved, but the idea remains the same. It has been shown that this procedure can be reduced to

$$\mathbb{P}_{1:N}(T) = \sum_{n=1}^{N} \frac{(-1)^{N-n} n^N}{n!(N-n)!} \mathbb{P}\left(\frac{T}{n}\right), \tag{1.4.10}$$

where the weights are now dependent on n (see Marchuk & Shaidurov [102] for details).

1.4.3 Wiener-Hopf factorisation

The Wiener-Hopf factorisation goes back to the early work of Wiener & Hopf [130], who used it to solve systems of integral equations. The Wiener-Hopf factorisation of a Lévy process, $(X_t)_{t\geq 0}$, is a collection of identities, which factorise the Laplace transform (in t) of the distribution of X_t into Laplace transforms (in t) of the distributions of the following processes:

$$\overline{X}_t := \sup\{X_s \,:\, s \leq t\}, \quad \underline{X}_t := \inf\{X_s \,:\, s \leq t\}, \quad Y_t := \overline{X}_t - X_t,$$

to which we refer as supremum process, infimum process and reflection (or drawdown) process of X_t, respectively.

Theorem 1.4.1 (Theorem 45.2 in Sato [121])**.** *(i) Let $q > 0$. There exists a unique pair of characteristic functions $\phi_q^+(z)$ and $\phi_q^-(z)$ of infinitely divisible distributions having drift 0 supported on $[0, \infty)$ and $(-\infty, 0]$, respectively, such that*

$$\frac{q}{q + \phi(z)} = \phi_q^+(z)\phi_q^-(z), \quad z \in \mathbb{R}. \tag{1.4.11}$$

(ii) The functions $\phi_q^+(z)$ and $\phi_q^-(z)$ have the following representations:

$$\begin{aligned}
\phi_q^+(z) &= \exp\left[\int_0^\infty t^{-1}\mathrm{e}^{-qt}\mathrm{d}t \int_0^\infty \left(\mathrm{e}^{\mathtt{i}zx} - 1\right)\mu_{X_t}(\mathrm{d}x)\right], \\
\phi_q^-(z) &= \exp\left[\int_0^\infty t^{-1}\mathrm{e}^{-qt}\mathrm{d}t \int_{-\infty}^0 \left(\mathrm{e}^{\mathtt{i}zx} - 1\right)\mu_{X_t}(\mathrm{d}x)\right].
\end{aligned}$$

The function $\phi_q^+(z)$ can be continuously extended to a bounded analytic function without zeros on the upper half plane and $\phi_q^-(z)$ can be similarly extended on the lower half plane. Unfortunately, the factors $\phi_q^+(z)$ and $\phi_q^-(z)$ are not known explicitly and must be evaluated numerically for most Lévy processes – the general class of mixed-exponential jump-diffusion (MEJD) models discussed in Section 1.2.3 and all models in that class are an exception however.

An extension to Equation (1.4.11) is given in the following theorem.

Theorem 1.4.2 (Theorem 45.7 in Sato [121])**.** *For any $q > 0$, $z \in \mathbb{R}$ and $w \in \mathbb{R}$,*

$$q \int_0^\infty \mathrm{e}^{-qt} \mathbb{E}\left[\mathrm{e}^{\mathrm{i}z\overline{X}_t + \mathrm{i}w(X_t - \overline{X}_t)}\right] \mathrm{d}t = \phi_q^+(z)\phi_q^-(w).$$

It should be noted that this theorem will be useful when calculating quantities involving the maximum of a Lévy process like barrier options, double barrier options and lookback options. It is also worth noting that $\overline{X}_t \stackrel{d}{=} X_t - \underline{X}_t$ and $\underline{X}_t \stackrel{d}{=} X_t - \overline{X}_t$ for all $t \geq 0$.

If we let

$$\begin{aligned} \phi_q^+(s) &= \int_0^\infty q\mathrm{e}^{-qt} \mathbb{E}\left[\mathrm{e}^{\mathrm{i}s\overline{X}_t}\right] \mathrm{d}t, \\ \phi_q^-(s) &= \int_0^\infty q\mathrm{e}^{-qt} \mathbb{E}\left[\mathrm{e}^{\mathrm{i}s\underline{X}_t}\right] \mathrm{d}t, \end{aligned}$$

it was shown by Rogozin [118] that $\phi_q^+(s), \phi_q^-(s)$ is the unique Wiener-Hopf factorisation of ψ. More details and the proofs of both theorems can be found in Sato [121].

Chapter 2

Fast computation of vanilla prices in time-changed models and implied volatilities using rational approximations

As discussed in the introduction, the need for models that can calibrate well to market prices has led to the generalisation of the GBM model. Many of these more general models can be expressed as time-changed Brownian motion models, to which we restrict in this chapter. We draw on the theory of rational functions to approximate the value function of a vanilla option in such models. The approximation takes the form of a linear combination of a number of negative exponential moments of the clock. This yields an explicit approximation for the value of a vanilla option in those time-changed models for which the Laplace transform (and hence any negative exponential moment) of the clock is available in tractable form.

For trading and risk management it is important to be able to (a) price vanilla options in models that provide an accurate description of market prices, and (b) generate the corresponding arbitrage-free volatility surface quickly and efficiently. Fast calculation of vanilla option prices in the specified model is also essential for carrying out the calibration of the prices to market quotes in a timely fashion.

To provide a numerical illustration, the method was implemented for the variance-gamma (VG) model, the KoBoL (also known as CGMY) model and the zero-correlation Heston model (the version of this model with correlation does not fall into the class of models studied here, but could be analysed by a two-dimensional extension). The rational function approximation method was found to yield stable, fast and accurate results. Comparison of the method to the standard fast Fourier transform (FFT) method introduced by Carr & Madan [40] (see Section 1.3.2 for a review) with respect to speed and accuracy, appears to be favourable for the rational function approximation method in the cases considered. At this point it is worth mentioning that several alternative and refined Fourier methods have been developed for the pricing of European options — see Boyarchenko & Levendorskiĭ [26] for a recent overview of several Fourier methods including an analysis of the different variations and recommendations for optimal parameter choices. A detailed comparative study of all the different pricing methods is left for future research.

The rational function approximation method is then applied to compute Black-Scholes implied volatilities. The method uses the fact that the computation of the implied volatilities that corresponds to a given set of arbitrage-free call option prices can be reduced to the computation of a single function of two variables. Contrary to Li [90], who proposes to approximate the entire resulting surface by a two-dimensional approximation, we perform a number of one-dimensional approximations and interpolate between these for any given combination of input parameters. For a wide range of parameters, the maximal approximation error of this approach is bounded by 5.5×10^{-5}, refining to our required level of accuracy the approximation of Li [90], which achieves a maximal error of 3.3×10^{-3} over the same region. It should be noted that this procedure can be used independently of the results derived for option pricing and is not limited to time-changed Brownian motion models. We refer the reader who is primarily interested in the implied volatility computation to Section 2.4.

The remainder of the chapter is organised as follows. In Section 2.1 the price of an option in a time-changed Brownian motion model is expressed in terms of a normalised Black-Scholes formula, and the approximation to the option price is presented in Section 2.2. Section 2.3 is devoted to a study of the error of the method, the application to computation of the implied volatility is given in Section 2.4, numerical results are reported in Section 2.5 and a summary is given in Section 2.6.

2.1 Vanilla options in time-changed Brownian motion models

In this chapter, we concentrate on the equity market and consider models in which the stock price process (S_t) under $\mathbb{Q}$ can be represented as follows:

$$S_t = S_0 \mathrm{e}^{(r-q)t+X_t-\omega t}, \tag{2.1.1}$$

$$X_t = \theta Z_t + \sigma W_{Z_t}, \tag{2.1.2}$$

where $(W_t)_{t\geq 0}$ is a Brownian motion and (Z_t) is the independent stochastic process called the clock (as introduced in Section 1.2.2). Hence, (Z_t) will be modelled either as a Lévy subordinator or as a time integral of a positive diffusion.

As before, $r \geq 0$ and $q \geq 0$ denote the constant risk-free interest rate and the constant dividend yield respectively, S_0 denotes the known stock price at time zero and (S_t) denotes the random stock price at time t. The condition that $S_t\mathrm{e}^{-(r-q)t}$ is a martingale will be guaranteed by an appropriate choice of the mean-correcting compensator ω_t as follows:

$$\omega_t = \frac{1}{t}\log \mathbb{E}[\mathrm{e}^{X_t}], \tag{2.1.3}$$

where $\mathbb{E}[\mathrm{e}^{X_t}]$ is assumed to be finite for all $t \geq 0$. In the case that X is a Lévy process, a necessary and sufficient condition for $\mathbb{E}[\mathrm{e}^{X_t}]$ to be finite is $\int_1^\infty \mathrm{e}^x v(\mathrm{d}x) < \infty$ (see Sato [121], Section 25). Note that only in the case that X_t is a Lévy process, w_t does not depend on t. Still, in the sequel we will suppress t from w for simplicity.

In Section 1.1.1 we introduced the payoff of plain vanilla options. In the Black-Scholes model, the risk-neutral dynamics of S are described by the exponential of a Brownian motion with drift,

$$S_t = S_0 \mathrm{e}^{(r-q-\frac{\sigma^2}{2})t+\sigma W_t}, \tag{2.1.4}$$

where $\sigma \geq 0$ is the volatility of the asset. The arbitrage-free value of a European call option (Equation (1.1.2)) in this model is then given by the Black-Scholes (BS) formula:

$$\begin{aligned} C_{BS}(S_0, K, T, r, q, \sigma) &= \mathrm{e}^{-rT}\mathbb{E}^{\mathbb{Q}}[(S_0\mathrm{e}^{(r-q-\frac{\sigma^2}{2})T+\sigma W_T} - K)^+] \qquad (2.1.5)\\ &= S_0\mathrm{e}^{-qT}\mathcal{N}(d_1) - K\mathrm{e}^{-rT}\mathcal{N}(d_2),\\ d_1 &= \frac{\log(S_0/K) + (r-q+\frac{\sigma^2}{2})T}{\sigma\sqrt{T}},\\ d_2 &= \frac{\log(S_0/K) + (r-q-\frac{\sigma^2}{2})T}{\sigma\sqrt{T}}, \end{aligned}$$

where $\mathcal{N}$ represents the standard normal cumulative distribution function. The following parametrisation of the Black-Scholes formula will be considered in what follows:

$$c_{BS}(v; x, \mu) = \mathrm{e}^{\mu v} \mathcal{N}\left(\frac{x}{\sqrt{v}} + \left(\mu + \frac{1}{2}\right)\sqrt{v}\right) - \mathrm{e}^{-x} \mathcal{N}\left(\frac{x}{\sqrt{v}} + \left(\mu - \frac{1}{2}\right)\sqrt{v}\right). \quad (2.1.6)$$

This normalisation is similar to the non-dimensional form of the Black-Scholes formula proposed by Lipton [92] (Chapter 9.3). The function c_{BS} is related to the original Black-Scholes formula as follows:

$$C_{BS}(S_0, K, T, r, q, \sigma) \quad = \quad S_0 \mathrm{e}^{-rT} c_{BS}\left(\sigma^2 T; \log(S_0/K), (r-q)/\sigma^2\right). \quad (2.1.7)$$

Typically, in time-changed models of the form given in Equations (2.1.1)–(2.1.2), no closed form formulas for call option prices are known. The next proposition shows how the call price of the time-changed model (C_{TC}) can be expressed in terms of the normalised Black-Scholes formula in (2.1.6).

Proposition 2.1.1. *If the process $(S_t)_{t\geq 0}$ under $\mathbb{Q}$ is given by the system of Equations (2.1.1) - (2.1.2), where (W_t) and (Z_t) are independent, the vanilla call option price with underlying S can be expressed as*

$$C_{TC}(S_0, K, T, r, q, \theta, \sigma) \quad = \quad S_0 \mathrm{e}^{-(q+\omega)T} \mathbb{E}^{\mathbb{Q}}\left[c_{BS}\left(\sigma^2 Z_T; x_{TC}, \mu_{TC}\right)\right], \quad (2.1.8)$$

where

$$\mu_{TC} = \frac{\theta}{\sigma^2} + \frac{1}{2} \qquad \textit{and} \qquad x_{TC} = \log\left(\frac{S_0}{K\mathrm{e}^{(q-r+\omega)T}}\right). \quad (2.1.9)$$

The parameters S_0, K, T, r, q, θ and σ are all constant and defined above. From Equation (2.1.3) it follows that the mean-correction ω is available in closed-form:

$$\mathbb{E}[\mathrm{e}^{X_t}] = \mathbb{E}\left[\mathrm{e}^{\theta Z_t + \sigma W_{Z_t}}\right] = \mathbb{E}\left[\mathrm{e}^{\left(\theta + \frac{\sigma^2}{2}\right) Z_t}\right] = \mathrm{e}^{\psi\left(-\theta - \frac{\sigma^2}{2}\right)t} = \mathrm{e}^{\omega t}, \quad (2.1.10)$$

so that ω is specified as follows:

$$\omega = \psi\left(-\theta - \frac{\sigma^2}{2}\right), \quad (2.1.11)$$

where $\psi(s) = \frac{1}{t}\log \mathbb{E}[\mathrm{e}^{-sZ_t}]$ is the Laplace exponent of (Z_t). In particular, it should be noted that ω only changes with θ and σ, and stays constant once these market parameters have been specified. In the Heston model with zero correlation, ω is equal to zero, which follows from the fact that e^{X_t} is a true martingale in the Heston model.

Remark. Note that μ_{TC} only depends on the *market* parameters θ and σ^2 while x_{TC} depends on r, q, S_0, T, K, θ, σ and ω. In particular, x_{TC} is *contract*-dependent as it varies with maturity T and strike K. We will refer to μ_{TC} and x_{TC} as the market-dependent parameter and the adjusted log-moneyness, respectively.

Proof. By conditioning on Z_T and given that (Z_t) and (W_t) are independent, we find the following:

$$\begin{aligned}
C_{TC}(S_0,K,T,r,q,\theta,\sigma) &= \mathrm{e}^{-rT}\mathbb{E}[(S_T-K)^+] = \mathrm{e}^{-rT}\mathbb{E}\left[\left(S_0\mathrm{e}^{(r-q)T+X_T-\omega T}-K\right)^+\right] \\
&= \mathrm{e}^{-rT}\mathbb{E}\left[\left(S_0\mathrm{e}^{(r-q)T+\theta Z_T+\sigma W_{Z_T}-\omega T}-K\right)^+\right] \\
&= \mathrm{e}^{-(q+\omega)T}\mathbb{E}\left[\left(S_0\mathrm{e}^{\theta Z_T+\sigma W_{Z_T}}-K\mathrm{e}^{(q-r+\omega)T}\right)^+\right] \\
&= \mathrm{e}^{-(q+\omega)T}\mathbb{E}\left[\left(S_0\mathrm{e}^{(\mu_{TC}\sigma^2-\frac{\sigma^2}{2})Z_T+\sigma W_{Z_T}}-K\mathrm{e}^{(q-r+\omega)T}\right)^+\right] \\
&= \mathrm{e}^{-(q+\omega)T}\mathbb{E}\left[\mathrm{e}^{\mu_{TC}\sigma^2 Z_T}C_{BS}(S_0,K\mathrm{e}^{(q-r+\omega)T},Z_T,\mu_{TC}\sigma^2,0,\sigma)\right] \\
&= S_0\mathrm{e}^{-(q+\omega)T}\mathbb{E}\left[c_{BS}\left(\sigma^2 Z_T,x_{TC},\mu_{TC}\right)\right],
\end{aligned}$$

where we used the Definitions (2.1.5) and (2.1.7) of C_{BS} and c_{BS}.

□

In the case that e^{X_t} is a martingale (or equivalently, $\theta=-\frac{\sigma^2}{2}$), the normalised Black-Scholes formula c_{BS} admits a symmetry:

Corollary 2.1.1. *If $\mu=0$, then the following holds true for all $v\in\mathbb{R}_+$ and $x\in\mathbb{R}$:*

$$c_{BS}(v;-x,0) = 1-\mathrm{e}^{-x}+\mathrm{e}^{-x}c_{BS}(v;x,0). \tag{2.1.12}$$

This identity thus applies, for example, to the Heston model with zero correlation.

Proof. By straightforward algebra we get the following equalities:

$$\begin{aligned}
c_{BS}(v;-x,0) &= \mathcal{N}\left(\frac{-x}{\sqrt{v}}+\frac{\sqrt{v}}{2}\right)-\mathrm{e}^{-x}\mathcal{N}\left(\frac{-x}{\sqrt{v}}-\frac{\sqrt{v}}{2}\right) \\
&= \left[1-\mathcal{N}\left(\frac{x}{\sqrt{v}}-\frac{\sqrt{v}}{2}\right)\right]-\mathrm{e}^{-x}\left[1-\mathcal{N}\left(\frac{x}{\sqrt{v}}+\frac{\sqrt{v}}{2}\right)\right] \\
&= 1-\mathrm{e}^{-x}+\mathrm{e}^{-x}\left[\mathcal{N}\left(\frac{x}{\sqrt{v}}+\frac{\sqrt{v}}{2}\right)-\mathrm{e}^{x}\mathcal{N}\left(\frac{x}{\sqrt{v}}-\frac{\sqrt{v}}{2}\right)\right] \\
&= 1-\mathrm{e}^{-x}+\mathrm{e}^{-x}c_{BS}(v;x,0).
\end{aligned}$$

□

The discussion so far has only considered call options. However, with the help of the put-call parity, one can easily obtain the value of a put option if the value of the corresponding call option is known. For convenience, we restate the put-call parity for the time-changed setting considered here at time 0:

$$P_{TC}(S_0, K, T, r, q, \theta, \sigma) = C_{TC}(S_0, K, T, r, q, \theta, \sigma) + K\mathrm{e}^{-rT} - S_0\mathrm{e}^{-qT}. \tag{2.1.13}$$

On account of Proposition 2.1.1, the problem of pricing a call option in a time-changed model reduces to the problem of evaluating $\mathbb{E}[c_{BS}(\sigma^2 Z_T; x, \mu)]$ for known values of x and μ, which we address in the following section.

2.2 Rational approximations used for option pricing

To evaluate C_{TC} given in Equation (2.1.8) we approximate the function $v \mapsto c_{BS}(v; x, \mu)$ on a specified range $v \in [a, b]$ by a rational function, for given values of x and μ. For an integer m, we denote the rational function approximation of $c_{BS}(v; x, \mu)$ with degree m by $c_{RA}^m(v; x, \mu)$:

$$c_{BS}(v; x, \mu) \approx c_{RA}^m(v; x, \mu) = \frac{\sum_{j=0}^m a_j^{x,\mu} v^j}{\sum_{j=0}^m b_j^{x,\mu} v^j}. \tag{2.2.1}$$

To obtain the parameters $a_j^{x,\mu}$ and $b_j^{x,\mu}$, for given x and μ, we use a rational Chebyshev approximation (see Section 1.4.1 for a summary).

Next, assuming that the roots of the denominator in Equation (2.2.1) are distinct, we use a partial fraction decomposition to rewrite the right-hand side of Equation (2.2.1) as follows:

$$c_{RA}^m(v; x, \mu) = A_0^{x,\mu} + \sum_{j=1}^m \frac{A_j^{x,\mu}}{v - B_j^{x,\mu}}. \tag{2.2.2}$$

In the remainder of this chapter it is assumed that the roots of the denominator in Equation (2.2.1) are distinct. The parameters $A_j^{x,\mu}$ and $B_j^{x,\mu}$ will usually be complex numbers. If $Re(B_j) < 0$, which will typically be the case (see also the remark below), we may rewrite any of the denominators $(v - B_j^{x,\mu})^{-1}$ in integral form as

$$\frac{1}{v - B_j^{x,\mu}} = \int_0^\infty \mathrm{e}^{-(v - B_j^{x,\mu})y} dy.$$

Interchanging sum and integration yields the following:

$$c_{RA}^{m}(v;x,\mu) = A_0^{x,\mu} + \int_0^{\infty} \left(\sum_{j=1}^{m} A_j^{x,\mu} \mathrm{e}^{B_j^{x,\mu} y} \right) \mathrm{e}^{-vy} dy. \tag{2.2.3}$$

To approximate the integral in Equation (2.2.3) efficiently, we truncate the integral and use a Gaussian quadrature:

$$\int_0^{\infty} f(x)dx \approx \int_c^d f(x)dx \approx \sum_{k=1}^{L} w_k f(x_k), \tag{2.2.4}$$

where $0 \leq c < d < \infty$, w_k are the quadrature weights, x_k the abscissas and f denotes the integrand in (2.2.3). We compared a number of different Gaussian quadrature methods and found that Gauss-Legendre performs particularly well; it results in small errors for all parameter values and models considered here. Abscissas and weights are calculated by the standard procedure (see Press *et al.* [113] for details) and do not depend on the integrand f in the case of Gauss-Legendre quadrature. We thus obtain the following approximation:

$$c_{RA}^{m}(v;x,\mu) \approx A_0^{x,\mu} + \sum_{k=1}^{L} \left(w_k \sum_{j=1}^{m} A_j^{x,\mu} \mathrm{e}^{B_j^{x,\mu} x_k} \right) \mathrm{e}^{-v x_k}, \quad \text{if } \; Re(B_j^{x,\mu}) < 0 \quad \forall j. \tag{2.2.5}$$

To summarise, given constant values for x and μ, $\mathbb{E}^{\mathbb{Q}}[c_{BS}(\sigma^2 Z_T; x, \mu)]$ can be approximated by a rational function of the form

$$\mathbb{E}^{\mathbb{Q}}[c_{BS}(\sigma^2 Z_T; x, \mu)] \approx A_0^{x,\mu} + \sum_{k=1}^{L} \left(w_k \sum_{j=1}^{m} A_j^{x,\mu} \mathrm{e}^{B_j^{x,\mu} x_k} \right) \mathbb{E}^{\mathbb{Q}} \left[\mathrm{e}^{-\sigma^2 Z_T x_k} \right], \tag{2.2.6}$$

if $Re(B_j^{x,\mu}) < 0$ for all j, where $A_j^{x,\mu}$ and $B_j^{x,\mu}$ are the parameters of a rational function approximation with degree m (after applying a partial fraction decomposition), all depending on x and μ.

Proof of Equation (2.2.6)**.** If $Re(B_j^{x,\mu}) < 0$ for all j, it follows from Equation (2.2.1) and Equation (2.2.5) that the following approximation is valid:

$$c_{BS}(v;x,\mu) \approx A_0^{x,\mu} + \sum_{k=1}^{L} \left(w_k \sum_{j=1}^{m} A_j^{x,\mu} \mathrm{e}^{B_j^{x,\mu} x_k} \right) \mathrm{e}^{-v x_k}.$$

Substituting $v = \sigma^2 Z_T$ and taking expectations on both sides yields the following expression:

$$\begin{aligned}\mathbb{E}^{\mathbb{Q}}\left[c_{BS}(\sigma^2 Z_T; x,\mu)\right] &\approx \mathbb{E}^{\mathbb{Q}}\left[A_0^{x,\mu} + \sum_{k=1}^{L}\left(w_k \sum_{j=1}^{m} A_j^{x,\mu} \mathrm{e}^{B_j^{x,\mu} x_k}\right)\mathrm{e}^{-\sigma^2 Z_T x_k}\right] \\ &= A_0^{x,\mu} + \sum_{k=1}^{L}\left(w_k \sum_{j=1}^{m} A_j^{x,\mu} \mathrm{e}^{B_j^{x,\mu} x_k}\right)\mathbb{E}^{\mathbb{Q}}\left[\mathrm{e}^{-\sigma^2 Z_T x_k}\right].\end{aligned}$$

□

Combining Equation (2.2.6) with Proposition 2.1.1 leads to an explicit approximation of the call option prices in the time-changed model in terms of the Laplace transform of the stochastic clock Z_T.

Remark. Typically, the values $B_j^{x,\mu}$ in the rational approximation have negative real part, but sometimes a coefficient $B_j^{x,\mu}$ has non-negative real part. If this is the case, the easiest way to proceed is to increase the order of the rational function approximation. In the cases where switching to a higher order approximation does not resolve the problem, one can deal with the approximation of terms for which $Re(B_j^{x,\mu}) \geq 0$ separately. For those terms, we define a new variable $v^* = \mathrm{e}^{-v}$ and approximate the resulting function by a Chebyshev approximation of order n to get

$$\begin{aligned}\mathbb{E}\left[\frac{A_j^{x,\mu}}{v - B_j^{x,\mu}}\right] &= \mathbb{E}\left[\frac{-A_j^{x,\mu}}{\log(v^*) + B_j^{x,\mu}}\right] \approx \mathbb{E}\left[\sum_{i=0}^{n} c_i^{x,\mu}(v^*)^i\right] \\ &= \mathbb{E}\left[\sum_{i=0}^{n} c_i^{x,\mu}\mathrm{e}^{-iv}\right] = \sum_{i=0}^{n} c_i^{x,\mu}\mathbb{E}\left[\mathrm{e}^{-iv}\right]\end{aligned} \tag{2.2.7}$$

(for a review of Chebyshev approximations see Section 1.4.1). Note that if more terms with $Re(B_j^{x,\mu}) \geq 0$ occur, only a single Chebyshev approximation is needed for all these terms simultaneously. Thus, in Equation (2.2.6) the terms in the sum corresponding to $B_j^{x,\mu}$ with non-negative real part should be replaced by an approximation of the form given in Equation (2.2.7).

Remark. In the case of the Heston model with correlation, a similar conditioning approach would lead to a family of functions of two variables that needs to be approximated. This follows since $\log(S_t/S_0)$ is normal when conditioning on V_t and $\int_0^t V_s ds$ (which can be found in Glasserman & Kim [67] or Broadie & Kaya [32]). For given values μ and x, one would therefore approximate a two-dimensional function, which can then be rewritten in terms of negative exponential moments of the clock. However, a detailed analysis of this case is left for future research, where one should investigate faster and more powerful two-dimensional approximation methods.

2.2.1 Example: variance-gamma model

This example illustrates how to price a vanilla call option in the VG model with the following parameters (taken from the original paper by Madan *et al.* [98])

$$\sigma = 0.1213, \qquad \nu = 0.1686 \qquad \text{and} \qquad \theta = -0.1436.$$

It follows that the time-change (Z_t) is now given by a gamma process independent of (W_t) with marginal distribution at time t given by a gamma distribution $G(\frac{t}{\nu}, \nu)$ with shape parameter $\frac{t}{\nu}$ and scale parameter ν (see Section 1.2.4 for more details). We assume that $S_0 = 1$, $K = 1.1$, $r = 0.03$, $q = 0.01$ and $T = 1$, so that we are pricing an out of the money call option with one-year maturity. It then follows from Equation (2.1.9) that μ_{TC} and x_{TC} take the following rounded values:

$$\mu_{TC} = -9.2596, \qquad x_{TC} = 0.0594.$$

A rational approximation of $c_{BS}(v; x, \mu)$ with degree $m = 5$ is then given as follows:

$$\begin{aligned} c^5_{RA}(v; x_{TC}, \mu_{TC}) &= -0.0041 - \frac{0.0009 + 0.0021\mathtt{i}}{v + (0.0387 - 0.0667\mathtt{i})} - \frac{0.0009 - 0.0021\mathtt{i}}{v + (0.0387 + 0.0667\mathtt{i})} \\ &+ \frac{0.0034}{v + 0.0356} + \frac{8.0 \times 10^{-5}}{v + 0.0098} + \frac{2.5 \times 10^{-5}}{v + 0.0014}, \end{aligned}$$

for $v \in [0.0027, 0.0405]$ after applying the partial fraction decomposition (it should be noted that we rounded these values only to present them here, but use more accurate values to derive the results stated below). Then, if we denote each ratio by $\frac{A_j}{v - B_j}$, using the Equation (2.2.3), the above can be rewritten as

$$c^5_{RA}(v; x_{TC}, \mu_{TC}) = A_0 + \int_0^\infty \left(A_1 \mathrm{e}^{B_1 y} + A_2 \mathrm{e}^{B_2 y} + A_3 \mathrm{e}^{B_3 y} + A_4 \mathrm{e}^{B_4 y} + A_5 \mathrm{e}^{B_5 y}\right) \mathrm{e}^{-yv} dy,$$

where all five B_js have negative real part.

In Figure 2.1, the difference of $c_{BS}(v; 0.0594, -9.2596)$ and $c^5_{RA}(v; 0.0594, -9.2596)$ is plotted for $v \in [0.0027, 0.0405]$. The maximum error for this example is 2.39×10^{-8}. Finally we use Gaussian quadrature to approximate the infinite integral (with $L = 500$, $c = 0$ and $d = 7000$). Employing Proposition 2.1.1 and Equation (2.2.6) to calculate the

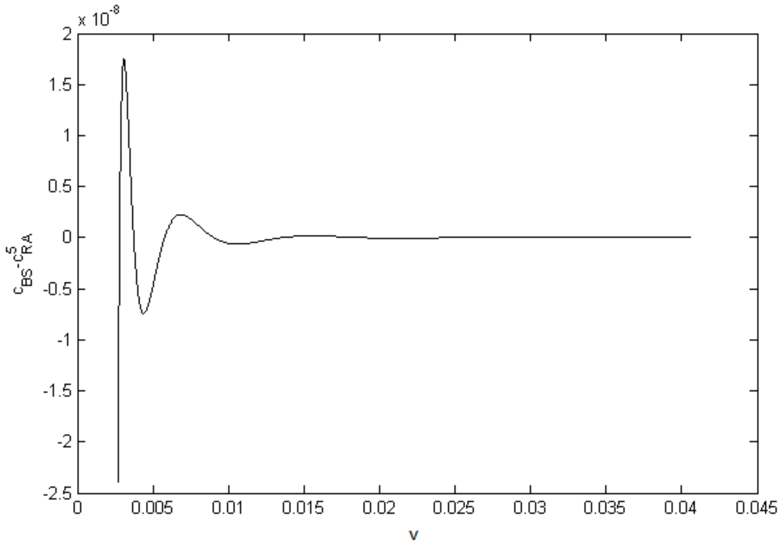

Figure 2.1: Difference between the normalised Black-Scholes formula, $c_{BS}(v; 0.0594, -9.2596)$, and the corresponding rational approximation with degree 5, $c^5_{RA}(v; 0.0594, -9.2596)$, for $v \in [0.0027, 0.0405]$ in the VG model with $\sigma = 0.1213$, $\nu = 0.1686$ and $\theta = -0.1436$ (Madan *et al.* [98]) and $S_0 = 1$, $K = 1.1$, $r = 0.03$, $q = 0.01$ and $T = 1$.

option price therefore yields $C_{TC} = 0.021403241$. Comparing this value to the option price computed using the FFT method (0.021403243) gives an error of 2×10^{-9}.

2.2.2 Offline calculation and interpolation

If one is interested in pricing a number of options with different strikes and maturities, some practical improvements that yield substantial gains in computation time can be made. Given the market parameters, and therefore μ_{TC}, one approximates the function $c_{BS}(v; x, \mu_{TC})$ for a number of values of the adjusted log-moneyness x between x^{min}_{TC} and x^{max}_{TC} (30 values of x should usually suffice). To calculate x^{min}_{TC} and x^{max}_{TC}, one only needs the smallest and largest strike and maturity that one is interested in pricing, as all other values of x_{TC} lie between these four corners. One then stores the corresponding approximation parameters $A^{x,\mu}_j$ and $B^{x,\mu}_j$ for each value of x and uses an interpolation method (cubic splining, for example) for values in between. As a consequence, one is able to speed up the method dramatically, since any option price with these market parameters can now be calculated without the need of performing rational approximations. Although the rational Chebyshev approximations can be performed very quickly, it should only be done once for a given set of market parameters.

Obviously, when approximating only a few values of x offline, which are then used for the interpolation, one should make sure that the errors of these approximations are sufficiently small. As illustrated in the next section, for some of the x values, errors are much bigger than for others, due to numerical instability. However, each approximation can be carefully checked by evaluating the resulting errors (see Section 2.3.2), as the computational time for these approximations should not matter as much (given that it is done only once offline). One can therefore search for a rational function approximation that performs well for the given value of x.

Remark. When using this method for fast calibration, one could pre-calculate approximations of $c_{BS}(v; x, \mu)$ for a number of parameter combinations of x and μ. The online calculation of an option price would then involve a two-dimensional interpolation between the values of x and μ calculated offline. This should be particularly feasible for calibrations where parameters are not allowed to vary too much from parameters obtained in the previous calibration, as one then has a well-defined range for μ. Investigation of this idea is left for future research.

2.3 Numerical error estimates

Observe that the error from our method arises from the approximation in Equation (2.2.6) only. This error can be subdivided into: (a) truncation error of v; (b) error in the rational function approximation; and (c) error in the Gaussian quadrature. In attempts to control the error, there will be a trade-off between the different sources of error (a) and (b), that is the size of the truncation interval for v and the quality of the rational approximation for a given degree. Since $c_{BS}(v; x, \mu)$ decays as $v^{1/2}$ for small v, approximating this function accurately for very small values of a requires a high order of the rational approximation. A suitable choice of the truncation limits a and b is therefore required to balance these two different sources of error. In order to balance these errors and to find suitable choices for a and b, we analyse the cumulative distribution function (CDF) of $\sigma^2 Z_T$ in Section 2.3.1. Later, we consider the resulting error of the rational function approximation for the range $[a, b]$ and outside the range $[a, b]$ in Section 2.3.2.

The third source of error is introduced by the numerical integration of the infinite

Case	Model	Parameters	Source	μ_{TC}	x_{TC}^{max}	x_{TC}^{min}
I	VG	$\sigma = 0.1213, \nu = 0.1686, \theta = -0.1436$	Madan *et al.* [98]	-9.2596	0.6099	-0.1436
II	VG	$\sigma = 0.178753, \nu = 0.13317, \theta = -0.30649$	Fiorani [58]	-9.0920	0.9857	-0.1061
III	Heston	$\kappa = 0.87, \delta = 0.07, \xi = 0.34, V_0 = 0.07$	Detlefsen & Härdle [53]*	0	0.2731	-0.1773
IV	Heston	$\kappa = 0.9, \delta = 0.04, \xi = 0.3, V_0 = 0.04$	Andersen [6]*	0	0.2731	-0.1773
V	CGMY	$C = 1, G = 5, M = 10, Y = 0.5$	Madan & Yor [100]	-2.0000	0.7264	-0.1320

Table 2.1: Computation of market-dependent parameter (μ_{TC}), and the maximum and minimum adjusted log-moneyness (x_{TC}^{max} and x_{TC}^{min}) for five sets of parameters found in the literature (*we have set ρ equal to zero in these models, as our framework only considers the zero-correlation Heston model, even though it was not zero in the original papers).

integral in Equation (2.2.3). The numerical integration method should be chosen such that the resulting error is comparable to the other two errors. If necessary, an adaptive quadrature method can be used to control for the error of this numerical integration.

In order to further analyse the error that arises from the method presented here, we have chosen five sets of market parameters from the literature. We consider options with strikes $K = 0.8, 0.81, 0.82, ..., 1.19, 1.2$ and maturities $T = 0.25, 0.5, 1, 1.5, 2, 2.5$ for each of the five parameter sets detailed below, and set $S_0 = 1$, $r = 0.03$ and $q = 0.01$. This leads to a total of 246 options and therefore 246 different values of x_{TC} for each set of market parameters. Table 2.1 summarises the five cases and states the source of each parameter set. Values of μ_{TC}, x_{TC}^{max} and x_{TC}^{min} are also given, where x_{TC}^{max} and x_{TC}^{min} represent the maximum and the minimum of the 246 values of the adjusted log moneyness x_{TC} for each case.

One can see from the table that the values for μ_{TC}, x_{TC}^{max} and x_{TC}^{min} vary substantially between different models and parameters. Note that μ_{TC} and ω are both zero in the case of the zero-correlation Heston model, implying that μ_{TC} and x_{TC} do not depend on the model parameters at all. From here on we refer to these sets of parameters as Case I-V, respectively.

2.3.1 Cumulative distribution functions

To choose appropriate values for a and b, the truncation values of v, we analyse the CDF of Z_T for Cases I - IV of Table 2.1. As stated in Section 1.2.4, Z_T is gamma-distributed

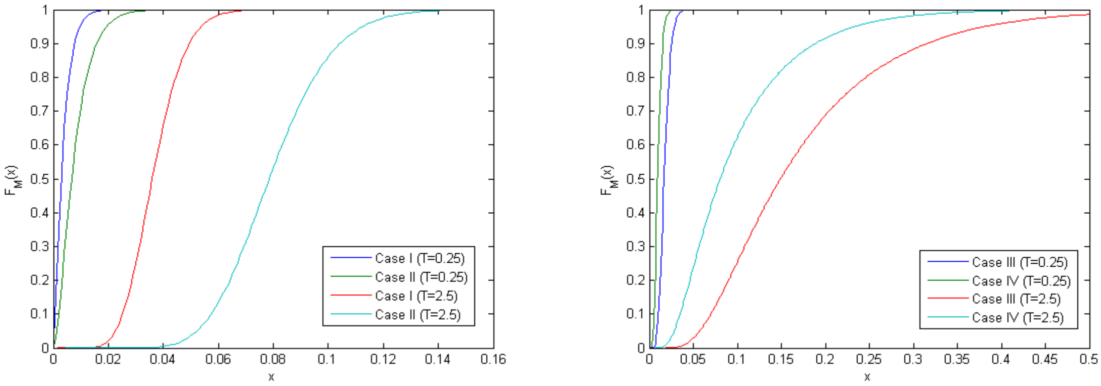

(a) Variance Gamma model (b) Heston model

Figure 2.2: Cumulative distribution function of $\sigma^2 Z_T$, where Z_T is the time-change of (a) the VG model with parameters as in Case I and II, and (b) the Heston model with parameters as in Case III and IV. For all cases we have plotted maturity $T = 0.25$ and $T = 2.5$.

($Z_T \sim G(\frac{T}{\nu}, \nu)$) for Cases I and II. By the scaling property of the gamma distribution, we obtain that $\sigma^2 Z_T \sim G(\frac{T}{\nu}, \sigma^2 \nu)$, with probability density function

$$f_{\sigma^2 Z_T}\left(x, \frac{T}{\nu}, \sigma^2\nu\right) = \frac{x^{\frac{t}{\nu}-1} \mathrm{e}^{-\frac{x\sigma^2}{\nu}}}{(\sigma^2\nu)^{\frac{t}{\nu}} \Gamma(\frac{t}{\nu})}. \tag{2.3.1}$$

Plotting the CDF for Cases I and II with maturity $T = 0.25$ and $T = 2.5$ results in Figure 2.2(a). For the CGMY model and the Heston model, we need to simulate Z_T to estimate its CDF as there are no closed-form expressions. Madan & Yor [100] describe a method to simulate Z_T in the case of the CGMY model. Glasserman & Kim [67] describe a method to simulate Z_T in the case of the Heston model. In particular, given V_0 in the Heston model, one can simulate V_T, the endpoint of the variance process, exactly as shown in Equation (1.2.15). Then, conditional on V_0 and V_T, the distribution of $Z_T = \int_0^T V_s ds$ is given by Theorem 2.1 in Glasserman & Kim [67], and can therefore be simulated easily. We implemented this procedure and estimated the CDF numerically for Cases III and IV. Results are represented in Figure 2.2(b). As can be seen, the ranges of the CDFs vary widely between the different models and different maturities (note that the scales of Figures 2.2(a) and 2.2(b) are not the same).

To ensure that only 0.1% of the mass of $\sigma^2 Z_T$ lies in the regions $[0, a]$ and $[b, \infty]$, we set a and b equal to the 0.1% and 99.9% quantiles of $\sigma^2 Z_T$, that is, we solve for x setting

Case	$a(T=0.25)$	$b(T=0.25)$	$a(T=2.5)$	$b(T=2.5)$
I	2.84×10^{-5}	0.0201	0.0141	0.0735
II	1.48×10^{-4}	0.0382	0.0347	0.1491
III	0.0048	0.0413	0.0286	0.7283
IV	0.0021	0.2600	0.0130	0.4841

Table 2.2: Computation of a and b, that is the 0.1% and 99.9% quantiles of the cumulative distribution function of $\sigma^2 Z_T$, for Case I - IV with maturity $T = 0.25$ and $T = 0.5$.

p equal to 0.001 and 0.999 in the following equation:

$$F^{-1}_{\sigma^2 Z_T}(p) = \inf\{x : F_{\sigma^2 Z_T}(x) \geq p\}. \tag{2.3.2}$$

For the gamma distribution, for example, this inverse is then given by

$$F^{-1}_{\sigma^2 Z_T}\left(p, \frac{T}{\nu}, \sigma^2\nu\right) = \inf\left\{x : F_{\sigma^2 Z_T}\left(x, \frac{T}{\nu}, \sigma^2\nu\right) \geq p\right\}, \tag{2.3.3}$$

where

$$F_{\sigma^2 Z_T}\left(x, \frac{T}{\nu}, \sigma^2\nu\right) = \int_0^x f_{\sigma^2 Z_T}(s)ds = \gamma\left(\frac{T}{\nu}, \frac{x}{\sigma^2\nu}\right),$$

and γ is the upper incomplete gamma function defined as

$$\gamma(a, b) = \Gamma(a)^{-1}\int_0^b t^{a-1}\mathrm{e}^{-t}dt.$$

For the Heston model, we use simulated values of $F_{\sigma^2 Z_T}(x)$ to calculate a and b (and the same could be done for the CGMY model). Results for Cases I - IV are presented in Table 2.2, where we have again chosen maturities $T = 0.25$ and $T = 2.5$ as an example and have calculated a and b for each case separately. These numbers confirm that the region of interest will depend heavily on the model and maturity under consideration.

Clearly, the more that is known about the possible range of $\sigma^2 Z_T$ and the smaller we are able to make the range $[a, b]$, the easier it will be to find an appropriate rational approximation for this range. There are also extreme parameter combinations for which the range of $[a, b]$ is rather large and the method does not perform as well (that is if the time change (Z_t) is too wide). Also, for maturities smaller than $T = 0.25$ we found that the resulting a might be too small for some of the parameter combinations and models, and the rational approximation may result in larger maximum errors. For options with short maturities we refer to the work of Levendorskiĭ [86] and Andersen & Lipton [8].

Case	$\epsilon^{max}_{[0,a]}$	$\epsilon^{max}_{[a,b]}$	$\epsilon^{max}_{[b,\infty]}$
I	1.44×10^{-6}	1.13×10^{-5}	2.84×10^{-6}
II	1.29×10^{-6}	2.70×10^{-5}	6.36×10^{-6}
III	2.73×10^{-10}	5.78×10^{-9}	2.67×10^{-10}
IV	5.93×10^{-8}	5.84×10^{-5}	2.88×10^{-8}

Table 2.3: Computation of maximum errors resulting from the rational function approximation for 246 parameter combinations over the region $[0, a]$, $[a, b]$ and $[b, \infty)$, which are denoted by $\epsilon^{max}_{[0,a]}$, $\epsilon^{max}_{[a,b]}$ and $\epsilon^{max}_{[b,\infty]}$ respectively.

2.3.2 Error from the rational function approximation

The error of most approximations looks similar to the error displayed in Figure 2.1, where we now choose a and b as described in the previous section. Note that the support of the time change in Equation (2.1.8) is over the whole positive real axis. The approximation in Equation (2.2.6) therefore leads to errors over $[0, \infty)$ as well. We subdivide this region into $[0, a]$, $[a, b]$ and $[b, \infty)$, and approximate the error for each region and for each of the five cases of Table 2.1 separately. The errors can be calculated as follows:

$$\begin{aligned}
\epsilon_{[0,a]} &= \int_0^a \left[c_{BS}\left(z; x, \mu\right) - \left(A_0^{x,\mu} + \sum_{i=0}^{n} b_i \mathrm{e}^{-iz} + \sum_{k=1}^{L} \left(w_k \sum_{j=1}^{m} A_j^{x,\mu} \mathrm{e}^{B_j^{x,\mu} x_k} \right) \mathrm{e}^{-x_k z} dy \right) \right] f_{\sigma^2 Z_t}(z) dz, \\
\epsilon_{[a,b]} &= \int_a^b \left[c_{BS}\left(z; x, \mu\right) - \left(A_0^{x,\mu} + \sum_{i=0}^{n} b_i \mathrm{e}^{-iz} + \sum_{k=1}^{L} \left(w_k \sum_{j=1}^{m} A_j^{x,\mu} \mathrm{e}^{B_j^{x,\mu} x_k} \right) \mathrm{e}^{-x_k z} dy \right) \right] f_{\sigma^2 Z_t}(z) dz, \\
\epsilon_{[b,\infty]} &= \int_b^\infty \left[c_{BS}\left(z; x, \mu\right) - \left(A_0^{x,\mu} + \sum_{i=0}^{n} b_i \mathrm{e}^{-iz} + \sum_{k=1}^{L} \left(w_k \sum_{j=1}^{m} A_j^{x,\mu} \mathrm{e}^{B_j^{x,\mu} x_k} \right) \mathrm{e}^{-x_k z} dy \right) \right] f_{\sigma^2 Z_t}(z) dz.
\end{aligned}$$

Computing these errors for each of the 246 options of Cases I - IV separately results in Table 2.3, where we represent the maximum absolute error for each case.

As can be seen, maximum logarithmic errors are of order -5 to -6. Even though these errors are already relatively small, we observed that most of the 246 errors are much smaller than these maximum errors for each case. To illustrate this point, we recalculate the errors shown in Table 2.3, deleting the largest 25 values from each maximum absolute error calculation. The results are given in Table 2.4, where we denoted these errors by ϵ^{max25}.

When pricing options, one could therefore delete x values that result in errors that are too large and interpolate between the x values prices that had smaller errors (*cf.* discussion

Case	$\epsilon_{[0,a]}^{max25}$	$\epsilon_{[a,b]}^{max25}$	$\epsilon_{[b,\infty]}^{max25}$
I	2.62×10^{-7}	3.70×10^{-6}	8.23×10^{-7}
II	9.32×10^{-7}	8.97×10^{-6}	3.39×10^{-6}
III	4.96×10^{-11}	9.56×10^{-10}	1.08×10^{-11}
IV	6.91×10^{-11}	3.67×10^{-10}	2.87×10^{-11}

Table 2.4: Computation of maximum errors resulting from the rational function approximation for 246 parameter combinations over the region $[0, a]$, $[a, b]$ and $[b, \infty)$ after deleting the 25 largest errors for each calculation, which are denoted by $\epsilon_{[0,a]}^{max25}$, $\epsilon_{[a,b]}^{max25}$ and $\epsilon_{[b,\infty]}^{max25}$ respectively.

in Section 2.2.2). From Table 2.4 we see that, especially for Cases III and IV (the Heston model), the deletion of values with large errors and consequent interpolating should yield a great improvement. We will detail this procedure further in the next section and give error estimates in Section 2.5.

2.4 Implied volatility

The Black-Scholes formula is often used to express option quotes in terms of the *implied volatility*: Given the option price and all parameters except σ in the Black-Scholes formula (2.1.5), one searches for the value of σ that solves the equation. This value of σ is referred to as implied volatility and we denote it by σ_{IV}. Since there is no closed-form formula for σ_{IV}, it is usually solved for by using a solver method, which is typically rather slow. To speed up the calculation Manaster & Kohler [101] developed a technique that provides a starting value and guarantees convergence. More recent methods, such as the methods developed by Brenner & Subrahmanyam [29], Corrado & Miller [46] and especially Jäckel [76], are faster and more accurate. Adopting the method described in this section, we seek an approximation of the inverse function by a rational function approximation, and therefore present another fast and accurate alternative to the standard solver methods.

We restate the normalisation of the Black-Scholes formula (2.1.6) with a slightly modified parametrisation:

$$c_{IV}(v, x) = c_{BS}(v^2, x, 0) = \mathcal{N}\left(\frac{x}{v} + \frac{v}{2}\right) - \mathrm{e}^{-x}\mathcal{N}\left(\frac{x}{v} - \frac{v}{2}\right). \tag{2.4.1}$$

Any call option price can then be written in terms of this normalised formula as follows:

$$C_{BS}(S_0, K, T, \sigma, r, q) = S_0 \mathrm{e}^{-qT} c_{IV}\left(\sigma\sqrt{T}, \log\left(\frac{S_0 \mathrm{e}^{(r-q)T}}{K}\right)\right). \tag{2.4.2}$$

Since the normalised Black-Scholes formula c_{IV} is a function of only two variables, finding a suitable rational approximation for any parameter combination becomes easier. Note that the question of finding σ_{IV} reduces to finding v_{IV} in Equation (2.4.1), where it follows from (2.4.2) that

$$\begin{aligned} c_{IV} &= \frac{C_{BS}(S_0, K, T, \sigma, r, q)}{S_0 \mathrm{e}^{-qT}}, \\ x &= \log\left(\frac{S_0 \mathrm{e}^{(r-q)T}}{K}\right), \end{aligned}$$

which are both given constants when searching for the implied volatility. We therefore need to solve for the value of v that solves Equation (2.4.1) for known values $c_{IV}(v, x) = c$ and x. Once we obtain v_{IV}, σ_{IV} is determined by $\sigma_{IV} = v_{IV}/\sqrt{T}$. It should also be noted that one can restrict, without loss of generality, to the case of call options, as the case of put options follows on account of the put-call parity as in Section 2.1. A re-parametrised version of the put-call parity can be stated as follows (see the proof of Corollary 2.1.1 for more details):

$$c_{IV}(v, -x) = \mathrm{e}^x c_{IV}(v, x) + 1 - \mathrm{e}^x, \qquad x \in \mathbb{R}, v \in \mathbb{R}_+,$$

so that the following relation holds for the implied volatility:

$$v_{IV}(c, x) = v_{IV}(\mathrm{e}^x c + 1 - \mathrm{e}^x, -x).$$

As a consequence, one can concentrate on the negative half-line $x \in \mathbb{R}^-$. All results presented in this section so far can be found in a recent article by Li [90], who concentrates on approximating the two-dimensional Black-Scholes implied volatility formula v_{IV} by a single two-dimensional rational approximation[1]. Li approximates the inverse of Equation (2.4.1) for $-0.5 \leq x \leq 0$ and $c_{LB}(x) \leq c \leq c_{UB}(x)$ where

$$\begin{aligned} c_{LB}(x) &= \frac{-0.00424532412773x + 0.00099075112125x^2}{1 + 0.26674393279214x + 0.03360553011959x^2}, \\ c_{UB}(x) &= \frac{0.38292495908775 + 0.31382372544666x + 0.07116503261172x^2}{1 + 0.01380361926221x + 0.11791124749938x^2}. \end{aligned}$$

[1]Note that it is also possible to build a lookup table for the entire two-dimensional function once and interpolate between values in the table for the purpose of option pricing. However, we find that the approximation approach presented here, is more efficient and accurate.

This means that bounds are widest for $x = 0$ and become narrower as x decreases to -0.5. These bounds are well chosen by Li, as it becomes more and more difficult to approximate the function well for small values of x. Still, it should be noted that the range is rather wide.

Note that the inverse is a function of two variables (c,x). Li therefore uses a two-parameter rational approximation of the form

$$v_{IV}(c,x) \approx v_{RA}^{Li}(c,x) = p_1 x + p_2\sqrt{c} + p_3 c + \frac{\sum_{1\le i+j\le 4} n_{i,j} x^i \sqrt{c}^j}{1 + \sum_{1\le i+j\le 4} m_{i,j} x^i \sqrt{c}^j},$$

and obtains the approximation parameters using the downhill simplex search method. Without further adjustments (like a Newton-Raphson polishing), Li states a maximum error of 3.3×10^{-3} for v_{IV} over this region. It should be noted that the error is of similar magnitude for many parameter combinations and that one still needs to divide by $\sqrt{T}$ to obtain σ_{IV} (making the error even bigger for short maturities). It should also be stressed that the approximation of Li applies to all combinations of c and x (within the bounds) and a total of 31 parameters is sufficient for any calculation. Having worked with the downhill simplex search method ourselves, we note that this is a remarkable result and that it should be used wherever this error bound is acceptable.

Rather than the ambitious attempt to approximate the whole function with one set of parameters, we repeat the approximation for 105 values of x given by $x = 0, -0.0025, -0.005, -0.0075, ..., -0.02$ and $x = -0.025, -0.03, -0.035, ..., -0.5$. For each of these x values we use a rational function approximation of the following form:

$$v_{IV}(c,x) \approx v_{RA}^{p}(c,x) = \frac{\sum_{i=0}^{p} n_i^x \sqrt{c}^i}{\sum_{i=0}^{p} m_i^x \sqrt{c}^i},$$

where p varies between 7 and 9 for different values of x[2]. The approximation parameters n_i^x and m_i^x, where these all depend on x, can be obtained again using the rational Chebyshev approximation (discussed in Section 1.4.1). However, we found that here it is

[2]For some values of x, the approximation is harder and we choose degree 9 for those. To approximate the function, we solved for v_{IV} using the Newton-Raphson method. For other values, degree 7 is sufficient to obtain the desired error bound. Note that rational approximations of degree 9 can still be performed easily with double precision. One can improve all the approximations performed in this section by switching to higher order rational approximations, although, high precision arithmetic would become necessary for degrees of 13 and higher.

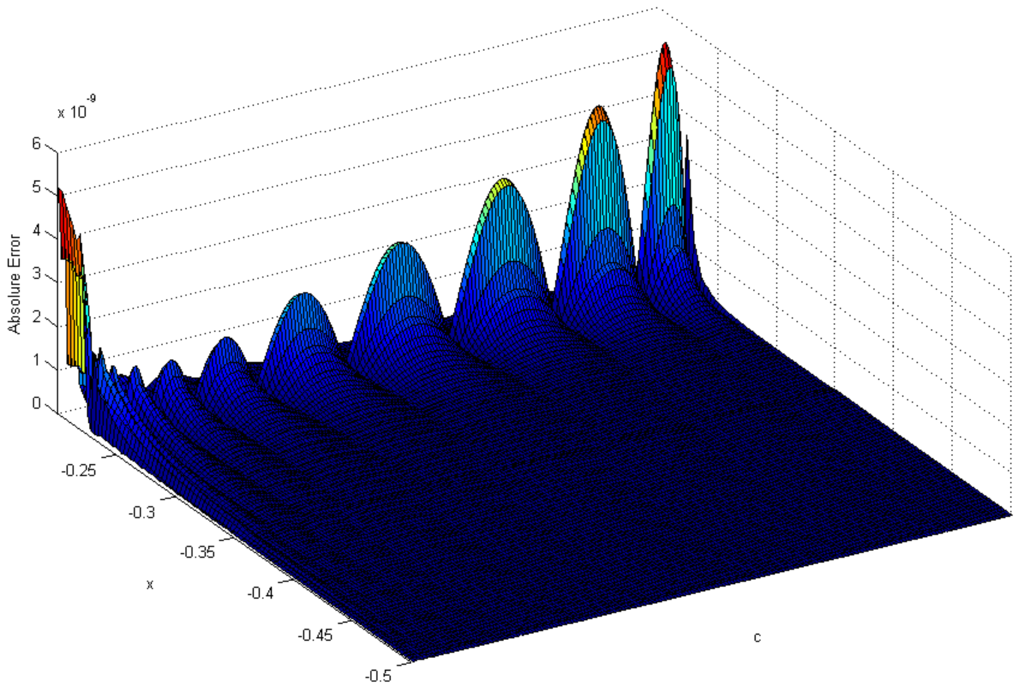

Figure 2.3: Error in the normalised Black-Scholes implied volatility, v_{imp}, for $x \in [-0.5; -0.2]$ and $c_{LB}(x) \leq c \leq c_{UB}(x)$ using rational function approximations.

advantageous to use the iterative algorithm discussed in Section 5.13 of Press *et al.* [113], using a maximum of six iterations to get closer to the so-called ideal 'minimax' solution. Once the approximation has been performed for each value of x, approximation parameters are stored to the computer and do not need to be recalculated, as detailed in Section 2.2.2. Note that these approximations neither depend on the model nor on the market parameters and can therefore be used for any option. To calculate v_{IV} for any value $-0.5 \leq x \leq 0$, one only needs to interpolate between the previously calculated values (using linear interpolation or a cubic spline, for example). We observe that the maximum absolute error for $-0.5 \leq x \leq -0.0075$ is 8.55×10^{-7}, whereas the maximum absolute error for $-0.0075 < x \leq 0$ is 5.54×10^{-5}. For most of the input values, the absolute error is even smaller than 1×10^{-8} and we plot the error for $x \in [-0.5; -0.2]$ in Figure 2.3. It is clear that the algorithm used is able to spread the error almost evenly for any of the x values and that all errors are rather small.

We would like to stress that this method, like the method presented by Li, does not require any approximation when calculating the implied volatility online. All approximations are done once and are stored to the hard-drive. The parameters one needs to store are all real and the calculation could easily be performed in Microsoft Excel, for example, without further adjustments. Evaluating the implied volatility for any model and any set of parameters (within the bounds) can then be carried out extremely quickly via interpolation. The region that is well approximated by this method is wide and applies to most parameter combinations and options. The region where this method struggles is the region where most methods do: options very close to maturity with only a few hours or days remaining. In these cases, asymptotic methods are appropriate (see *e.g.* Gao & Lee [61]). If some of the options being priced do not fall within the defined bounds (the bound on x should hardly ever be an issue, but the bounds on c might be), there is no harm in using your favourite solver method for these few cases. For all other cases, the method presented here should yield a great improvement of computational efficiency and is easy to implement.

2.5 Numerical results: case studies

This section comprises the numerical results of the rational approximation method. Section 2.5.1 compares numerical results for option prices of the developed rational approximation method to those obtained by employing the standard FFT method. Section 2.5.2 compares the speeds of both methods, and Section 2.5.3 contains a comparison of accuracy and speed for the implied volatility calculations.

2.5.1 Comparision of option prices to the FFT

As discussed in Section 1.3, other methods have been developed to evaluate options numerically when the asset dynamics are assumed to be different than in the Black-Scholes setting. Monte Carlo methods and finite difference schemes are two widely used examples. In the case of asset dynamics following Equations (2.1.1) - (2.1.2), the standard methodology to evaluate vanilla options is to use Fourier-based option pricing methods (see Section 1.3.2). We compare the rational approximation approach presented here to the standard FFT method developed by Carr & Madan [40] since this method is well-known and widely used in practice. Note that several more efficient methods have been proposed in the literature and that the choice of parameters of the numerical scheme proposed by Carr and Madan does not hold in general (we refer the reader to Boyarchenko & Levendorskiĭ [26], to Levendorskiĭ [88] especially for the case of the Heston model, and to De Innocentis [51] for the Variance Gamma model). Note that for the FFT method, one usually requires the characteristic function of the log of the stock price at time t (where the stock price at time t is assumed to be as in Equation (2.1.1)), which is

$$\mathbb{E}[\mathrm{e}^{\mathtt{i}z\log(S_t)}] = \mathrm{e}^{\mathtt{i}z(\log(S_0)+(r-q-\phi(-\mathtt{i}))t)}\mathbb{E}^{\mathbb{Q}}[\mathrm{e}^{\mathtt{i}zX_t}]. \tag{2.5.1}$$

As can be seen, one therefore requires the Fourier transform of (X_t) as defined in Equation (1.2.1) rather than the Laplace transform of (Z_t). The general formula to obtain the resulting characteristic function $\Phi_{X_t}(z)$ for (X_t) from that of (Z_t) is

$$\begin{aligned} \mathbb{E}^{\mathbb{Q}}[\mathrm{e}^{\mathtt{i}zX_t}] &= \mathbb{E}^{\mathbb{Q}}[\mathrm{e}^{\mathtt{i}z(\sigma W_{Z_t}+\theta Z_t)}] \qquad (2.5.2)\\ &= \mathbb{E}^{\mathbb{Q}}[\mathrm{e}^{(\mathtt{i}z\theta-\frac{z^2\sigma^2}{2})Z_t}], \quad z\in\mathbb{R}, \end{aligned}$$

for all three models discussed above. From this it follows that, for example, the characteristic function of (X_t) in the VG model is equal to

$$\mathbb{E}^{\mathbb{Q}}[\mathrm{e}^{\mathtt{i}zX_t}] = (1-\nu z\mathtt{i}\theta+\sigma^2\nu z^2/2)^{-\frac{t}{\nu}}. \tag{2.5.3}$$

We next compare prices of vanilla call options computed from both methods for the three models discussed in Section 1.2.2. For each of the models, we select one set of market parameters from Table 2.1 and compare plain vanilla call option prices for strikes $K\in[0.8,1.2]$ and maturities $T\in[0.25,2.5]$. Tables 2.5 - 2.7 give absolute errors between the option price obtained by the FFT method and the rational approximation method. In particular, Table 2.5 represents errors for Case I, Table 2.6 represents errors for Case V and Table 2.7 represents errors for Case III. In these three tables, we set $S_0=1$, $r=0.03$ and $q=0.01$. As can be seen, maximum errors in Table 2.5, 2.6 and 2.7 are 1.61×10^{-5}, 1.14×10^{-6} and 8.59×10^{-8}, respectively.

For all three tables, we pre-calculated 30 values of x_{TC} equally spaced between x_{TC}^{max} and x_{TC}^{min} such that strikes $K\in[0.8,1.2]$ and maturities $T\in[0.25,2.5]$ are included. We iterate over ten different values for a and b, and calculate errors for each of the ten cases, rather than calculating the value for a and b with the help of the CDF, as this procedure is much quicker. We take those values of a and b that lead to errors smaller than 1×10^{-6} and delete x values for which no such combination can be found. In Equation (2.2.7), n

was set to 7. The rational Chebyshev approximation in Equation (2.2.1) starts with degree 6 and increases to degree 8 to avoid positive roots, and the Gauss-Legendre quadrature in Equation (2.2.4) was performed with 500 points, where $c = 0$ and $d = 7000$.

Remark. Note that these degrees (that is rational approximations with degree 6 and 8) can be performed with double precision. If one is interested in improving on the error bounds given here, it might be worth investigating how switching to higher order rational approximations, which will require high precision arithmetics, influences the errors. This could be particularly relevant for the few approximations performed offline, for which computational effort is not the main concern. We leave a detailed comparison of different Gaussian quadrature methods for further research.

2.5.2 Comparison of speed

The relative computational speeds of the FFT method (with 2048 points) and of the rational function method depend on the number of strikes and the number of maturities that are considered. In the FFT method, all strikes can be computed in one go, given that they have the same maturity. The rational function approximation, on the other hand, approximates the normalised Black-Scholes formula (2.1.6) for a given strike, which can then be used for any maturity. Therefore, pricing relatively few strikes and relatively many maturities should be advantageous for the rational approximation method and vice versa. Table 2.8 gives approximate computational times for the two different methods, for different numbers of strikes and maturities. The first row resembles the example of Table 2.5, where we can see that the rational function approximation clearly outperforms the FFT method. As can also be seen, the rational function approximation is about five to ten times faster than the FFT method, depending on the number of strikes and maturities that need to be priced. The computational times given here were measured by Matlab (version R2009b) on a Lenovo ThinkPad R60 (1.8 GHZ, 2GB RAM) and are given in seconds.

2.5.3 Numerical results for implied volatility

We use our method presented in Section 2.4 to determine the volatility surface of the CGMY model for $T \in [0.1, 1.0]$ (steps of 0.01) and $K \in [0.7, 1.3]$ (steps of 0.01) with $C = 1$, $G = 5$, $M = 10$ and $Y = 0.5$ (these parameters are taken from Madan & Yor [100]).

K	T = 0.25	T = 0.5	T = 1	T = 1.5	T = 2	T = 2.5
0.80	3.89E-06	1.02E-07	9.25E-06	3.60E-06	6.82E-06	8.25E-06
0.81	3.46E-06	3.06E-08	9.54E-06	5.13E-06	4.26E-06	8.35E-06
0.82	1.04E-06	4.47E-08	5.27E-06	6.65E-06	1.99E-06	8.90E-06
0.83	6.84E-07	1.80E-07	3.78E-07	6.89E-06	1.11E-06	9.57E-06
0.84	6.39E-07	2.81E-07	1.28E-06	5.58E-06	1.88E-06	1.01E-05
0.85	3.98E-07	1.50E-07	5.89E-07	2.80E-06	3.17E-06	1.03E-05
0.86	1.65E-06	3.58E-07	2.46E-07	5.73E-07	3.75E-06	1.02E-05
0.87	2.17E-06	3.92E-07	3.03E-07	2.90E-06	3.23E-06	9.60E-06
0.88	7.26E-07	8.94E-08	2.93E-09	2.86E-06	2.16E-06	8.62E-06
0.89	1.13E-06	1.84E-07	5.28E-08	1.27E-06	9.45E-07	7.26E-06
0.90	4.48E-07	3.90E-07	4.83E-08	1.70E-07	3.16E-07	5.73E-06
0.91	3.54E-06	4.24E-07	1.03E-07	4.26E-07	1.88E-06	4.24E-06
0.92	4.12E-06	3.28E-07	9.98E-08	1.27E-07	4.12E-06	3.09E-06
0.93	1.65E-06	6.39E-08	7.38E-08	1.70E-07	6.21E-06	2.81E-06
0.94	4.24E-07	9.95E-08	1.89E-08	1.88E-07	6.89E-06	3.24E-06
0.95	3.07E-07	1.14E-07	5.36E-10	1.11E-08	5.42E-06	3.75E-06
0.96	7.42E-07	1.11E-07	7.96E-08	3.95E-08	2.58E-06	4.01E-06
0.97	4.44E-07	8.60E-08	1.25E-07	5.21E-08	2.61E-08	3.73E-06
0.98	1.54E-06	3.07E-07	6.27E-08	6.28E-08	7.55E-07	2.61E-06
0.99	2.87E-06	4.47E-07	1.73E-07	2.01E-07	4.55E-07	7.06E-07
1.00	2.06E-06	6.61E-08	3.40E-08	1.42E-07	4.76E-08	1.59E-06
1.01	2.35E-06	1.05E-06	1.01E-07	1.41E-07	3.10E-07	3.57E-06
1.02	4.92E-06	2.06E-06	1.12E-07	1.41E-07	1.77E-07	4.15E-06
1.03	8.92E-06	9.71E-07	1.16E-08	4.51E-10	2.02E-08	2.98E-06
1.04	1.61E-05	2.41E-07	1.77E-07	9.86E-08	1.85E-08	1.21E-06
1.05	4.25E-07	9.88E-07	2.58E-08	1.10E-07	5.21E-09	1.63E-07
1.06	1.98E-06	7.80E-07	1.16E-07	5.74E-08	2.82E-08	6.32E-07
1.07	3.00E-06	3.22E-08	1.09E-07	1.31E-07	1.40E-07	3.75E-07
1.08	2.18E-06	3.68E-07	1.19E-08	3.58E-08	1.12E-07	5.33E-08
1.09	2.63E-06	8.86E-07	1.28E-07	3.46E-08	9.61E-08	1.21E-07
1.10	1.95E-06	3.44E-07	1.33E-08	7.36E-08	1.11E-07	5.65E-08
1.11	2.70E-06	1.49E-06	4.10E-08	1.82E-09	2.33E-08	1.63E-09
1.12	2.05E-06	7.31E-07	5.48E-08	5.10E-08	1.95E-08	7.60E-08
1.13	9.87E-07	1.14E-07	3.67E-09	4.54E-08	6.25E-08	7.01E-08
1.14	5.68E-08	6.47E-07	3.83E-08	1.07E-10	3.08E-08	8.57E-10
1.15	1.01E-06	3.59E-07	7.05E-09	3.31E-08	4.20E-08	2.93E-08
1.16	1.27E-06	6.50E-08	2.64E-08	1.38E-08	4.78E-08	7.66E-08
1.17	1.03E-06	9.28E-08	8.06E-09	2.44E-09	4.45E-09	7.42E-08
1.18	9.50E-08	7.57E-08	3.20E-08	1.53E-08	5.20E-09	7.77E-08
1.19	1.10E-06	1.07E-07	6.20E-08	8.27E-09	1.35E-08	6.56E-08
1.20	2.17E-07	6.09E-09	3.24E-09	9.02E-09	1.73E-09	1.86E-08

Table 2.5: Absolute errors between FFT method and rational function method for call options in the VG model with parameters $\sigma = 0.1213$, $\nu = 0.1686$ and $\theta = -0.1436$ (Case I of Table 2.1) for varying strikes and maturities ($S_0 = 1$, $r = 0.03$, $q = 0.01$).

K	T = 0.25	T = 0.5	T = 1	T = 1.5	T = 2	T = 2.5
0.80	3.89E-06	1.02E-07	9.25E-06	3.60E-06	6.82E-06	8.25E-06
0.81	3.46E-06	3.06E-08	9.54E-06	5.13E-06	4.26E-06	8.35E-06
0.82	1.04E-06	4.47E-08	5.27E-06	6.65E-06	1.99E-06	8.90E-06
0.83	6.84E-07	1.80E-07	3.78E-07	6.89E-06	1.11E-06	9.57E-06
0.84	6.39E-07	2.81E-07	1.28E-06	5.58E-06	1.88E-06	1.01E-05
0.85	3.98E-07	1.50E-07	5.89E-07	2.80E-06	3.17E-06	1.03E-05
0.86	1.65E-06	3.58E-07	2.46E-07	5.73E-07	3.75E-06	1.02E-05
0.87	2.17E-06	3.92E-07	3.03E-07	2.90E-06	3.23E-06	9.60E-06
0.88	7.26E-07	8.94E-08	2.93E-09	2.86E-06	2.16E-06	8.62E-06
0.89	1.13E-06	1.84E-07	5.28E-08	1.27E-06	9.45E-07	7.26E-06
0.90	4.48E-07	3.90E-07	4.83E-08	1.70E-07	3.16E-07	5.73E-06
0.91	3.54E-06	4.24E-07	1.03E-07	4.26E-07	1.88E-06	4.24E-06
0.92	4.12E-06	3.28E-07	9.98E-08	1.27E-07	4.12E-06	3.09E-06
0.93	1.65E-06	6.39E-08	7.38E-08	1.70E-07	6.21E-06	2.81E-06
0.94	4.24E-07	9.95E-08	1.89E-08	1.88E-07	6.89E-06	3.24E-06
0.95	3.07E-07	1.14E-07	5.36E-10	1.11E-08	5.42E-06	3.75E-06
0.96	7.42E-07	1.11E-07	7.96E-08	3.95E-08	2.58E-06	4.01E-06
0.97	4.44E-07	8.60E-08	1.25E-07	5.21E-08	2.61E-08	3.73E-06
0.98	1.54E-06	3.07E-07	6.27E-08	6.28E-08	7.55E-07	2.61E-06
0.99	2.87E-06	4.47E-07	1.73E-07	2.01E-07	4.55E-07	7.06E-07
1.00	2.06E-06	6.61E-08	3.40E-08	1.42E-07	4.76E-08	1.59E-06
1.01	2.35E-06	1.05E-06	1.01E-07	1.41E-07	3.10E-07	3.57E-06
1.02	4.92E-06	2.06E-06	1.12E-07	1.41E-07	1.77E-07	4.15E-06
1.03	8.92E-06	9.71E-07	1.16E-08	4.51E-10	2.02E-08	2.98E-06
1.04	1.61E-05	2.41E-07	1.77E-07	9.86E-08	1.85E-08	1.21E-06
1.05	4.25E-07	9.88E-07	2.58E-08	1.10E-07	5.21E-09	1.63E-07
1.06	1.98E-06	7.80E-07	1.16E-07	5.74E-08	2.82E-08	6.32E-07
1.07	3.00E-06	3.22E-08	1.09E-07	1.31E-07	1.40E-07	3.75E-07
1.08	2.18E-06	3.68E-07	1.19E-08	3.58E-08	1.12E-07	5.33E-08
1.09	2.63E-06	8.86E-07	1.28E-07	3.46E-08	9.61E-08	1.21E-07
1.10	1.95E-06	3.44E-07	1.33E-08	7.36E-08	1.11E-07	5.65E-08
1.11	2.70E-06	1.49E-06	4.10E-08	1.82E-09	2.33E-08	1.63E-09
1.12	2.05E-06	7.31E-07	5.48E-08	5.10E-08	1.95E-08	7.60E-08
1.13	9.87E-07	1.14E-07	3.67E-09	4.54E-08	6.25E-08	7.01E-08
1.14	5.68E-08	6.47E-07	3.83E-08	1.07E-10	3.08E-08	8.57E-10
1.15	1.01E-06	3.59E-07	7.05E-09	3.31E-08	4.20E-08	2.93E-08
1.16	1.27E-06	6.50E-08	2.64E-08	1.38E-08	4.78E-08	7.66E-08
1.17	1.03E-06	9.28E-08	8.06E-09	2.44E-09	4.45E-09	7.42E-08
1.18	9.50E-08	7.57E-08	3.20E-08	1.53E-08	5.20E-09	7.77E-08
1.19	1.10E-06	1.07E-07	6.20E-08	8.27E-09	1.35E-08	6.56E-08
1.20	2.17E-07	6.09E-09	3.24E-09	9.02E-09	1.73E-09	1.86E-08

Table 2.6: Absolute errors between FFT method and rational function method for call options in the CGMY model with parameters $C = 1$, $G = 5$, $M = 10$ and $Y = 0.5$ (Case V of Table 2.1) for varying strikes and maturities ($S_0 = 1$, $r = 0.03$, $q = 0.01$).

K	T = 0.25	T = 0.5	T = 1	T = 1.5	T = 2	T = 2.5
0.80	3.33E-09	1.84E-10	6.13E-09	3.44E-09	1.86E-08	8.36E-10
0.81	8.19E-10	1.10E-09	1.13E-09	8.08E-09	6.10E-09	2.07E-08
0.82	1.36E-08	1.27E-09	2.09E-09	2.63E-09	5.13E-09	3.04E-10
0.83	5.67E-09	2.33E-09	5.48E-09	2.36E-09	2.79E-09	5.42E-10
0.84	1.56E-09	2.96E-09	3.44E-09	5.04E-09	2.83E-09	2.06E-09
0.85	9.52E-09	4.86E-09	3.01E-09	4.02E-09	3.81E-09	3.24E-09
0.86	2.05E-08	2.49E-09	6.01E-09	2.18E-09	3.86E-09	1.89E-09
0.87	6.16E-08	8.58E-09	2.88E-09	4.85E-09	1.28E-09	1.54E-09
0.88	6.76E-08	1.31E-08	2.91E-09	3.10E-09	1.31E-09	4.22E-09
0.89	7.48E-08	5.79E-09	5.69E-09	1.55E-09	1.39E-09	1.42E-08
0.90	7.27E-08	1.21E-08	1.56E-09	4.20E-09	5.16E-09	2.93E-08
0.91	7.25E-08	1.62E-08	3.57E-09	2.19E-09	4.17E-09	4.55E-08
0.92	6.47E-08	6.48E-09	7.01E-09	2.47E-09	3.39E-09	5.05E-08
0.93	3.50E-08	1.39E-08	2.83E-09	5.19E-09	4.23E-11	3.89E-08
0.94	3.58E-08	1.52E-08	5.63E-09	2.59E-09	3.64E-09	1.64E-08
0.95	2.68E-08	8.73E-10	6.79E-09	3.16E-09	1.23E-10	4.96E-09
0.96	6.57E-09	6.81E-09	6.62E-10	4.37E-09	3.68E-09	1.93E-08
0.97	4.79E-09	1.24E-08	3.55E-09	1.61E-09	5.66E-10	4.03E-08
0.98	3.66E-08	9.89E-09	7.21E-09	3.51E-09	2.20E-09	2.42E-08
0.99	5.90E-08	1.92E-08	6.14E-09	4.72E-09	3.67E-09	2.24E-09
1.00	6.93E-08	1.54E-08	7.81E-09	2.70E-09	3.50E-09	4.25E-09
1.01	6.18E-08	3.47E-09	4.50E-09	3.73E-09	1.70E-09	3.40E-10
1.02	5.41E-08	1.20E-08	4.80E-10	2.68E-09	2.01E-09	1.09E-09
1.03	3.89E-08	1.01E-08	4.10E-09	1.05E-09	1.18E-09	5.24E-09
1.04	1.10E-08	2.49E-09	4.23E-09	3.23E-09	4.80E-09	2.49E-08
1.05	3.85E-10	8.45E-09	2.75E-09	3.30E-09	1.55E-09	4.42E-08
1.06	6.61E-09	3.29E-09	4.35E-09	2.79E-09	2.01E-09	2.93E-08
1.07	5.51E-09	2.04E-09	2.28E-09	3.55E-09	4.32E-09	1.11E-08
1.08	1.41E-08	4.55E-09	1.28E-09	2.57E-09	4.39E-09	1.02E-08
1.09	2.97E-08	5.54E-09	3.69E-09	2.75E-09	2.16E-09	4.30E-09
1.10	4.24E-08	4.46E-09	2.55E-09	3.15E-09	1.91E-09	9.78E-10
1.11	6.83E-08	7.55E-09	1.94E-09	2.14E-09	3.31E-09	1.54E-09
1.12	8.59E-08	9.40E-09	2.83E-09	2.16E-09	1.79E-09	3.90E-09
1.13	8.15E-08	1.06E-08	2.39E-09	2.28E-09	3.13E-09	1.05E-09
1.14	7.68E-08	8.75E-09	2.28E-09	1.76E-09	3.56E-09	3.15E-08
1.15	7.10E-08	7.58E-09	2.09E-09	1.85E-09	2.69E-10	4.10E-08
1.16	7.37E-08	8.91E-09	1.68E-09	1.69E-09	1.21E-09	1.68E-08
1.17	6.19E-08	9.94E-09	1.94E-09	1.62E-09	2.14E-09	7.82E-09
1.18	7.01E-09	1.25E-09	2.95E-09	1.63E-09	6.07E-09	2.41E-08
1.19	5.69E-08	2.98E-10	1.37E-09	1.81E-09	6.81E-09	5.02E-08
1.20	2.40E-09	3.74E-08	3.94E-10	1.78E-09	5.95E-09	5.77E-08

Table 2.7: Absolute errors between FFT method and rational function method for call options in the zero-correlation Heston model with parameters $\kappa = 0.87$, $\delta = 0.07$, $\xi = 0.34$,$V_0 = 0.07$ and $\rho = 0$ (Case III of Table 2.1) for varying strikes and maturities ($S_0 = 1$, $r = 0.03$, $q = 0.01$).

# Maturities	# Strikes	Time in sec. FFT	Time in sec. RA
41	7	0.404	0.044
7	41	0.074	0.011
100	100	1.006	0.106
300	300	2.816	0.460
300	5	2.795	0.298
5	300	0.049	0.009

Table 2.8: Time comparison between FFT method and rational function method in seconds.

Again $S_0 = 1$, $r = 0.03$ and $q = 0.01$. This gives a total of $5,551$ options and results in a maximum error of 4.35×10^{-7}. As stated before, this procedure is faster than the usual solver methods. When comparing to Matlab's built-in solver method (which uses Newton's method) for implied volatility (setting accuracy to 1×10^{-8}), calculating these $5,551$ implied volatilities takes 80.22 seconds with our rational function method and 320.42 seconds with Matlab's method. For details on how to construct a non-arbitrageable implied volatility surface, we refer to Lipton & Sepp [96] and references therein.

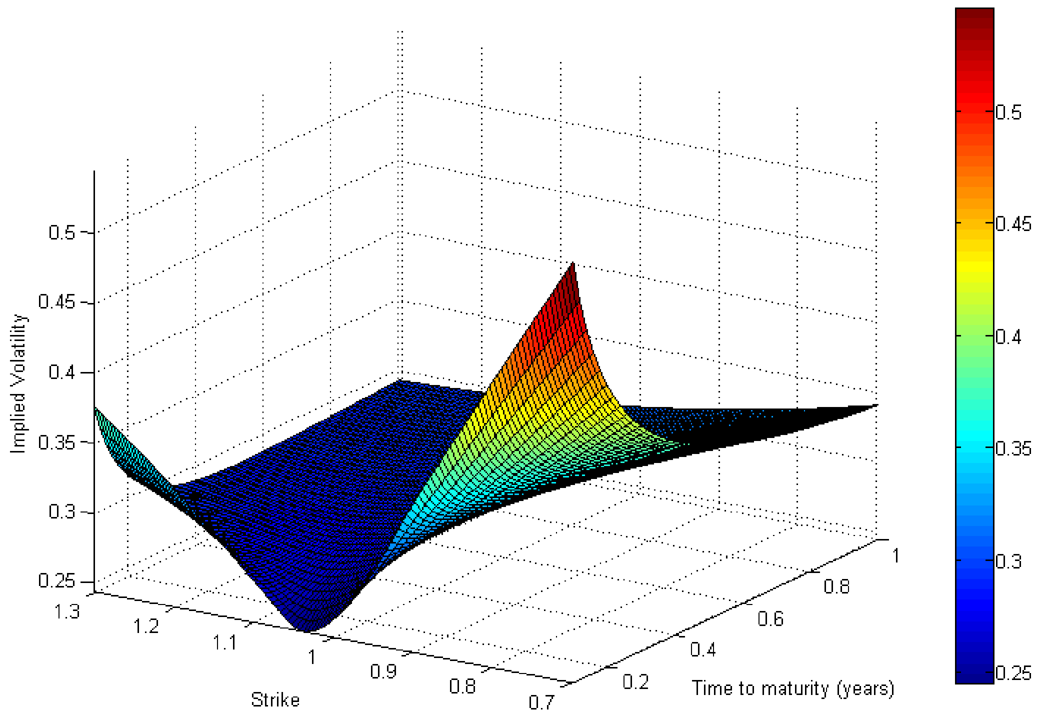

Figure 2.4: Volatility surface of CGMY model for $T \in [0.1, 1.0]$ and $K \in [0.7, 1.3]$ with $C = 1$, $G = 5$, $M = 10$ and $Y = 0.5$ (these parameters are taken from Madan & Yor [100]). Again $S_0 = 1$, $r = 0.03$ and $q = 0.01$.

2.6 Summary

In this chapter, we illustrated how to use rational function approximations to derive an alternative approach for calculating vanilla option prices and Black-Scholes implied volatilities. In particular, by approximating a normalisation of the Black-Scholes formula, a two-parameter function of one variable, we derived a pricing formula for any time-changed Brownian motion model. The method was found to be stable and fast, since it is possible to rewrite the rational approximation in terms of negative exponential moments (the Laplace transform) of the time change. The method can therefore be used for any model for which the Laplace transform of the time change is available in tractable form. It is important to note that also stochastic volatility Lévy models are included in this framework. Although rational Chebyshev approximations can be performed with little computational effort, we showed that one can significantly speed up the method by pre-calculating the approximations and interpolating between them for the purpose of option pricing.

By way of illustration, we implemented the method for three popular models from the literature, and found that the method compares favourably to the standard FFT with respect to speed and accuracy.

Additionally, we used the methodology to approximate the inverse of the Black-Scholes formula in order to compute implied volatilities, and found this method to be significantly faster than existing methods. We are able to approximate the resulting two-dimensional function by a total of 105 rational approximations. Implied volatilities for a wide range of input parameters can then be obtained, for any given set of arbitrage-free vanilla option prices, by interpolating between the previously calculated approximations. The absolute error for this method was shown to be bounded by 5.5×10^{-5}, although this can be refined if necessary by choosing rational approximations with higher order.

Chapter 3

Lévy bridge Monte Carlo method: Pricing of barrier options and range accruals

Outline. The Markov-bridge sampling method presented in this chapter concerns the estimation of the expectation $\mathbb{E}[F(T,\xi)]$ of a given path-functional F of a Markov process ξ and the time horizon $T > 0$. It consists of averaging conditional expectations $\widetilde{F}(\xi_{t_0}, \ldots, \xi_{t_N})$ over M independent copies $(\xi_{t_0}^{(i)}, \ldots, \xi_{t_N}^{(i)})$, $i = 1, \ldots, M$, of the random vector $(\xi_{t_0}, \ldots, \xi_{t_N})$ for values of the process ξ on an equidistant grid $\mathbb{T}_N = \{0 = t_0 < t_1 < \ldots < t_N = T\}$:

$$\mathbb{E}[F(T,\xi)] \approx \frac{1}{M} \sum_{i=1}^{M} \widetilde{F}(\xi_{t_0}^{(i)}, \ldots, \xi_{t_N}^{(i)}), \tag{3.0.1}$$

where $\widetilde{F}(\xi_{t_0}, \ldots, \xi_{t_N})$ denotes the regular version of the conditional expectation $\mathbb{E}[F(T,\xi)|\xi_{t_0}, \ldots, \xi_{t_N}]$. The name of the method derives from the fact that, conditional on the values $(\xi_{t_0}, \ldots, \xi_{t_N})$, the stochastic processes $\{\xi_t, t \in [t_i, t_{i+1}]\}$, $i = 0, \ldots, N-1$, are equal in law to Markov-bridge processes. The estimator in Eqn. (3.0.1) is unbiased and has strictly smaller variance than the standard Monte Carlo estimator, as a consequence of the tower property of conditional expectation and the conditional variance formula. The Markov-bridge sampling method has the advantage that it allows for refinements of the generated paths to the required level of accuracy, and that it can be combined with importance sampling. Such a bridge method is especially suited for the evaluation of expectations of path-dependent functionals (see Boyle *et al.* [28], for example). Since $\widetilde{F}$ is, in general, not available in closed or analytically tractable form, the viability of the Markov-bridge sampling method hinges on the ability to efficiently approximate this function. In this chapter we derive such an approximation method for the conditional expectation $\widetilde{F}$ of certain path-functionals given in terms of occupation times and first-passage times, and present a Markov-bridge method for the estimation of the corresponding expectation $\mathbb{E}[F(T, \xi)]$ under the stochastic volatility model with jumps defined in Eqns. (3.5.1) and (3.5.2) below, which is a two-dimensional Markov process. The definition includes the Heston model [72] and the variation of the Bates model [17] with mixed-exponential jumps. We apply the method to the valuation of barrier options and range accruals, which are common path-dependent derivative securities.

Several bridge sampling methods exist in the literature dealing with the case that ξ belongs to the class of one-dimensional Lévy processes. In Figueroa-Lopez & Tankov [57] an adaptive bridge sampling method is developed for the case of real-valued Lévy processes based on short-time asymptotics of stopped Lévy processes. By conditioning on the jump-skeleton and exploiting the explicit form of the distribution of the maximum of a Brownian bridge, a simulation method for pricing of barrier options under jump-diffusions is presented in Metwally & Atiya [106], and a refinement of this algorithm and application to the pricing of corporate bonds is given in Ruf & Scherer [120].

Approximation of bridge functionals. As mentioned above, a key step in the development of the Markov-bridge method is the availability of an efficient approximation of the conditional expectation $\widetilde{F}$. Since generally the transition probabilities of the Markov processes considered here are not explicitly available, the first step is to approximate the Markov process in question by its continuous Euler-Maruyama (EM) scheme. The approximation of expectations of path-dependent functionals using the continuous EM-scheme is based on the *harness property* of a Lévy process: the collection of values of the Lévy process at times t in between t_1 and t_2 is independent of the collection of values at times t outside this interval, given the values of the process at t_1 and t_2. Note that a Lévy process that is conditioned to start from position z and is pinned down to y at the horizon T, is equal in law to a Lévy bridge process from $(0, z)$ to (T, y) (for a visualisation see Figure 3.1, where two paths of a Lévy bridge on the unit interval $[0, 1]$ starting and ending at 0 are depicted). We are led to the problem of evaluating the first-passage probabilities and the expected occupation times of a Lévy bridge.

Randomisation method. The approximation method of the Lévy bridge quantities that we present is based in part on a randomisation of the time-parameter. A related randomisation method was used successfully by Carr [35] for the valuation of American put options, and was extended to the Lévy case in Boyarchenko & Levendorskiĭ [21] and Levendorskiĭ [87], for example. As observed in Feller [56, Ch. VII.6], the approximation of the value $f(t)$ of a continuous and bounded function f at $t > 0$, by the expectation $\mathbb{E}[f(\Gamma_{n,n/t})]$ of f evaluated at an independent random time $\Gamma_{n,n/t}$ with Gamma$(n, n/t)$ distribution (which has mean t and variance t^2/n) is asymptotically exact. Since $\Gamma_{n,n/t}$ converges in distribution to a point mass at t, it follows that the expectation $\mathbb{E}[f(\Gamma_{n,n/t})]$ converges to $f(t)$ as n tends to infinity. With regard to the rate of convergence, the form of the probability density function (PDF) of $\Gamma_{n,n/t}$ implies that, in the case that f is C^2 at t, the decay of the error $\mathbb{E}[f(\Gamma_{n,n/t})] - f(t)$ is linear in $1/n$. Moreover, $\mathbb{E}[f(\Gamma_{n,n/t})]$ admits the following expansion if the function f is C^{2k} at t:

$$\mathbb{E}[f(\Gamma_{n,n/t})] - f(t) = \sum_{m=1}^{k} b_m(t) \left(\frac{1}{n}\right)^m + o(n^{-k}) \qquad \text{as } n \to \infty,$$

for certain functions $b_1, \ldots, b_k$ (proved in Thm. 3.1.1 below). We show that the functions f, which we consider, are sufficiently smooth, so that the use of the Richardson extrapolation is fully justified in order to increase the rate of convergence. We show that the first-passage probability and expected occupation time, observed at the independent random time $\Gamma_{n,n/t}$, are solutions to certain recursions. Restricting ourselves to the dense class of Lévy processes of mixed-exponential jump-diffusion type (the definition of which is recalled in Def. 3.3.1 below), we present explicit solutions to these two recursions. To illustrate the efficiency, the method was implemented for a number of models in this class, and the numerical outcomes are reported in Section 3.4. We observed that the outcomes of the recursion, based on a small number (about ten) of recursive steps, already yielded highly accurate approximations, when combined with the Richardson extrapolation.

Markov-bridge method. Subsequently, we combine these approximations with a continuous EM scheme to estimate the conditional expectations $\widetilde{F}$ corresponding to the first-passage times and expected occupation times of the Bates-type model (Eqns. (3.5.1)—(3.5.2)). We numerically investigate the rate of convergence corresponding to the continuous EM scheme and find that the error estimates established in Gobet [68], for the case

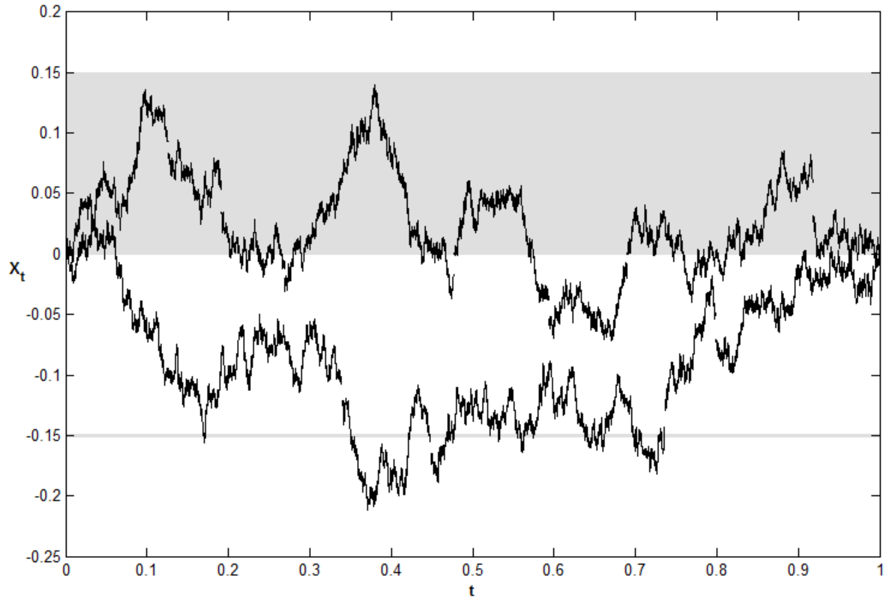

Figure 3.1: The figure displays two realisations of a Lévy bridge $X^{(0,0)\to(1,0)}$ starting and ending at 0, where the process X is a hyper-exponential jump-diffusion with parameters given in Table 3.1. A barrier level is drawn at -0.15 and the range from 0 to 0.15 is shaded.

of killed diffusion processes, appear to also hold in the current setting. The study of theoretical rates of convergence and error bounds is left for future research. To illustrate the effectiveness of the method, we evaluated a barrier option and a range note under the Heston model and Bates-type models.

Contents. The remainder of this chapter is organised as follows. In Section 3.1 the error expansion of the randomisation method is derived. Sections 3.2 is devoted to the derivation of recursive formulas for the first-passage probabilities and expected occupation times of Lévy bridges. Section 3.3 considers the special case of mixed-exponential jump-diffusions. The continuous Euler-Maruyama scheme used to evaluate the path-functionals in the class of stochastic volatility models with jumps is described in Section 3.5. Numerical illustrations are presented in Sections 3.4 and 3.6, and summarising remarks are given in Section 3.7.

3.1 The randomisation method

In general, option pricing formulas for randomised maturities are simpler than those for fixed maturities. The simplest expressions arise when the option matures at the first jump time of a Poisson process, in which case the maturity date is exponentially distributed. The randomisation method is based on the fact that by the strong law of large numbers, the sum of n i.i.d. exponential random variables with mean t/n, which we denote $\Gamma_{n,n/t}$, converges to t almost surely as n tends to infinity. The method therefore consists in approximating the value $f(t)$ of a function f at time $t > 0$ by the expectation $\mathbb{E}[f(\Gamma_{n,n/t})]$ evaluated at a random time $\Gamma_{n,n/t}$ that follows a Gamma(n, n/t) distribution. Since $\Gamma_{n,n/t}$ converges in distribution to t as n tends to infinity, the error $\mathbb{E}[f(\Gamma_{n,n/t})] - f(t)$ converges to zero for any bounded and continuous function f. The error can be expanded in terms of powers of $1/n$ provided that f is sufficiently smooth, as shown in the following result (which we label as theorem because of its importance in the sequel):

Theorem 3.1.1. *Let k be a given non-negative integer and consider $f \in C^{2k+2}(\mathbb{R}_+)$. There exist functions $b_1, \ldots, b_{k+1} : \mathbb{R}_+ \to \mathbb{R}$ such that we have, for any $t \in \mathbb{R}_+$,*

$$n^{k+1}\left[\mathbb{E}[f(\Gamma_{n,n/t})] - f(t) - \sum_{m=1}^{k} b_m(t)\left(\frac{1}{n}\right)^m\right] = b_{k+1}(t) + o(1) \qquad \text{as } n \to \infty. \tag{3.1.1}$$

In particular, denoting by $f^{(m)}$ the mth derivative of f, we have

$$\begin{aligned}
b_1(t) &= \frac{t^2}{2} f^{(2)}(t), \qquad b_2(t) = \frac{t^4}{8} f^{(4)}(t) + \frac{t^3}{3} f^{(3)}(t),\\
b_3(t) &= \frac{t^6}{48} f^{(6)}(t) + \frac{t^5}{6} f^{(5)}(t) + \frac{t^4}{4} f^{(4)}(t),\\
b_4(t) &= \frac{t^8}{384} f^{(8)}(t) + \frac{t^7}{24} f^{(7)}(t) + \frac{13t^6}{72} f^{(6)}(t) + \frac{t^5}{5} f^{(5)}(t).
\end{aligned}$$

Remark 3.1.1. (i) Thm. 3.1.1 implies that for $f \in C^2(\mathbb{R}_+)$ the error of the approximation of $f(t)$ by $\mathbb{E}[f(\Gamma_{n,n/t})]$ decays linearly in $1/n$, that is, $\mathbb{E}[f(\Gamma_{n,n/t})] - f(t) = \frac{b_1(t)}{n} + o\left(\frac{1}{n}\right)$ as n tends to infinity.

(ii) Thm. 3.1.1 also provides a justification of the use of the Richardson extrapolation to increase the rate of convergence if the function f is sufficiently smooth. Since the error of the approximation is given in terms of positive integer powers of $1/n$, the Richardson extrapolation that utilises the first N values $\mathbb{E}[f(\Gamma_{1,1/t})], \ldots, \mathbb{E}[f(\Gamma_{N,N/t})]$ is explicitly given by

$$P_{1:N} \quad := \quad \sum_{k=1}^{N} \frac{(-1)^{N-k} k^N}{k!(N-k)!} \mathbb{E}[f(\Gamma_{k,k/t})], \tag{3.1.2}$$

(see Marchuk and Shaidurov [102] for a derivation of this formula). In the case $f \in C^{2k+2}(\mathbb{R}_+)$, $k < N$, Theorem 3.1.1 implies that the error $P_{1:N} - f(t)$ of the extrapolation

$P_{1:N}$ is given by $o(N^{-k-1})$. In particular, if f is C^∞ then the error $P_{1:N} - f(t)$ is $o(N^{-k-1})$ for every k, as N tends to infinity. We refer to Sidi [126] for background on the theory of extra- and interpolation.

Proof of Theorem 3.1.1. Taylor's theorem and the fact that $f \in C^{2k+2}$ implies that we have

$$f(s) - f(t) = \sum_{m=1}^{2k+1} \frac{(s-t)^m}{m!} f^{(m)}(t) + R_k(s,t),$$

where the remainder term is given by $R_k(s,t) = \frac{(s-t)^{2k+2}}{(2k+2)!} f^{(2k+2)}(\xi)$ for some ξ between s and t. Replacing s by the independent Gamma random variable $\Gamma_{n,n/t}$ we get

$$\mathbb{E}[f(\Gamma_{n,n/t}) - f(t)] = \sum_{m=2}^{2k+1} \frac{a_{m,n}}{m!} f^{(m)}(t) + \mathbb{E}[R_k(\Gamma_{n,n/t}, t)]$$

with $a_{m,n} = \mathbb{E}[(\Gamma_{n,n/t} - t)^m]$, where we have $a_{1,n} = 0$ as the expectation $\mathbb{E}[\Gamma_{n,n/t}]$ is equal to t. The numbers $a_{m,n}$ are equal to $a_{m,n} = \frac{\mathrm{d}^m}{\mathrm{d}u^m}\big|_{u=0} M(u)$ where M denotes the moment-generating function of the random variable $\Gamma_{n,n/t} - t$ which is given by

$$M(u) = \left(1 - \frac{ut}{n}\right)^{-n} \exp\{-ut\}, \qquad u \leq \frac{n}{t}.$$

In particular, it follows from the form of M that the $a_{m,n}$ are linear combinations of positive integer powers of $1/n$. Reordering of terms results in the identity in Eqn (3.1.1), where the formulas of the functions $b_1(t), \ldots, b_4(t)$ can be derived by straightforward calculations. $\square$

3.2 Supremum and occupation time of a Lévy bridge

A Lévy bridge process is a time-inhomogeneous Markov process defined on a finite time-interval $[s,t]$ with transition probabilities that are equal to those of a Lévy process conditioned on its values at times s and t (see Bertoin [18]). While the standard Lévy process $X = \{X_t, t \in [0,T]\}$ is normalised to start from zero, $X_0 = 0$, we also consider the family of Lévy processes starting from $z \in \mathbb{R}$, and denote the corresponding probability measures by $\{\mathbb{P}_z, z \in \mathbb{R}\}$, with $\mathbb{P} = \mathbb{P}_0$. We refer to Bertoin [18], Kyprianou [83] and Sato [121] for general treatments of the theory of Lévy processes. To avoid degeneracies we exclude the case that $|X|$ is a subordinator in the sequel.

For any given non-negative numbers s and t with $s \leq t$ and any real numbers z and y, we will denote by $X^{(s,z)\to(t,y)} = \{X_u^{(s,z)\to(t,y)}, u \in [s,t]\}$ the *Lévy bridge process* that is defined as follows:

Definition 3.2.1. The *Lévy bridge process* $X^{(s,z)\to(t,y)} = \{X_u^{(s,z)\to(t,y)}, u \in [s,t]\}$ associated to X is a time-inhomogeneous Markov process with transition probabilities that are equal to those of a Lévy process X conditioned on $\{X_s = z, X_t = y\}$.

In this section we consider the problem of identifying the distribution of the supremum $\overline{X}^{(0,0)\to(t,y)} = \sup_{u\in[0,t]} X_u^{(0,0)\to(t,y)}$ of the Lévy bridge process,

$$\vec{d}_t(x,y) := \mathbb{P}\left(\overline{X}^{(0,0)\to(t,y)} \leq x\right), \tag{3.2.1}$$

and the expected occupation time of the set $(-\infty, x]$,

$$\vec{\omega}_t(x,y) := \mathbb{E}\left[\int_0^t I_{\left\{X_u^{(0,0)\to(t,y)} \leq x\right\}} \mathrm{d}u\right]. \tag{3.2.2}$$

We note that there is no loss of generality in restricting to Lévy bridges starting from the point $(0,0)$. By the spatial and temporal homogeneity of the Lévy process X, the corresponding quantities in the case of a general starting point (s,z) are explicitly given in terms of the functions $\vec{d}$ and $\vec{\omega}$ by $\vec{d}_{t-s}(x-z, y-z)$ and $\vec{\omega}_{t-s}(x-z, y-z)$.

Deploying the randomisation method described in Section 3.1, we construct approximations of the first-passage time probabilities and expected occupation times of Lévy bridge processes in terms of *randomised* Lévy bridge processes that are defined as follows:

Definition 3.2.2. For any two random times τ_1 and τ_2 with $\tau_1 < \tau_2$ that are independent of X, the randomised Lévy bridge $X^{(\tau_1,z)\to(\tau_2,y)}$ is the stochastic process that, conditional on $\{\tau_1 = s, \tau_2 = t\}$, has the same law as the Lévy bridge $X^{(s,z)\to(t,y)}$.

To ensure that the random variable $X_{\Gamma_{1,q}}$ admits a continuous density u_1 we adopt the following assumption:

Assumption 3.2.1. The Lévy process X satisfies the integrability condition

$$\int_{\mathbb{R}} \frac{\mathrm{d}s}{|\phi(s)|} < \infty, \tag{3.2.3}$$

where ϕ is the characteristic exponent of X.

Lemma 3.2.1. *Under the condition in Eqn.* (3.2.3)*, the density $u_{1,q}$ exists and is continuous and bounded.*

Proof. Since the Fourier-transform of the measure μ on $(\mathbb{R}, \mathcal{B}(\mathbb{R}))$ given by $\mu(\mathrm{d}x) = \mathbb{P}(\{X_{\Gamma_{1,q}} \in \mathrm{d}x\})$ satisfies the bound $\int |\widehat{\mu}(s)|\mathrm{d}s \leq \int \left|\mathbb{E}[\mathrm{e}^{\mathbf{i}sX_{\Gamma_{1,q}}}]\right| \mathrm{d}s$ and the characteristic function of the random variable $X_{\Gamma_{1,q}}$ is given in terms of the characteristic exponent ϕ by

$$\mathbb{E}[\exp(\mathbf{i}\theta X_{\Gamma_{1,q}})] = \frac{q}{q+\phi(\theta)}, \tag{3.2.4}$$

it follows, in view of Assumption 3.2.1 (*e.g.*, Sato [121]) that the measure μ has a continuous bounded density. □

Specifying the random times τ_1 to be equal to zero and τ_2 to be equal to the independent random time $\Gamma_{n,n/t}$, we can define the analogues of the functions $\vec{d}$ and $\vec{\omega}$ in terms of the randomised bridge $X^{(0,0)\to(\Gamma_{n,n/t},y)}$, as follows:

$$\begin{aligned}
\vec{D}_t^{(n)}(x,y) &:= \mathbb{P}\left(\overline{X}^{(0,0)\to(\Gamma_{n,n/t},y)} \leq x\right), \\
\vec{\Omega}_t^{(n)}(x,y) &:= \mathbb{E}\left[\int_0^{\Gamma_{n,n/t}} I_{\left\{X_u^{(0,0)\to(\Gamma_{n,n/t},y)} \leq x\right\}} \mathrm{d}u\right].
\end{aligned}$$

Below, we derive semi-analytical formulas for the functions $\vec{D}_t^{(1)}(x,y)$ and $\vec{\Omega}_t^{(1)}(x,y)$. We show that for any real x and y, the values $\vec{d}_t(x,y)$ and $\vec{\omega}_t(x,y)$ are equal to the limits of $\vec{D}_t^{(n)}(x,y)$ and $\vec{\Omega}_t^{(n)}(x,y)$ as n tends to infinity, which in turn are given by the solutions of n-step recursions that are explicitly given in terms of the functions $\vec{D}_t^{(1)}$ and $\vec{\Omega}_t^{(1)}$ (see Theorem 3.2.1 below). The decay of the error of this approximation procedure is linear as a function of $1/n$, provided that the functions $\vec{d}_t(x,y)$ and $\vec{\omega}_t(x,y)$ are sufficiently regular.

Proposition 3.2.1. *Let x, y and t be given real numbers with $t > 0$, and assume that the distribution of X_t has a continuous density p_t. If the functions $s \mapsto \vec{d}_s(x,y)$, $s \mapsto \vec{\omega}_s(x,y)$ (as defined in Eqns.* (3.2.1) *and* (3.2.2)*) and $s \mapsto p_s(y)$ are C^2 at $s = t$ with $p_t(y) > 0$, then constants C^d and C^ω exist such that we have, for all positive integers n,*

$$\left|\vec{D}_t^{(n)}(x,y) - \vec{d}_t(x,y)\right| \leq \frac{C^d}{n}, \qquad \left|\vec{\Omega}_t^{(n)}(x,y) - \vec{\omega}_t(x,y)\right| \leq \frac{C^\omega}{n}. \tag{3.2.5}$$

Proof. The estimates in Eqn. (3.2.5) follow directly by applying Theorem 3.1.1 to the functions $t \mapsto \vec{d}_t(x,y)p_t(y)$, $t \mapsto \vec{\omega}_t(x,y)p_t(y)$ and $t \mapsto p_t(y)$. □

The derivation of the expressions for the functions $\vec{D}_t^{(1)}(x,y)$ and $\vec{\Omega}_t^{(1)}(x,y)$ is based on the following auxiliary result concerning the differentiability of two related functions under the condition in Eqn. (3.2.3).

Lemma 3.2.2. *Let q be any strictly positive number.*

(i) For any fixed x, the map $y \mapsto \mathbb{P}(\overline{X}_{\Gamma_{1,q}} \le x, X_{\Gamma_{1,q}} \le y)$ is continuously differentiable and its derivative $D_1(x,y)$ is bounded.

(ii) The map $(x,y) \mapsto \mathbb{E}\left[\int_0^{\Gamma_{1,q}} I_{\{X_u \le x\}} \mathrm{d}u \, I_{\{X_{\Gamma_{1,q}} \le y\}}\right]$ is continuously differentiable with respect to x and y. The mixed derivative $\Omega_1(x,y)$ with respect to x and y is given by

$$\Omega_1(x,y) = \frac{1}{q} u_1(y-x)\, u_1(x), \tag{3.2.6}$$

for arbitrary real x and y, where u_n denotes the continuous density of random variable $X_{\Gamma_{n,q}}$.

Proof of Lemma 3.2.2. (i) Note that

$$\int \left| \mathbb{E}\left[\mathrm{e}^{\mathbf{i} s X_{\Gamma_{1,q}}} \right] \right| \mathrm{d}s = q \int \frac{\mathrm{d}s}{|\phi(s)+q|} < \infty$$

in view of Assumption 3.2.1. Hence it follows (*e.g.* Sato [121]) that $\mathbb{P}\left(X_{\Gamma_{1,q}} \in \mathrm{d}x\right)$ has a continuous bounded density. Define $\tau_x^+ = \inf\{t : X_t > x\}$ and note that the following holds:

$$\begin{aligned}
\mathbb{P}(\overline{X}_{\Gamma_{1,q}} \le x, X_{\Gamma_{1,q}} \le y) &= \mathbb{P}(X_{\Gamma_{1,q}} \le y) - \mathbb{P}(\overline{X}_{\Gamma_{1,q}} > x, X_{\Gamma_{1,q}} \le y) \\
&= \mathbb{P}(X_{\Gamma_{1,q}} \le y) - \int_x^\infty \mathbb{P}_z(X_{\Gamma_{1,q}} \le y) \mathbb{P}(X_{\tau_x^+} \in \mathrm{d}z, \tau_x^+ < \Gamma_{1,q}).
\end{aligned}$$

So it follows by Lebesgue's dominated convergence theorem and the fact that $\mathbb{P}\left(X_{\Gamma_{1,q}} \in \mathrm{d}x\right)$ has a continuous bounded density, that $\mathbb{P}(\overline{X}_{\Gamma_{1,q}} \le x, X_{\Gamma_{1,q}} \le y)$ has a continuous bounded density with respect to y.

(ii) Denote the joint distribution of X_s and X_t by $P_{t,s}$. To see that the identity in Eqn. (3.2.6) holds true, note first that for any $s < t$ the joint distribution of X_s and X_t satisfies

$$P_{t,s} = \mathbb{P}\left[X_s \in \mathrm{d}a, X_t \in \mathrm{d}y\right] = \mathbb{P}\left[X_s \in \mathrm{d}a\right] \mathbb{P}_a\left[X_{t-s} \in \mathrm{d}y\right]$$

by the Markov property and stationarity of increments. An application of Fubini's theorem then yields

$$\begin{aligned} & q\int_0^\infty \mathrm{e}^{-qt}\int_0^t P_{t,s}\mathrm{d}s\mathrm{d}t \\ = & \; q\int_0^\infty \mathrm{e}^{-qs}\mathbb{P}\left[X_s\in\mathrm{d}a\right]\int_s^\infty \mathrm{e}^{-q(t-s)}\mathbb{P}_a\left[X_{t-s}\in\mathrm{d}y\right]\mathrm{d}t\mathrm{d}s \\ = & \; q\int_0^\infty \mathrm{e}^{-qs}\mathbb{P}\left[X_s\in\mathrm{d}a\right]\mathrm{d}s\int_0^\infty \mathrm{e}^{-qu}\mathbb{P}_a\left[X_u\in\mathrm{d}y\right]\mathrm{d}u, \end{aligned}$$

which is equal to $q^{-1}u_1(y-a)\,u_1(a)\mathrm{d}a\mathrm{d}y$. □

Notation. In the sequel, if a measure μ on $(\mathbb{R},\ \mathcal{B}(\mathbb{R}))$ given by $\mu(A) = \mathbb{E}[BI_{\{Z\in A\}}]$, where B and Z denote integrable random variables, admits a density, then we denote this density by $\mathbb{E}[BI_{\{Z=z\}}]$.
It therefore follows that

$$D_1(x,y) = \mathbb{P}(\overline{X}_{\Gamma_{1,q}}\le x, X_{\Gamma_{1,q}}=y) \quad\text{and}\quad \Omega_1(x,y) = \mathbb{E}\left[\int_0^{\Gamma_{1,q}} I_{\{X_u=x\}}\mathrm{d}u\, I_{\{X_{\Gamma_{1,q}}=y\}}\right].$$

The functions D_1 and Ω_1 admit semi-analytical expressions, which can be derived using the Markov property and the Wiener-Hopf factorisation of X (see Section 1.4.3 for more details on the Wiener-Hopf factorisation). Denoting by $\overline{X}_t = \sup_{s\le t}X_s$ and $\underline{X}_t = \inf_{s\le t}X_s$ the running supremum and infimum of X at time $t>0$, we recall (see *e.g.* Bertoin [18, Ch. VI]) that the probabilistic form of the Wiener-Hopf factorisation of X states that (a) the running supremum $\overline{X}_{\Gamma_{1,q}}$ and the *drawdown* $\overline{X}_{\Gamma_{1,q}} - X_{\Gamma_{1,q}}$ of X at the random time $\Gamma_{1,q}$ are independent, and (b) the drawdown $\overline{X}_{\Gamma_{1,q}} - X_{\Gamma_{1,q}}$ has the same law as the negative of the running infimum $-\underline{X}_{\Gamma_{1,q}}$. The probabilistic form of the Wiener-Hopf factorisation implies that the characteristic function of the random variable $X_{\Gamma_{1,q}}$ given in Eqn. (3.2.4) is equal to the product of the characteristic functions ϕ_q^+ and ϕ_q^- of the random variables $\overline{X}_{\Gamma_{1,q}}$ and $\underline{X}_{\Gamma_{1,q}}$,

$$\phi_q^+(\theta) = \mathbb{E}[\exp(\mathtt{i}\theta\overline{X}_{\Gamma_{1,q}})], \qquad \phi_q^-(\theta) = \mathbb{E}[\exp(\mathtt{i}\theta\underline{X}_{\Gamma_{1,q}})].$$

Proposition 3.2.2. *For any strictly positive real q, we have*

$$D_1(x,y) = \mathcal{L}^{-1}_{u,v}\left[\frac{1}{u}\phi_q^-(\mathtt{i}u)\phi_q^+(\mathtt{i}(u+v))\right](x,y), \qquad x\ge y, \tag{3.2.7}$$

$$\Omega_1(x,y) = \mathcal{F}^{-1}_\xi\left[\frac{1}{q+\phi(\xi)}\right](y-x)\cdot\mathcal{F}^{-1}_\xi\left[\frac{q}{q+\phi(\xi)}\right](x), \qquad x,y\in\mathbb{R}, \tag{3.2.8}$$

$$u_n(x) = \mathcal{F}^{-1}_\xi\left[\frac{q^n}{(q+\phi(\xi))^n}\right](x), \quad x\in\mathbb{R}, \tag{3.2.9}$$

where $\mathcal{L}^{-1}_{u,v}$ *and* $\mathcal{F}^{-1}_{\xi}$ *denote the inverses of the two-dimensional Laplace transform and the Fourier transform, respectively.*

Proof. The probabilistic form of the Wiener-Hopf factorisation of X implies that the joint distribution of $\overline{X}_{\Gamma_{1,q}}$ and $X_{\Gamma_{1,q}}$ is given by

$$\begin{aligned}\mathbb{P}\left[\overline{X}_{\Gamma_{1,q}} \in \mathrm{d}x, X_{\Gamma_{1,q}} \in \mathrm{d}y\right] &= \mathbb{P}\left[\overline{X}_{\Gamma_{1,q}} \in \mathrm{d}x, \overline{X}_{\Gamma_{1,q}} - X_{\Gamma_{1,q}} \in \mathrm{d}(x-y)\right] \qquad (3.2.10)\\ &= \mathbb{P}\left[\overline{X}_{\Gamma_{1,q}} \in \mathrm{d}x\right] \mathbb{P}\left[-\underline{X}_{\Gamma_{1,q}} \in \mathrm{d}(x-y)\right] \qquad \text{for } x \geq y.\end{aligned}$$

As a consequence, it follows that the joint Laplace transform of the random variables $\overline{X}_{\Gamma_{1,q}}$ and $X_{\Gamma_{1,q}}$ is given by $\frac{1}{u}\phi^-_q(\mathtt{i}u)\phi^+_q(\mathtt{i}(u+v))$, from which Eqn. (3.2.7) follows. By combining Eqns. (3.2.4) and (3.2.6), we arrive at Eqn. (3.2.8). The final equation, Eqn. (3.2.9), follows in view of Eqn. (3.2.4) and the fact that the Fourier transform of a convolution is equal to a product of Fourier transforms. □

In view of the fact that the process $X^{(s,z)\to(t,y)}$ is equal in law to the process $\{X_u, u \in [s,t]\}$ conditioned on $\{X_s = z, X_t = y\}$, it follows that the functions $\vec{D}^{(n)}_t(x,y)$ and $\vec{\Omega}^{(n)}_t(x,y)$ are equal to the ratio of the solutions D_n and Ω_n (of certain recursions given below), and $u_n(y)$. That is,

$$\begin{aligned}D_n(x,y) = \quad & \vec{D}^{(n)}_t(x,y)u_n(y) &= \mathbb{P}(\overline{X}_{\Gamma_{n,q}} \leq x, X_{\Gamma_{n,q}} = y), \qquad (3.2.11)\\ \Omega_n(x,y) = \quad & \tfrac{\mathrm{d}}{\mathrm{d}x}\vec{\Omega}^{(n)}_t(x,y)u_n(y) &= \mathbb{E}\left[\int_0^{\Gamma_{n,q}} I_{\{X_u = x, X_{\Gamma_{n,q}} = y\}}\mathrm{d}u\right]. \qquad (3.2.12)\end{aligned}$$

The form of the three recursions is given as follows:

Theorem 3.2.1. *Let q be a strictly positive real number. The maps D_n and $\Omega_n : \mathbb{R}^2 \to \mathbb{R}^+$, and the map $u_n : \mathbb{R} \to \mathbb{R}^+$ $n \in \mathbb{N}$, satisfy the recursions*

$$\begin{aligned}D_{n+1}(x,y) &= \int_{-\infty}^{x} D_n(x-w,y-w)D_1(x,w)\mathrm{d}w, & x \in \mathbb{R}_+, y \in \mathbb{R}, y \leq x, \quad (3.2.13)\\ \Omega_{n+1}(x,y) &= \int_{\mathbb{R}} \left[\Omega_1(x,w)u_n(y-w) + \Omega_n(x-w,y-w)u_1(w)\right]\mathrm{d}w, & x,y \in \mathbb{R}, \quad (3.2.14)\\ u_{n+1}(x) &= \int_{\mathbb{R}} u_1(w)u_n(x-w)\mathrm{d}w, & x \in \mathbb{R}, \quad (3.2.15)\end{aligned}$$

where u_n is the probability density function of the random variable $X_{\Gamma_{n,q}}$.

Proof of Theorem 3.2.1. Let q and n be strictly positive numbers, real and integer respectively. Since we may write

$$\overline{X}_t = \max\left\{X_s + \sup_{0\leq u\leq t-s}(X_{u+s} - X_s), \overline{X}_s\right\}, \qquad \text{for any } s,t \text{ with } 0 \leq s \leq t,$$

it follows as a consequence of the stationarity and independence of increments of X, and the fact that a $\Gamma_{n,q}$ random variable is equal in distribution to the sum of independent $\Gamma_{n-1,q}$ and $\Gamma_{1,q}$ random variables, that we have

$$\begin{aligned} & \mathbb{P}\left(\overline{X}_{\Gamma_{n,q}} \leq x, X_{\Gamma_{n,q}} \in \mathrm{d}y\right) \\ = \; & \mathbb{P}\left(\max\left\{X_{\Gamma_{1,q}} + \overline{X}'_{\Gamma_{n-1,q}}, \overline{X}_{\Gamma_{1,q}}\right\} \leq x, X_{\Gamma_{1,q}} + X'_{\Gamma_{n-1,q}} \in \mathrm{d}y\right) \qquad (3.2.16) \\ = \; & \int_{-\infty}^{x} \mathbb{P}(\overline{X}_{\Gamma_{1,q}} \leq x, X_{\Gamma_{1,q}} \in \mathrm{d}z)\mathbb{P}_z(\overline{X}_{\Gamma_{n-1,q}} \leq x, X_{\Gamma_{n-1,q}} \in \mathrm{d}y), \end{aligned}$$

where the random variables $\overline{X}'_{\Gamma_{n-1,q}}$ and $X'_{\Gamma_{n-1,q}}$ are independent of X. We arrive at the identity in Eqn. (3.2.13) since the Lévy process X is spatially homogeneous.

To show that the second recursion holds true, we note that another application of the Markov property yields that, for any real x,

$$\begin{aligned} \mathbb{E}\left[\int_0^{t+u} I_{\{X_s \leq x\}} \mathrm{d}s \; I_{\{X_{t+u} \in \mathrm{d}b\}}\right] &= \int_{-\infty}^{\infty} \mathbb{E}\left[\int_0^{t} I_{\{X_s \leq x\}} \mathrm{d}s \; I_{\{X_{t} \in \mathrm{d}y\}}\right] \mathbb{P}_y\left[X_u \in \mathrm{d}b\right] \\ &+ \int_{-\infty}^{\infty} \mathbb{E}_y\left[\int_0^{u} I_{\{X_s \leq x\}} \mathrm{d}s \; I_{\{X_{u} \in \mathrm{d}b\}}\right] \mathbb{P}\left[X_t \in \mathrm{d}y\right]. \end{aligned}$$

Replacing t and u by the independent random times $\Gamma_{1,q}$ and $\Gamma_{n-1,q}$, again using the fact that their sum follows a $\Gamma_{n,q}$ random variable, and using that the random variables $X_{\Gamma_{n,q}}$ and $X_{\Gamma_{1,q}}$ have continuous densities denoted by u_n and u_1, completes the proof of the identity.

Using the same properties as above, the third recursion holds true since we have,

$$\mathbb{P}\left(X_{\Gamma_{n,q}} \in \mathrm{d}x\right) = \int_{\mathbb{R}} \mathbb{P}\left(X_{\Gamma_{1,q}} \in \mathrm{d}z\right) \mathbb{P}_z\left(X_{\Gamma_{n-1,q}} \in \mathrm{d}x\right).$$

□

3.3 Special case: mixed-exponential jump-diffusions

We show in this section that the recursions in Eqns. (3.2.13) and (3.2.14) admit explicit solutions in the case that the Lévy process X is from the class of mixed-exponential jump-diffusions as defined in Section 1.2.3. We recall the definition here for convenience.

Definition 3.3.1. (i) A random variable has a *mixed-exponential density* if it has PDF f

given by

$$f(x) = \sum_{i=1}^{m^+} p_i^+ \alpha_i^+ \mathrm{e}^{-\alpha_i^+ x} I_{(0,\infty)}(x) + \sum_{j=1}^{m^-} p_j^- \alpha_j^- \mathrm{e}^{-\alpha_j^- |x|} I_{(-\infty,0)}(x), \text{ where} \tag{3.3.1}$$

$$\sum_{k=1}^{m^\pm} p_k^\pm = q^\pm, \quad q^+ + q^- = 1 \quad \text{and} \quad -\alpha_{m^-}^- < \cdots < -\alpha_1^- < 0 < \alpha_1^+ < \cdots < \alpha_{m^+}^+.$$

(ii) A Lévy process $X = \{X_t, t \in \mathbb{R}_+\}$ is a *mixed-exponential jump-diffusion* (MEJD) if it is of the form

$$X_t \quad = \quad \mu t + \sigma W_t + \sum_{i=1}^{N_t} U_i, \tag{3.3.2}$$

where μ is a real number, σ is strictly positive, W is a standard Brownian motion, N is a Poisson process with intensity λ, and the jump-sizes $\{U_i, i \in \mathbb{N}\}$ are distributed according to a mixed-exponential density. Here, the collections $W = \{W_t, t \in \mathbb{R}_+\}$, $N = \{N_t, t \in \mathbb{R}_+\}$ and $\{U_i, i \in \mathbb{N}\}$ are independent.

Remark 3.3.1. (i) If one adds in Definition 3.3.1 the restriction that the weights $p_k^\pm$ are non-negative, the jump-size distribution is a hyper-exponential distribution, and the corresponding Lévy process is a hyper-exponential jump-diffusion (HEJD). It reduces to Kou's double-exponential jump-diffusion process if in addition we restrict to $m^+ = m^- = 1$. While hyper-exponential jump diffusions are dense in the class of all Lévy processes with a completely monotone Lévy density, the collection of mixed-exponential jump-diffusions is dense in the class of all Lévy processes, in the sense of weak convergence of probability measures (see Botta & Harris [19]). That is, any Lévy process can be approximated arbitrarily closely by MEJD processes.

(ii) The parameters $\{p_k^\pm, k = 1, \dots, m^\pm\}$ cannot be chosen arbitrarily but need to satisfy a restriction to guarantee that f is a PDF. A necessary condition for f to be a PDF is

$$p_1^\pm > 0, \qquad \sum_{k=1}^{m^\pm} p_k^\pm \alpha_k^\pm \geq 0,$$

while a sufficient condition is

$$\sum_{k=1}^{l} p_k^\pm \alpha_k^\pm \geq 0 \quad \forall l = 1, ..., m^\pm,$$

which are both easily verified. For a proof of these results and alternative conditions see Bartholomew [16]. In Section 3.5 we will impose the additional condition $\alpha_1^+ > 1$, which ensures that the expectation $\mathbb{E}[S_t]$ of the exponential Lévy process $S_t = \exp\{X_t\}$ is finite for any non-negative t.

(iii) Samples can be drawn from the mixed-exponential distribution by using the acceptance-rejection method (see Section 1.3.1) and taking as the instrumental distribution the hyper-exponential distribution that is obtained by setting equal to 0 all the weights p_i^+ and p_i^- in the mixed-exponential distribution that are negative, and renormalising the remaining weights for the density to have total mass equal to 1. The described hyper-exponential density multiplied by a constant will dominate the original mixed-exponential density.

From the definition of the MEJD process X, it is straightforward to verify that the characteristic exponent $\phi(s) = -\log \mathbb{E}[\mathrm{e}^{\mathtt{i}sX_1}]$ is a rational function of the form

$$\phi(s) = -\mathtt{i}\mu s + \frac{\sigma^2 s^2}{2} - \lambda \left(\sum_{i=1}^{m^+} p_i^+ \frac{\alpha_i^+}{\alpha_i^+ - \mathtt{i}s} + \sum_{j=1}^{m^-} p_j^- \frac{\alpha_j^-}{\alpha_j^- + \mathtt{i}s} - 1 \right), \qquad s \in \mathbb{R}.$$

The distributions of X, the running supremum $\overline{X}$ and the running infimum $\underline{X}$ at the random time $\Gamma_{1,q}$, and also the functions D_1 and Ω_1 can be expressed, as we shall see below, in terms of the roots $\{\rho_k^+, k = 1, \ldots, m^+ + 1\}$ and $\{\rho_k^-, k = 1, \ldots, m^- + 1\}$ with positive and negative real parts of the Cramér-Lundberg equation

$$\phi(-\mathtt{i}s) = -q, \quad q > 0. \tag{3.3.3}$$

The Wiener-Hopf factors ϕ_q^+ and ϕ_q^- of a mixed-exponential jump-diffusion can be shown to be equal to certain rational functions:

Lemma 3.3.1. *Let $q > 0$ be given and suppose that the roots of Eqn.* (3.3.3) *are distinct. The functions ϕ_q^+ and ϕ_q^- are given explicitly by*

$$\phi_q^+(s) := \prod_{i=1}^{m^+} \left(1 - \mathtt{i}s/\alpha_i^+\right) \prod_{i=1}^{m^+ +1} \left(1 - \mathtt{i}s/\rho_i^+(q)\right)^{-1}, \tag{3.3.4}$$

$$\phi_q^-(s) := \prod_{j=1}^{m^-} \left(1 + \mathtt{i}s/\alpha_j^-\right) \prod_{j=1}^{m^- +1} \left(1 - \mathtt{i}s/\rho_j^-(q)\right)^{-1}. \tag{3.3.5}$$

Proof. The assertion holds by following the line of reasoning presented in Asmussen *et al.* [10] for the case of a phase-type Lévy process. □

The fact that the Wiener-Hopf factors ϕ_q^+ and ϕ_q^- are rational functions implies that, when the roots of the Cramér-Lundberg equation are distinct, the running supremum $\overline{X}_{\Gamma_{1,q}}$ and the running infimum $\underline{X}_{\Gamma_{1,q}}$ also follow mixed-exponential distributions.

Lemma 3.3.2. *Let $q > 0$ be given and suppose that the roots of Eqn.* (3.3.3) *are distinct. The random variables $\overline{X}_{\Gamma_{1,q}}$, $-\underline{X}_{\Gamma_{1,q}}$ and $X_{\Gamma_{1,q}}$ have mixed-exponential distributions with densities $\overline{u}_1$, $\underline{u}_1$ and u_1 given by*

$$\overline{u}_1(x) = \sum_{i=1}^{m^++1} A_i^+(q)\rho_i^+(q)\mathrm{e}^{-\rho_i^+(q)x}, \qquad x > 0, \quad (3.3.6)$$

$$\underline{u}_1(x) = \sum_{j=1}^{m^-+1} A_j^-(q)(-\rho_j^-(q))\mathrm{e}^{\rho_j^-(q)x}, \qquad x > 0, \quad (3.3.7)$$

$$u_1(x) = \sum_{i=1}^{m^++1} B_i(q)\mathrm{e}^{-\rho_i^+(q)x}I_{(0,\infty)}(x) + \sum_{j=1}^{m^-+1} C_j(q)\mathrm{e}^{-\rho_j^-(q)x}I_{(-\infty,0)}(x), \quad x \in \mathbb{R}, \quad (3.3.8)$$

with

$$A_i^+(q) := \frac{\prod_{k=1}^{m^+}(1-\rho_i^+(q)/\alpha_k^+)}{\prod_{k\neq i}(1-\rho_i^+(q)/\rho_k^+(q))}, \qquad A_j^-(q) := \frac{\prod_{k=1}^{m^-}(1+\rho_j^-(q)/\alpha_k^-)}{\prod_{k\neq j}(1-\rho_j^-(q)/\rho_k^-(q))}, \qquad (3.3.9)$$

$$B_i(q) := A_i^+(q)\phi_q^-(\rho_i^+(q))\rho_i^+(q), \qquad C_j(q) := A_j^-(q)\phi_q^+(\rho_j^-(q))(-\rho_j^-(q)), \quad (3.3.10)$$

*for $i = 1, \dots, m^+ + 1$ and $j = 1, \dots, m^- + 1$, where we define $A_k^\pm \equiv 1$ in the case $m^\pm = 0$ (*i.e. *if there are no positive and/or negative jumps).*

Proof. Note that the coefficients of the function $(1 - \mathtt{i}s/\rho_i^+(q))^{-1}$ in the partial-fraction decompositions of the functions $q/(q - \phi(s))$ and $\phi_q^+(s)$ are given by $C_i(q)$ and $A_i^+(q)$, respectively, while the coefficients of the function $(1 - \mathtt{i}s/\rho_j^-(q))^{-1}$ in the partial-fraction decompositions of the functions $q/(q - \phi(s))$ and $\phi_q^-(s)$ are given by $B_j(q)$ and $A_j^-(q)$ respectively. Subsequently inverting the Fourier transforms $(1 - \mathtt{i}s/\rho_i^+(q))^{-1}$ and $(1 - \mathtt{i}s/\rho_j^-(q))^{-1}$ yields the stated expressions for the densities of $\overline{X}_{\Gamma_{1,q}}$, $-\underline{X}_{\Gamma_{1,q}}$ and $X_{\Gamma_{1,q}}$. □

Remark 3.3.2. *In case that there are multiple roots to Equation* (3.3.3)*, analogous expressions as in Lemmas 3.3.1 and 3.3.2 can be derived using the corresponding form of the partial fraction decomposition.*

By combining Lemma 3.3.2 with the identity in Eqn. (3.2.10) and performing a one-dimensional integration, we identify an explicit expression for the function D_1. The form of the function Ω_1 follows directly by combining the identity in Eqn. (3.2.6) with the form of the potential density in Eqn. (3.3.8).

Proposition 3.3.1. *Let $q > 0$ be given and suppose that the roots of Eqn.* (3.3.3) *are distinct. For any real x and y, it holds that*

$$D_1(x,y) = u_1(y) - \sum_{i=1}^{m^+ +1} \sum_{j=1}^{m^- +1} E_{ij}(q) \left(\mathrm{e}^{-\rho_j^-(q)y + (\rho_j^-(q) - \rho_i^+(q))x} \right), \tag{3.3.11}$$

with $y \leq x$, $x \geq 0$, and

$$\Omega_1(x,y) = \frac{1}{q} \begin{cases} \sum_{i=1}^{m^+ +1} \sum_{j=1}^{m^- +1} B_i(q) C_j(q) \left(\mathrm{e}^{(\rho_j^-(q) - \rho_i^+(q))x - \rho_j^-(q)y} \right), \\ \sum_{i=1}^{m^+ +1} \sum_{j=1}^{m^- +1} B_i(q) C_j(q) \left(\mathrm{e}^{(\rho_i^+(q) - \rho_j^-(q))x - \rho_i^+(q)y} \right), \\ \sum_{i=1}^{m^+ +1} \sum_{j=1}^{m^+ +1} B_i(q) B_j(q) \left(\mathrm{e}^{(\rho_i^+(q) - \rho_j^+(q))x - \rho_i^+(q)y} \right), \\ \sum_{i=1}^{m^- +1} \sum_{j=1}^{m^- +1} C_i(q) C_j(q) \left(\mathrm{e}^{(\rho_i^-(q) - \rho_j^-(q))x - \rho_i^-(q)y} \right), \end{cases} \tag{3.3.12}$$

for the cases $\{x > 0, x > y\}$, $\{y > x, 0 > x\}$, $\{y > x > 0\}$ and $\{0 > x > y\}$ respectively, where the coefficients $B_i(q)$ and $C_j(q)$ are given in Lemma 3.3.2 and $E_{ij}(q) := (A_i^+(q) A_j^-(q) \rho_i^+(q) \rho_j^-(q))/(\rho_j^-(q) - \rho_i^+(q))$.

3.3.1 Solutions to the recursions

The functions Ω_n and D_n, and the density u_n can be explicitly identified by combining the forms of the functions Ω_1 and D_1 given in Proposition 3.3.1 and the form of the function u_1 given in Lemma 3.3.2, with the recursive relations in Eqns. (3.2.13), (3.2.14) and (3.2.15). From the form of these recursive relations it follows that the functions Ω_n, D_n and u_n can be expressed as linear combinations of exponentials with the weights given by polynomials $P_{i,n}^{\pm}(x)$ and $P_{i,j,n}(x,y)$ for $i = 1, \dots, m^+ + 1$ and $j = 1, \dots, m^- + 1$. Associated to these polynomials are other polynomials $\widetilde{P}_{k,i,n}^{\pm}$, $\widetilde{P}_{i,j,k,n}^{\pm}$ and real numbers $\widetilde{c}_{i,j,n}^{\pm}$ defined by

$$\int_0^x P_{k,n}^+(y) \mathrm{e}^{-\rho_k^+ y - \rho_i^+(x-y)} \mathrm{d}y = \mathrm{e}^{-\rho_k^+ x} \widetilde{P}_{k,i,n}^+(x) - \mathrm{e}^{-\rho_i^+ x} \widetilde{c}_{k,i,n}^+,$$

$$\int_x^0 P_{k,n}^-(y) \mathrm{e}^{-\rho_k^- y - \rho_i^-(x-y)} \mathrm{d}y = \mathrm{e}^{-\rho_k^- x} \widetilde{P}_{k,i,n}^-(x) - \mathrm{e}^{-\rho_i^- x} \widetilde{c}_{k,i,n}^-,$$

$$\int_0^x \mathrm{e}^{\rho_i^+(z-x)} P_{i,j,n}(x-z, y-z) u_1(z) \mathrm{d}z = \sum_{k=1}^{m^+ +1} \widetilde{P}_{i,j,k,n}^+(x,y) \mathrm{e}^{-\rho_k^+ x},$$

$$\int_0^x \mathrm{e}^{\rho_j^-(z-x)} P_{i,j,1}(x-z, y-z) u_n(z) \mathrm{d}z = \sum_{k=1}^{m^- +1} \widetilde{P}_{i,j,k,n}^-(x) \mathrm{e}^{-\rho_k^- x}.$$

The fact that there are polynomials and constants satisfying the above relations follows by repeated integration by parts. By induction, the following expressions for the functions u_n, D_n and Ω_n can be derived:

Proposition 3.3.2. *For any $n \in \mathbb{N} \cup \{0\}$ we have*

$$\begin{aligned}
u_{n+1}(x) &= \sum_{k=1}^{m^++1} P^+_{k,n+1}(x)\mathrm{e}^{-\rho_k^+ x} I_{(0,\infty)}(x) + \sum_{k=1}^{m^-+1} P^-_{k,n+1}(x)\mathrm{e}^{-\rho_k^- x} I_{(-\infty,0)}(x), \quad x \in \mathbb{R}, \\
D_{n+1}(x,y) &= u_{n+1}(y) - \sum_{i=1}^{m^++1}\sum_{j=1}^{m^-+1} P_{i,j,n+1}(x,y)\mathrm{e}^{-\rho_j^-(y-x)-\rho_i^+ x}, \qquad x \in \mathbb{R}_+,\ x \geq y, \\
\Omega_{n+1}(x,y) &= q^{-(n+1)} \cdot \sum_{k=1}^{n+1} u_{n+2-k}(x) u_k(y-x), \qquad x, y \in \mathbb{R},
\end{aligned}$$

with $P^+_{k,1} = B_k(q)$, $P^-_{k,1} = C_k(q)$ and $P_{i,j,1} = E_{ij}(q)$ (as defined in Proposition 3.3.11), and where $P^{\pm}_{k,n+1}$ and $P_{i,j,n+1}$ are polynomials, and $c^{\pm}_{k,i,n}$ are real numbers that are defined recursively for $n \in \mathbb{N}$, as follows:

$$\begin{aligned}
P^+_{k,n+1}(x) &= \sum_{r=1}^{m^-+1}\left(C_r(q)\int_0^\infty \mathrm{e}^{(\rho_r^- - \rho_k^+)z} P^+_{k,n}(x+z)\mathrm{d}z + B_k(q) c^-_{k,r,n}\right) \\
&+ \sum_{r=1}^{m^++1} B_r(q)\left(\widetilde{P}^+_{k,r,n}(x) - \widetilde{c}^+_{r,k,n}\right), \\
P^-_{k,n+1}(x) &= \sum_{r=1}^{m^++1}\left(B_r(q)\int_{-\infty}^0 \mathrm{e}^{(\rho_r^+ - \rho_k^-)z} P^-_{k,n}(x+z)\mathrm{d}z + C_k(q) c^+_{k,r,n}\right) \\
&+ \sum_{r=1}^{m^-+1} C_r(q)\left(\widetilde{P}^-_{k,r,n}(x) - \widetilde{c}^-_{r,k,n}\right),
\end{aligned}$$

and

$$\begin{aligned}
P_{i,j,n+1}(x,y) &= \int_{-\infty}^0 P_{i,j,n}(x-z, y-z)\mathrm{e}^{\rho_i^+ z} u_1(z)\mathrm{d}z - \sum_{k=1}^{m^-+1} \widetilde{P}^-_{i,k,j,n}(y-x) \\
&+ B_i(q)\int_0^\infty P^-_{j,n}(y-x-z)\mathrm{e}^{(\rho_j^- - \rho_i^+)z}\mathrm{d}z + \frac{E_{i,j}(q)}{\rho_j^- - \rho_i^+}\int_0^\infty u_n(z)\mathrm{e}^{\rho_j^- z}\mathrm{d}z \\
&+ \sum_{k=1}^{m^++1} \widetilde{P}^+_{k,j,i,n}(x,y) \\
&- \sum_{k=1}^{m^++1}\sum_{l=1}^{m^-+1} \frac{E_{k,l}(q)}{\rho_l^- - \rho_k^+}\int_{-\infty}^0 P_{i,j,n}(-z, y-x-z)\mathrm{e}^{\rho_i^+ z - \rho_l^- z}\mathrm{d}z, \\
c^-_{k,r,n} &= \int_{-\infty}^0 \mathrm{e}^{(\rho_k^+ - \rho_r^-)z} P^-_{r,n}(z)\mathrm{d}z, \qquad c^+_{k,r,n} = \int_0^\infty \mathrm{e}^{(\rho_k^- - \rho_r^+)z} P^+_{r,n}(z)\mathrm{d}z.
\end{aligned}$$

Proof. The expressions for u_{n+1}, D_{n+1} and Ω_{n+1} follow by induction with respect to n, utilising (i) the fact that u_{n+1} is equal to the convolution of u_n and u_1, as a consequence of the independence and stationarity of the increments of X, (ii) the form of D_1 in Eqn. (3.3.11) and the recursive relation in Eqn. (3.2.13), and (iii) the form of Ω_1 in Eqn. (3.2.6) and the recursive relation in Eqn. (3.2.14). □

Remark 3.3.3. In view of the fact that the CDF of the running maximum up to time t and the expected occupation time up to time t below a fixed level of a Brownian motion is C^∞ as function of t, it follows by conditioning on jump-times and -sizes that the functions $t \mapsto \vec{d}_t(x,y)$ and $t \mapsto \vec{\omega}_t(x,y)$ corresponding to a mixed-exponential jump-diffusion X are C^∞ for any fixed x and y. In particular, the error estimates in Thm. 3.1.1 hold true for the quantities $D_n(x,y)$ and $\Omega_n(x,y)$ (identified in Prop. 3.3.2).

3.4 Numerical illustration: first-passage probabilities and occupation times

To provide a numerical illustration of the randomisation method, we implemented the recursive formulas (given in Prop. 3.3.2). We report numerical results in the cases that the underlying Lévy process is equal to a linear Brownian motion, a Kou process, a HEJD process and a MEJD process with typical parameters, which are detailed in Table 3.1. The parameters used for the HEJD (taken from Jeannin & Pistorius [77]) approximate the Lévy density of the NIG model with $\alpha = 8.858$, $\beta = -5.808$, and $\delta = 0.174$. The parameters used for the MEJD (taken from Cai & Kou [34]) approximate the Merton model with jump size distribution $\mathcal{N}(0, 0.01^2)$, the normal distribution with mean 0 and standard deviation 0.01 (for an analysis on the approximation of Lévy processes by HEJD processes, we refer to Crosby *et al.* [48]).

Example: Brownian motion Consider a Brownian bridge process with starting point 1.0, end point 1.1 and barrier level 1.2, and assume a constant risk-free interest rate of 5% and a dividend yield of 0%. The bridge process is assumed to start at time 0 and end at time 1. To compute the first-passage probability of a Brownian bridge over the barrier level with $\sigma = 0.2$ using the procedure developed here, one needs to first find the roots of the corresponding Cramér-Lundberg equation (3.3.3). The equation simplifies to

$$0.05s + 0.02s^2 - q = 0,$$

which leads to two roots: $\rho_1^{\pm}(q) = \frac{-0.05 \pm \sqrt{0.0025+0.08q}}{0.04}$, where $q = T/n = n^{-1}$ and n is the number of recursive steps. Since for this example $y > 0$ and $m^{\pm} = 0$, the joint probability $D_n(x,y) = \mathbb{P}(\overline{X}_{\Gamma_{n,q}} \leq x, X_{\Gamma_{n,q}} = y)$ in Proposition 3.3.2 can be simplified to:

$$D_n(x,y) = P_{1,n}^{+}(y)\mathrm{e}^{-\rho_1^{+}y} - P_{1,1,n}(x,y)\mathrm{e}^{-\rho_1^{-}(y-x)-\rho_1^{+}x}.$$

For $n = 1, 2, 3$ this leads to

$$\begin{aligned}
D_1(x,y) &= \left(\frac{\rho_1^{+}\rho_1^{-}}{\alpha}\right)\left[\mathrm{e}^{-\rho_1^{-}(y-x)-\rho_1^{+}x} - \mathrm{e}^{-\rho_1^{+}y}\right] \\
D_2(x,y) &= \left(\frac{\rho_1^{+}\rho_1^{-}}{\alpha}\right)^2\left[(y-2x-2\alpha^{-1})\mathrm{e}^{-\rho_1^{-}(y-x)-\rho_1^{+}x} + (2\alpha^{-1}+y)\mathrm{e}^{-\rho_1^{+}y}\right] \\
D_3(x,y) &= \left(\frac{\rho_1^{+}\rho_1^{-}}{\alpha}\right)^3\Big[(0.5y^2 - 2xy + 2x^2 - (3y-6x)\alpha^{-1} + 6\alpha^{-2})\mathrm{e}^{-\rho_1^{-}(y-x)-\rho_1^{+}x} \\
&- (0.5y^2 + 3y\alpha^{-1} + 6\alpha^{-2})\mathrm{e}^{-\rho_1^{+}y}\Big],
\end{aligned}$$

for $x \in \mathbb{R}_+,\ x \geq y$, where $\alpha = \rho_1^{+} - \rho_1^{-} > 0$. To obtain the first passage probabilities, one still needs to divide by u_n (see Equation (3.2.11)), which yields 0.2367, 0.2801 and 0.3016 for $n = 1, 2, 3$. Note that these are the first three values listed in Table 3.2.

$\square$

The outcomes of the randomisation method applied to the parameters in Table 3.1 are reported in Table 3.2, Table 3.3 and Figure 3.2. Table 3.2 lists the values of the first-passage probabilities of the randomised Lévy bridge corresponding to a $\Gamma_{n,n/T}$-randomisation of the fixed time $T = 1$ for a number of values of n. Table 3.3 lists the corresponding values of the expected occupation times. These values are denoted P_n for the four Lévy processes under consideration. We also report the results obtained by applying a Richardson extrapolation $P_{1:n}$ (see Section 1.4.2) of order n, using the first n outcomes (as defined in Eqn. (3.1.2)). The results given in Tables 3.2 and Table 3.3 were subsequently used to compute the logarithms of the absolute errors in the cases of the first-passage probabilities (in subfigures (a), (b) and (c)) and the expected occupation times (in subfigures (d), (e) and (f)) that are plotted in Figure 3.2. In the case of the linear Brownian motion the errors were computed with respect to the exact values, which are given in the bottom row of Tables 3.2 and 3.3.

	BS	KOU	HEJD†	MEJD†
σ	0.2	0.2	$\sqrt{0.042}$	0.2
λ		3.0	11.5	1.0
α^+		50	(5,10,15,25,30,60,80)	(213.0215,236.0406,237.1139,939.7441,939.8021)
α^-		25	(5,10,15,25,30,60,80)	(213.0215,236.0406,237.1139,939.7441,939.8021)
p^+		0.3	$(0.05, 0.05, 0.1, 0.6, 1.2, 1.9, 6.1) * 0.51/\lambda$	(4.36515,1.0833,-5,0.0311,0.02045)
p^-		0.7	$(0.5, 0.3, 1.1, 0.8, 1, 4, 2.3) * 0.64/\lambda$	(4.36515,1.0833,-5,0.0311,0.02045)

Table 3.1: Chosen model parameters found in the literature and used throughout this chapter. The parameters for the Kou model are taken from Kou & Wang [80], the ones for the HEJD model from Jeannin & Pistorius [77] and the ones for the MEJD model from Cai & Kou [34]. †These parameters have been re-expressed using our notation.

The first-passage density is known in closed form (see Eqn. (3.A.1) in Appendix 3.A), while the expected occupation time is given in terms of a double integral of a Gaussian density (see Eqn. (3.B.1) in Appendix 3.B), which we evaluated with the help of an adaptive quadrature method. In the case of the other three processes the errors were computed with respect to the value $P_{1:11}$ that was obtained after Richardson extrapolation with $n = 11$ stages. In the case of the BM model, we see from Tables 3.2 and 3.3 that the extrapolated values for $n = 11$ are highly accurate: these coincide with the exact values for the first five and seven decimal digits in the case of the first-passage time probability and the expected occupation time, respectively.

From Figure 3.2 a number of observations can be made. Each subfigure displays the errors of the recursive values (in black) and the Richardson extrapolated values (in grey). Empirically we observe that the rate of decay of the error of the un-extrapolated outcomes appears to be (approximately) linear across the two different functionals and the three considered models, in line with the theoretical error bound given in Proposition 3.2.1. Indeed, the ordinary least squares (OLS) regression lines (in black) in the log-log plots have slopes equal to -0.94 (-0.98), -0.95 (-0.99) and -0.98 (-0.99) in the case of the first-passage probabilities (and expected occupation times) of the Lévy bridges corresponding to the BM, Kou and HEJD processes, respectively. In line with the theoretical error estimates given in Section 3.1, we observe that the application of the Richardson extrapolation leads to a significantly faster decay of the error.

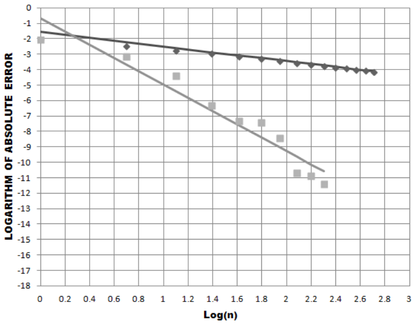

(a) Brownian motion

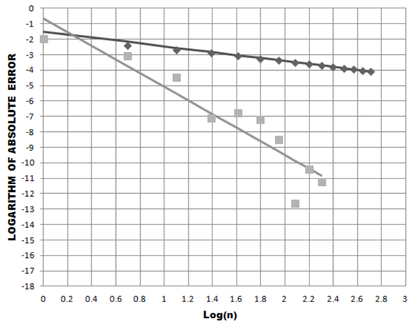

(b) Kou process

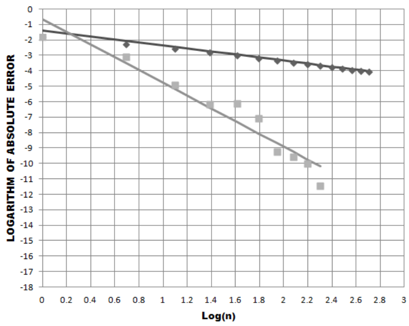

(c) HEJD process

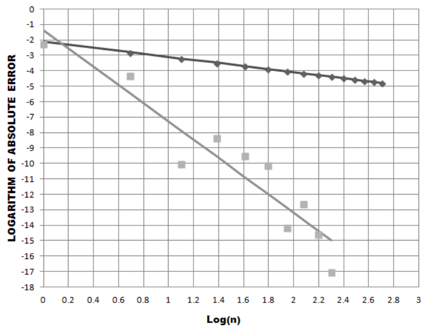

(d) Brownian motion

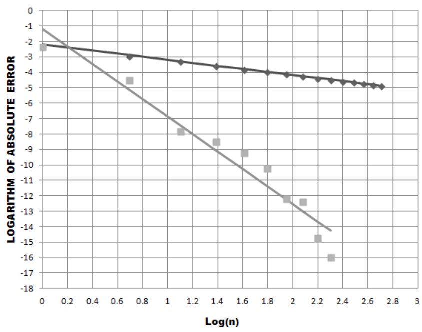

(e) Kou process

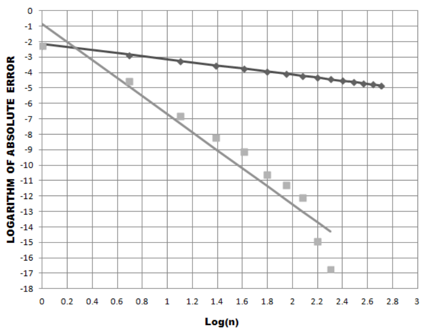

(f) HEJD process

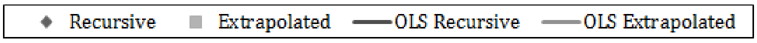

Figure 3.2: Displayed is the logarithm of the absolute errors of the outcomes generated by the recursive algorithm for (1) the one-sided first-passage probabilities under the (a) BM, (b) Kou and (c) HEJD process, and (2) the occupation time under the (d) BM, (e) Kou and (f) HEJD process as a function of $\log(n)$, where n is the number of recursion steps. Ordinary least square estimations of each series are plotted (in the case of the un-extrapolated values the OLS line was estimated using the last six values only). The starting point of the bridge is 1.0, the end point is 1.1, the barrier level is 1.2 and the range is $(1.05, 1.25)$. We assumed a constant risk-free interest rate of 5% and a dividend yield of 0%. In all cases the Lévy bridge process is assumed to start at time 0 and to end at time 1. The model parameters that were used are given in Table 3.1.

n	P_n BM	$P_{1:n}$ BM	P_n Kou	$P_{1:n}$ Kou	P_n HEJD	$P_{1:n}$ HEJD	P_n MEJD	$P_{1:n}$ MEJD
1	0.2366952	0.2366952	0.2610700	0.2610700	0.3006853	0.3006853	0.2416393	0.2416393
2	0.2801451	0.3235950	0.3088900	0.3567186	0.3617512	0.4228170	0.2699507	0.2982620
3	0.3016241	0.3550757	0.3324100	0.3908162	0.3911554	0.4635372	0.2903759	0.3477084
4	0.3146973	0.3659765	0.3466200	0.4017172	0.4084846	0.4734619	0.3044856	0.3673021
5	0.3235182	0.3685654	0.3561300	0.4037245	0.4198448	0.4735378	0.3145421	0.3701236
6	0.3298679	0.3685139	0.3629300	0.4032856	0.4278257	0.4720958	0.3219877	0.3693867
7	0.3346518	0.3681077	0.3680200	0.4027494	0.4337174	0.4713210	0.3276902	0.3689724
8	0.3383814	0.3679032	0.3719800	0.4025372	0.4382332	0.4711443	0.3321834	0.3688065
9	0.3413680	0.3678600	0.3751300	0.4025104	0.4417979	0.4711707	0.3358082	0.3689589
10	0.3438118	0.3678680	0.3777000	0.4025274	0.4446794	0.4712065	0.3387906	0.3687423
11	0.3458473	0.3678773	0.3798400	0.4025384	0.4470546	0.4712177	0.3412854	0.3696835
Exact		0.3678794		-		-		-

Table 3.2: Displayed are the one-sided first-passage probabilities obtained recursively (P_n) and with Richardson extrapolation ($P_{1:n}$) for the BM, Kou, HEJD and MEJD process as a function of n, where n is the number of recursions. The starting point of the bridge is assumed to be 1.0, the end point is 1.1 and the barrier level is 1.2. We assumed a constant risk-free interest rate of 5% and a dividend yield of 0%. In all cases the Lévy bridge is assumed to start at time 0 and to end at time 1. The model parameters are as given in Table 3.1.

For the Brownian motion we observe the error plot also for larger n (see Figure 3.3 for $n = 1, ..., 25$). The slopes of the shown OLS regression lines, obtained using the final ten outcomes, are -0.97 and -0.99 for the first-passage probabilities and expected occupation times respectively. This indicates that the slopes are indeed approaching -1 for larger n.

By comparing the error plots across models, we note that the rate of decay of the error is very similar across the three models under consideration. By comparing the error plots of the first-passage probabilities and the expected occupation time, we note that the logarithmic errors for the expected occupation times (for a given n) are smaller than the corresponding errors in the case of the first-passage probability, suggesting that the randomisation method converges faster in the case of the expected occupation times. This feature is likely to be related to the higher degree of smoothness in the case of the expected occupation time.

n	P_n BM	$P_{1:n}$ BM	P_n Kou	$P_{1:n}$ Kou	P_n HEJD	$P_{1:n}$ HEJD	P_n MEJD	$P_{1:n}$ MEJD
1	0.3865063	0.3865063	0.3875916	0.3875916	0.3680801	0.3680801	0.3789600	0.3789600
2	0.4307253	0.4749444	0.4298457	0.4720999	0.4142655	0.4604509	0.4201725	0.4613850
3	0.4483632	0.4879860	0.4465221	0.4837622	0.4322124	0.4719338	0.4366033	0.4735048
4	0.4577436	0.4881793	0.4553273	0.4835609	0.4415893	0.4711338	0.4453382	0.4736600
5	0.4635418	0.4878660	0.4607453	0.4832435	0.4473202	0.4707490	0.4507360	0.4733648
6	0.4674753	0.4879019	0.4644099	0.4833092	0.4511786	0.4708328	0.4543970	0.4733951
7	0.4703175	0.4879423	0.4670525	0.4833526	0.4539517	0.4708704	0.4570412	0.4733295
8	0.4724668	0.4879448	0.4690480	0.4833517	0.4560403	0.4708630	0.4590410	0.4733286
9	0.4741489	0.4879420	0.4706080	0.4833478	0.4576699	0.4708578	0.4606062	0.4733246
10	0.4755011	0.4879415	0.4718610	0.4833473	0.4589767	0.4708575	0.4618607	0.4733241
11	0.4766119	0.4879416	0.4728896	0.4833474	0.4600480	0.4708575	0.4628994	0.4733241
Exact		0.4879416		-		-		-

Table 3.3: Displayed are the occupation times obtained recursively (P_n) and with Richardson extrapolation ($P_{1:n}$) for the BM, Kou, HEJD and MEJD process as a function of n, where n is the number of recursions. The starting point of the bridge is assumed to be 1.0, the end point is 1.1 and the range is $1.05 - 1.25$. We assumed a constant risk-free interest rate of 5% and a dividend yield of 0%. In all cases the Lévy bridge is assumed to start at time 0 and to end at time 1. The model parameters are as given in Table 3.1.

Figure 3.4 displays the run times of the recursive method. Again the first three subfigures relate to the one-sided first-passage probabilities and the last three subfigures relate to the occupation time. From all six subfigures it seems evident that the computational effort is growing exponentially in n, the number of recursive steps. Note that the scaling of the y-axis is different in all subfigures, so that the BS case is about ten times faster than the Kou case, which is $150 - 200$ times faster than the HEJD case - analysing this in more detail shows that the computational effort also grows rapidly with the number of roots of the Cramér-Lundberg equation, where BS has 2, Kou has 4 and the HEJD used here has 16 roots. It can be seen that the one-sided first-passage probabilities are obtained $3 - 7$ times faster than the occupation times.

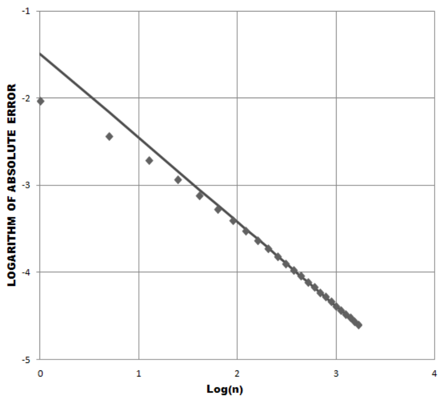

(a) First-passage probability

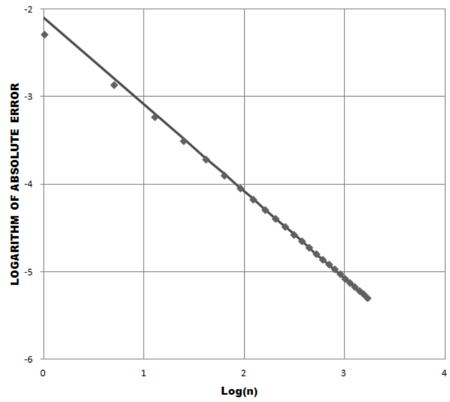

(b) Occupation time

Figure 3.3: Displayed is the logarithm of the absolute error of the recursive algorithm for (a) the one-sided first-passage probabilities and (b) the expected occupation time applied to the Brownian motion as a function of n, where n is the number of recursions. The starting point of the bridge is 1.0, end point is 1.1, barrier level is 1.2, range is $1.05 - 1.35$ and maturity is 1 year. We assume a constant risk-free interest rate of 5%, a dividend yield of 0% and a volatility of 20%. The slopes of the OLS lines are given by -0.97 and -0.99, respectively.

Remark 3.4.1. The numerical evaluation of the recursions in Eqns. (3.2.13) and (3.2.14) requires the computation of the roots of the Cramér-Lundberg equation, which, except in the cases of the linear Brownian motion and the Kou model, are not available in closed form. We used a High Precision Arithmetic Library to investigate the roundoff error resulting from the computation of the roots and found that, in the case of the HEJD and MEJD model, the computed roots were accurate up to an error of $1.0\mathrm{e}^{-11}$ without using higher order precision arithmetic.

3.5 Continuous Euler scheme for stochastic volatility models with jumps

We assume that the stock price process $S = \{S_t, t \in \mathbb{R}_+\}$ evolves according to a Bates-type stochastic volatility model with mixed-exponential jumps[1]. The process S is thus specified

[1]We consider a modification of the Bates model, replacing the distribution of the jumps in the log-price process to be a mixed-exponential jump-diffusion distribution rather than the original log-normal distribution.

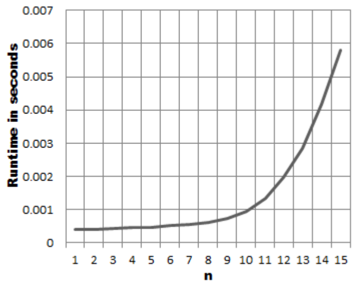

(a) Brownian motion

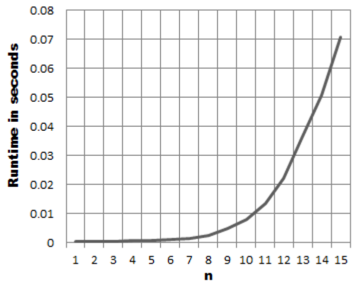

(b) Kou process

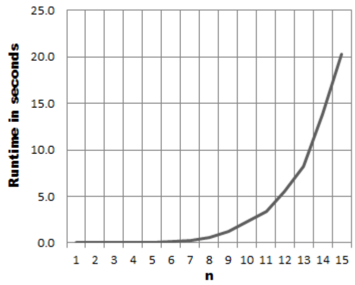

(c) HEJD process

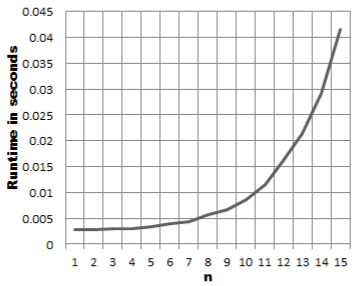

(d) Brownian motion

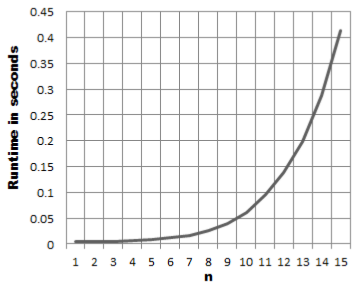

(e) Kou process

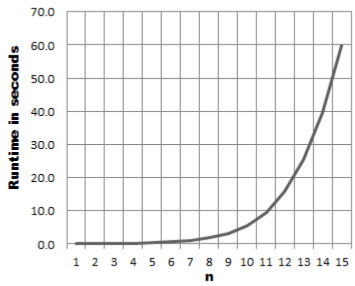

(f) HEJD process

Figure 3.4: Displayed are the run times in seconds of the recursive algorithm for (1) the one-sided first-passage probabilities applied to the (a) BM, (b) Kou and (c) HEJD process, and (2) the occupation time applied to the (d) BM, (e) Kou and (f) HEJD process as a function of $\log(n)$, where n is the number of recursions. Note that the scaling of the y-axis is different in each subfigure. Bridge and model parameters are as in Figure 3.2.

by the exponential model

$$S_t = \exp\{Y_t\}, \qquad t \in \mathbb{R}_+,$$

where the log-price process $Y = \{Y_t, t \in \mathbb{R}_+\}$ satisfies the stochastic differential equation

$$\begin{aligned} \mathrm{d}Y_t &= \left(\mu - \frac{Z_t}{2}\right)\mathrm{d}t + \sqrt{Z_t}\mathrm{d}B_t + \mathrm{d}J_t, && (3.5.1)\\ \mathrm{d}Z_t &= \kappa(\delta - Z_t)\mathrm{d}t + \xi\sqrt{Z_t}\mathrm{d}W_t, \qquad t \in \mathbb{R}_+, && (3.5.2)\\ Y_0 &= x = \log S_0 \quad \text{and} \quad Z_0 = v, \end{aligned}$$

where x and v are strictly positive, and (B, W) is a two-dimensional Brownian motion with correlation parameter ρ. Process J_t is an independent compound Poisson process with intensity λ and jump-sizes are distributed according to a mixed-exponential distribution F with mean m. The parameters κ, δ, and ξ of the model are positive and represent the speed of mean-reversion of the volatility, the long term volatility level and the volatility of volatility parameter. The parameter μ is set equal to $\mu = r - q - \lambda m$ which ensures that the moment condition $\mathbb{E}[\exp\{Y_t\}] = \exp\{(r-q)t + Y_0\}$ is satisfied for all non-negative t, where the constants r and q are, as before, non-negative constants representing the risk-free rate of return and the dividend yield. Under this moment condition it holds that the process $\{\mathrm{e}^{-(r-q)t} S_t, t \in \mathbb{R}_+\}$ is a martingale. Note that by choosing κ and ξ equal to zero we find back the mixed-exponential jump-diffusion process. For background on the application of jump processes and stochastic volatility processes in quantitative finance, we refer to Cont & Tankov [43] and Gatheral [62], respectively.

The first step is to approximate the log-price process Y by a process that has piecewise constant drift and volatility. To define such an approximation, observe that the Euler-Maruyama approximation of the process (Y, Z) on the equidistant partition $\mathbb{T}_N$ can be expressed as

$$Y'_{\tau_{n+1}} = Y'_{\tau_n} + \left(\mu - \frac{Z'_{\tau_n}}{2}\right)\Delta_n + \sqrt{|Z'_{\tau_n}|}\Delta W_n + \Delta J_n, \tag{3.5.3}$$

$$Z'_{\tau_{n+1}} = Z'_{\tau_n} + \kappa(\delta - Z'_{\tau_n})\Delta_n + \xi\sqrt{|Z'_{\tau_n}|}\Delta B_n, \qquad n \in \mathbb{N}, \tag{3.5.4}$$

with $\Delta W_n = W_{\tau_{n+1}} - W_{\tau_n}$, $\Delta B_n = B_{\tau_{n+1}} - B_{\tau_n}$, $\Delta J_n = J_{\tau_{n+1}} - J_{\tau_n}$ and $\Delta_n = (\tau_{n+1} - \tau_n) = T/N$. For a proof of convergence we refer to Higham & Mao [73]. We consider the continuous Euler scheme that is obtained by defining the values of Y'_t for t not contained in the grid by evolving the SDE with frozen coefficients, leaving the (piecewise constant) approximation $(Z'_{\tau_n})_{n\in\mathbb{N}}$ for Z' given in Eqn. (3.5.4) unchanged. We arrive at the approximation

$$Y'_t = Y'_{\tau_n} + \left(\mu - \frac{Z'_{\tau_n}}{2}\right)(t - \tau_n) + \sqrt{|Z'_{\tau_n}|}(W_t - W_{\tau_n}) + (J_t - J_{\tau_n}),$$

for $t \in [\tau_n, \tau_{n+1}]$. Observe that with this choice of interpolation it holds that, conditional on the values of the random variable Z'_{τ_n}, the process $\{Y'_{t-\tau_n}, t \in [\tau_n, \tau_{n+1}]\}$ is a Lévy process, for each $n = 0, \ldots, N-1$. The described bridge sampling algorithm is summarised in Table 3.4.

Remark 3.5.1. The choice $N = 1$ in the above algorithm corresponds to the case of a *single* large step bridge sampling, which is the version of the algorithm that was implemented to produce the results reported in Section 3.4 in the cases where the underlying is a Lévy process.

Next we focus on the application of the bridge sampling method to the approximation of the expectation of two path-functionals that are given in terms of the running maximum

Table 3.4: Bridge sampling algorithm for approximating $\mathbb{E}[F(T,Y,Z)]$.

1. Fix M, $N \in \mathbb{N}$ sufficiently large.
2. Sample M IID copies $\xi^{(1)},\ldots,\xi^{(M)}$ from the law of $\left(Y'_{\tau_1}, Z'_{\tau_1},\ldots,Y'_{\tau_N}, Z'_{\tau_N}\right)$,
3. Evaluate the estimator $\frac{1}{M}\sum_{i=1}^{M}\widetilde{F}^{(N)}\left(\xi^{(i)}\right)$,

with $\widetilde{F}^{(N)}(y_0,z_0,\ldots,y_N,z_N) = \mathbb{E}\left[F(T,Y',Z')\middle| Y'_{\tau_0}=y_0, Z'_{\tau_0}=z_0,\ldots,Y'_{\tau_N}=y_N, Z'_{\tau_N}=z_N\right]$.

and the occupation time of Y as follows:

$$F_S(T,Y,Z) := g(Y_T) I_{\{\overline{Y}_T \le a\}}, \quad a>0, \text{ with } \overline{Y}_t := \sup\{Y_s \,:\, s \le t\},$$
$$F_O(T,Y,Z) := \int_0^T g(Y_s)\mathrm{d}s,$$

for some function $g:\mathbb{R}_+\to\mathbb{R}$. The functionals F_S and F_O admit the following multiplicative and additive decompositions into parts that only involve the processes $Y^{i-1,i} := \{Y_{t+\tau_{i-1}}, t\in[0,\tau_i-\tau_{i-1}]\}$, for $i=1,\ldots,N$:

$$F_S(T,Y,Z) = g(Y_T)\prod_{i=1}^{N} F_S^{(i)}(Y,Z), \qquad F_S^{(i)}(Y,Z) = I_{\left\{\sup_{s\in[\tau_{i-1},\tau_i]} Y_s \le a\right\}},$$
$$F_O(T,Y,Z) = \sum_{i=1}^{N} F_O^{(i)}(Y,Z), \qquad F_O^{(i)}(Y,Z) = \int_{\tau_{i-1}}^{\tau_i} g(Y_s)\mathrm{d}s.$$

These decompositions in turn imply that the conditional expectations

$$\widetilde{F}_S^{(N)}(y_0,z_0,\ldots,y_N,z_N) = \mathbb{E}\left[F_S(T,Y',Z')\middle| Y'_{\tau_0}=y_0, Z'_{\tau_0}=z_0,\ldots,Y'_{\tau_N}=y_N, Z'_{\tau_N}=z_N\right], \tag{3.5.5}$$
$$\widetilde{F}_O^{(N)}(y_0,z_0,\ldots,y_N,z_N) = \mathbb{E}\left[F_O(T,Y',Z')\middle| Y'_{\tau_0}=y_0, Z'_{\tau_0}=z_0,\ldots,Y'_{\tau_N}=y_N, Z'_{\tau_N}=z_N\right], \tag{3.5.6}$$

can be expressed in terms of Lévy bridge processes.

Utilising the fact that the process $X^{(s,z)\to(t,y)}$ is equal in law to the process $\{X_u, u\in[s,t]\}$ conditioned on $\{X_s=z, X_t=y\}$, we express below the laws of the two path-functionals of the Lévy bridge in terms of the law of the Lévy process X.

Proposition 3.5.1. *For any $N \in \mathbb{N}$ the following decompositions hold true:*

$$\widetilde{F}_S^{(N)}((y_0, z_0), \dots, (y_N, z_N)) = g(y_N) \prod_{i=1}^{N} \widetilde{F}_S^{(i)}(y_{i-1}, y_i, z_{i-1}), \tag{3.5.7}$$

$$\widetilde{F}_O^{(N)}((y_0, z_0), \dots, (y_N, z_N)) = \sum_{i=1}^{N} \widetilde{F}_O^{(i)}(y_{i-1}, y_i, z_{i-1}), \tag{3.5.8}$$

where the functions $x \mapsto \widetilde{F}_S^{(i)}(x, y, z)$ and $x \mapsto \widetilde{F}_O^{(i)}(x, y, z)$ are given by

$$\widetilde{F}_S^{(i)}(x, y, z) = \mathbb{E}\left[I_{\left(\overline{L}^{(0,x)\to(\Delta,y)} \le a\right)}\right], \qquad \widetilde{F}_O^{(i)}(x, y, z) = \mathbb{E}\left[\int_0^{\Delta} g\left(L_s^{(0,x)\to(\Delta,y)}\right) \mathrm{d}s\right],$$

with $\Delta = T/N$, where $L^{(0,x)\to(\Delta,y)}$ denotes the Lévy bridge process corresponding to the Lévy process $L = L^{(i)}$ that is equal in law to $Y^{i-1,i} - Y'_{\tau_i}$ conditional on $Z'_{\tau_{i-1}} = z$.

Proof. The decompositions hold as a consequence of the harness property of a Lévy process, the definition of a Lévy bridge and the fact that a Lévy process is spatially homogeneous. □

The first-passage time probability and expected occupation time of the process Y' can then be calculated using the recursive algorithm that was presented in Section 3.2.

Remark 3.5.2. (i) In order to increase the accuracy of the approximation we will use in the implementation the values obtained in the previous section combined with Richardson extrapolation.

(ii) In order to efficiently approximate the first-passage time probability and the expected occupation time of the Lévy bridge process, seen as function of the endpoint of the bridge, one could combine the procedure described in (i) with interpolation: One would then compute these quantities for a number of points and construct subsequently functions on the real line $\mathbb{R}$ by using (linear) interpolation.

(iii) Samples from the mixed-exponential distribution can be drawn by using the acceptance-rejection method described in Section 1.3.1. Since the MEJD distribution considered here is symmetric, we have chosen a symmetric double-exponential distribution with only one positive and negative exponent. The corresponding PDF is:

$$g(x) = 0.5 \times \alpha_1 \mathrm{e}^{-\alpha_1 |x|},$$

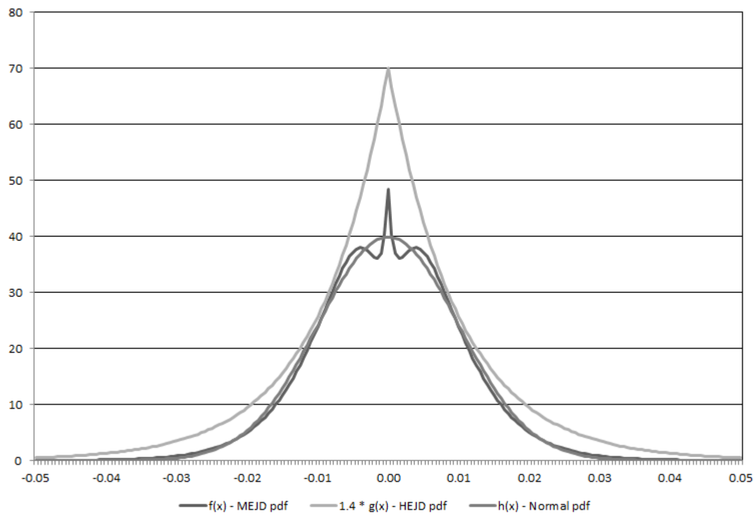

Figure 3.5: The figure displays the PDF of three different jump size distributions. Firstly, it gives the PDF of $\mathcal{N}(0, 0.01^2)$, the normal distribution with mean 0 and standard deviation 0.01, which could be used in the Merton model. Secondly, it gives the distribution of the MEJD model with parameters as detailed in Table 3.1, which tries to approximate the normal distribution. Lastly, it plots the distribution of a HEJD model multiplied with 1.4, which we sample from and use in the acceptance-rejection method.

where α_1 was chosen to be 100. With this choice, the constant c for the acceptance-rejection method can be set to 1.4 and $c \times g(x)$ still strictly dominates $f(x)$ for any x. Figure 3.5 plots $f(x)$ for the MEJD model of Table 3.1 together with $1.4 \times g(x)$ and the PDF of $\mathcal{N}(0, 0.01^2)$, the distribution the MEJD tries to approximate. It can be seen that the MEJD approximates the normal distribution reasonably well, and that the double-exponential distribution multiplied by the constant strictly dominates the MEJD distribution, which is a prerequisite for the acceptance-rejection method. Note that it should always be straight forward to find a HEJD distribution dominating the MEJD distribution with a relatively small constant, which makes the acceptance-rejection method very efficient to use (see Remark 3.3.1 (iii)).

(iv) Note that other variance reduction techniques (reviewed in Section 1.3.1) such as stratified sampling, importance sampling and quasi Monte-Carlo, could be used to further improve the efficiency of the bridge sampling Monte Carlo method. To focus on the newly developed method however, we have omitted use of these techniques here.

3.6 Numerical results: pricing barrier options and range accruals

By way of illustration we next present the numerical results that were obtained by valuing an up-and-in (UIC) barrier call option and a range note (RN) under a number of models by using the bridge algorithm described in Table 3.4. See Section 1.1 for a definition of these two derivatives. To do so, we use the recursive method for the approximation of first-passage time probabilities and expected occupation times that was described in the previous section.

By arbitrage pricing theory, the UIC option and the RN have values at time 0 given by

$$\begin{aligned} UIC_0(K,H) &= \mathbb{E}\left[\mathrm{e}^{-rT}(S_T-K)^+ I_{\{\sup_{0\le t\le T} S_t>H\}}\right], \\ RN_0(a_1,a_2) &= \mathbb{E}\left[\mathrm{e}^{-rT}\cdot\frac{C}{T}\int_0^T I_{\{a_1\le S_u\le a_2\}}\mathrm{d}u\right], \end{aligned}$$

where K is the strike price, H is the barrier level, C is the nominal, and a_1 and a_2 are the lower and upper bound of the range respectively.

We consider Lévy jump-diffusion models in Section 3.6.1 and Bates-type stochastic volatility models with jumps in Section 3.6.2.

3.6.1 Lévy jump-diffusion models

Under the Black-Scholes, Kou, HEJD and MEJD models, we compute the values of up-and-in call options and range notes for typical values of the option parameters using the single-step bridge algorithm described in Table 3.4 (with $N=1$) and evaluating the bridge probabilities by the recursive procedure that was described in the previous section. To provide a comparison, we also report the results that were obtained by running the discrete Euler-Maruyama (EM) scheme. Table 3.5 and Table 3.6 contain approximations of the values of the UIC option and the range note together with the run times, respectively. The option prices are stated as the Monte Carlo midpoint followed by the error at the 95% confidence level (as defined in Equation (1.3.1)) while computational times are given in seconds (all computations in this chapter were obtained in C++ on an Intel(R) Core(TM) i5 CPU M450 @ 2.40 GHz and 4GB RAM).

In Table 3.5 we report the value of an up-and-in call option with maturity 1 year, a barrier level of 120, and strike and spot prices of 100 (only in the case of the MEJD, the barrier level was assumed to be 115 and the strike price 101, in order to compare to the prices reported in Cai & Kou [34]). The values of the range note presented in Table 3.6 correspond to a maturity of 1 year, lower and upper barrier levels of 1.15 and 1.35, a nominal of 100, and a spot price of 1.00. At maturity, the range note pays the ratio of time spent within the range (of upper and lower barrier) and total time to maturity. The range note defined as such is equivalent to the corridor option with $K = 0$ defined in Fusai [60] and Cai & Kou [34]. The UIC option and range note were considered under the Black-Scholes (BS), Kou, HEJD and MEJD models with parameters as given in Table 3.1 assuming a constant risk-free interest rate of 5% and a dividend yield of 0%. In Table 3.5 we also report the values of the UIC option in those cases that could be extracted from the literature. In particular, the value under the Black-Scholes model is given by an analytical formula (see, *e.g.*, Haug [71]), while Kou & Wang [80] and Cai & Kou [34] report the values under the Kou and MEJD model, which were obtained by different methods. In Table 3.6 the only reference value stated is the value under the Black-Scholes model, which follows by a triple integration (see Appendix 3.B).

The parameters of the discrete EM scheme and the bridge method are collected in Tables 3.5 and 3.6. The outcomes of the Lévy bridge method were obtained using the method described in Section 3.3 with Richardson extrapolation. We varied the number of interpolation points as stated in the caption of the tables (see also Remark 3.5.2 (ii)). We have chosen 50 or 100 interpolation points for the evaluation of the barrier option in Table 3.5, and 100 or 200 interpolation points for the evaluation of the range note in Table 3.6. The reason for choosing fewer points for the barrier option is that one only need to consider endpoints between the strike and the barrier level in this case. In particular, note that the option is worthless below and the probability that the barrier was hit is 1.0 above this region. For the range note the region of endpoints is not as restricted and we therefore pre-calculate a larger number of endpoints (equally spaced between 40% and 200% of spot). We checked that at least 99.9% of the paths end up within this region (for paths that end up below/above the range, we use the lowest/highest pre-calculated value). Making this region slightly smaller/larger or increasing/decreasing the number of pre-calculated points, does not change the option prices notably. To obtain the outcomes of the discrete Euler-Maruyama scheme, each of the M sample paths was generated at

		Black-Scholes		Kou	
Method	Steps N	Midpoint (Error)	Time	Midpoint (Error)	Time
Discrete EM	100	9.044 (±0.0297)	3.3	9.851 (±0.0318)	4.5
Discrete EM	1,000	9.189 (±0.0297)	32.0	10.019 (±0.0318)	42.9
Discrete EM	10,000	9.254 (±0.0297)	313.7	10.021 (±0.0317)	453.6
Bridge method	1	9.270 (±0.0292)	0.1	10.071 (±0.0313)	0.2
Bridge method	1	9.276 (±0.0053)	2.5	10.054 (±0.0057)	7.2
Reference value		9.275^*	0.0	$10.053^\dagger$	169.3

		HEJD		MEJD	
Method	Steps N	Midpoint (Error)	Time	Midpoint (Error)	Time
Discrete EM	100	12.581 (±0.0407)	4.8	9.418 (±0.0287)	5.8
Discrete EM	1,000	12.724 (±0.0405)	42.4	9.519 (±0.0287)	53.0
Discrete EM	10,000	12.727 (±0.0404)	417.8	9.533 (±0.0287)	523.0
Bridge method	1	12.764 (±0.0403)	1.1	9.557 (±0.0285)	0.9
Bridge method	1	12.755 (±0.0073)	24.9	9.546 (±0.0052)	9.4
Reference value				$9.546^\ddagger$	6.0

Table 3.5: A comparison of different Monte Carlo methods (all ran with antithetic variate reduction) for an up-and-in call option with a barrier level of 120, a strike price of 100, a spot price of 100 and a maturity of 1 year (only the MEJD methods were run with a barrier level of 115 and a strike price of 101 to match prices reported in Cai & Kou [34]). We assumed a constant risk-free interest rate of 5% and a dividend yield of 0%. The results for the Euler-Maruyama scheme and the bridge scheme (first lines) were obtained using $M = 1$ million runs. The enhanced results for the bridge scheme (reported in the second lines) were obtained with $M = 30$ million runs and using twice the number of interpolation points (100 instead of the 50 that were used in the corresponding first line). We used the model parameters listed in Table 3.1 and $n = 7$ for the bridge sampling method with Richardson extrapolation. Run-times of the various schemes are reported in seconds in the columns 'Time'. *Exact value (see Appendix 3.A). †As reported in Kou & Wang [80]. ‡As reported in Cai & Kou [34].

N time steps, where M and N vary for the outcomes that are reported in Tables 3.5 and 3.6. For the results obtained using the Monte Carlo bridge method the number of recursive steps n and the number of runs is reported. All simulations were performed

		Black-Scholes		**Kou**	
Method	Steps N	Midpoint (Error)	Time	Midpoint (Error)	Time
Discrete EM	100	13.222 (±0.0375)	3.5	13.803 (±0.0376)	4.4
Discrete EM	1,000	13.119 (±0.0373)	32.2	13.739 (±0.0374)	44.0
Discrete EM	10,000	13.111 (±0.0372)	321.0	13.699 (±0.0373)	443.1
Bridge method	1	13.113 (±0.0273)	0.2	13.700 (±0.0264)	0.3
Bridge method	1	13.113 (±0.0050)	2.5	13.696 (±0.0049)	7.6
Reference value		13.116*	3.5		

		HEJD		**MEJD**	
Method	Steps N	Midpoint (Error)	Time	Midpoint (Error)	Time
Discrete EM	100	14.858 (±0.0371)	4.9	13.206 (±0.0374)	4.7
Discrete EM	1,000	14.816 (±0.0370)	44.1	13.138 (±0.0373)	43.7
Discrete EM	10,000	14.784 (±0.0369)	435.6	13.124 (±0.0373)	431.4
Bridge method	1	14.787 (±0.0251)	3.8	13.129 (±0.0273)	7.0
Bridge method	1	14.789 (±0.0046)	32.5	13.121 (±0.0050)	20.62

Table 3.6: A comparison of different Monte Carlo methods (all ran with antithetic variate reduction) for a range note with a nominal of 100, an upper barrier level of 1.35, a lower barrier level of 1.15, a spot price of 1.00 and a maturity of 1 year. We assumed a constant risk-free interest rate of 5% and a dividend yield of 0%. The results for the Euler-Maruyama scheme and the bridge scheme (first lines) were obtained using $M = 1$ million runs. The enhanced results for the bridge scheme (reported in the second lines) were obtained with $M = 30$ million runs and using twice the number of interpolation points (200 instead of the 100 that were used in the corresponding first line). We used the model parameters listed in Table 3.1 and $n = 5$ for the bridge sampling method with Richardson extrapolation. *Exact value obtained by numerical integration of Equation (3.B.2).

on the logarithm of the underlying, and the antithetic variance reduction technique was utilised in all cases (see Section 1.3.1 for background on Monte Carlo simulations and variance reduction techniques).

From the results in Table 3.5 and Table 3.6, we see that using the discrete Euler-Maruyama scheme, a large number of time steps and runs is required for the outcome to converge to the true value (the slow convergence, especially for values of path-dependent options, was also observed in Boyle *et al.* [28], for example). The outcomes generated by

κ	δ	ξ	ρ	V_0	K	H	(a_1, a_2)	S_0	r	d	T
1.0	0.1	0.2	-0.5	0.07	100	120	(1.15,1.35)	100	0.05	0.0	1.0

Table 3.7: Market parameters (spot level, interest rate, dividend yield), option parameters (maturity, strike, barrier, range) and the model parameters of the Bates-type model used for the valuation of the up-and-in call option and the range note in Figure 3.6 and Table 3.8 (with jump-parameters as given in Table 3.1).

the bridge sampling Monte Carlo method however converge more rapidly. In contrast to the discrete EM scheme, only the value at the final time needs to be generated for the bridge sampling algorithm. As a consequence, many more runs can be performed per unit computational time in the bridge algorithm in comparison with the discrete EM scheme, resulting in a smaller statistical error.

3.6.2 Bates-type stochastic volatility model with jumps

We computed the approximate values of an up-and-in call option and a range note under the Heston model, and Bates-type models with double-exponential and hyper-exponential jumps, by running the algorithm described in Table 3.4 with 10 million paths ($M = 10^6$), on the grid $\mathbb{T}_N$ with $N = 2^i$ steps for $i = 0, 1, 2, ..., 10$. We used the Richardson extrapolated value with $n = 7$ steps and approximated the functions $\widetilde{F}^{(i)}_{(S,O)}(x, y, z)$ by evaluating these on a grid of points. We use (double) interpolation to obtain approximations of the values of the function outside the grid. For a comparison, we also report the results obtained by a standard (discrete) Euler-Maruyama approximation with 10 million paths and a varying number of (equidistant) time-steps. For both methods, if the variance process becomes negative in the discretisation method, we reflect the value at 0.

For the results displayed in Figure 3.6 we take the value corresponding to $N = 1024$ as true value and compute the logarithm of the absolute errors for all other outcomes with respect to this value. To estimate the rate of decay of the error as the number of time steps tends to infinity, we performed an ordinary least-square regression on the generated values for each of the models. For the OLS regression, we use the values corresponding to the six largest numbers of steps (only the three largest numbers were used for the continuous Euler scheme in case of the range note). The slopes of the OLS lines of the continuous Euler scheme for the Heston model, and the Bates-type model with double-

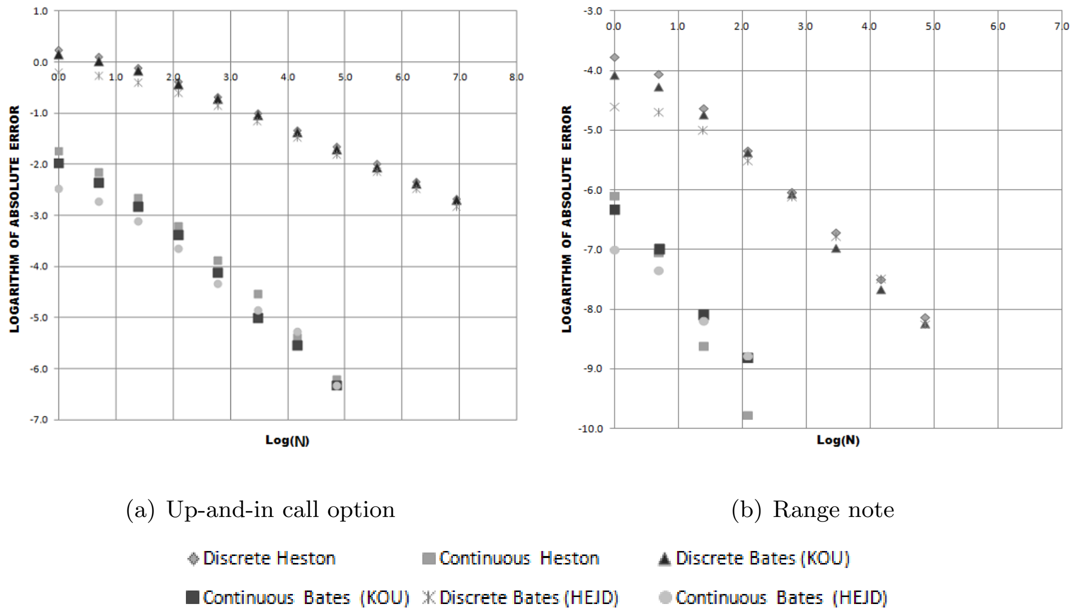

(a) Up-and-in call option (b) Range note

Figure 3.6: The absolute error of the values of an up-and-in barrier option and range note under the Heston and Bates-type models plotted on a log-log scale against the number of time-steps N. Parameters are as given in Tables 3.7 and 3.1.

exponential and hyper-exponential jumps that we found are -1.03, -1.02 and -1.04 in the case of the up-and-in call option, and -1.36, -0.96 and -1.02 in the case of the range note. This suggests a rate of decay of the error that is linear in the reciprocal of the number of steps. By way of comparison we also implemented the standard (discrete) Euler-Maruyama scheme for each of the three models, and found the corresponding slopes of the OLS lines to be equal to -0.485, -0.482 and -0.485 in the case of the up-and-in call option values, and -0.996, -1.005 and -1.005 in the case of range notes. These results suggest that, in the case of an UIC option, a square-root rate rather than a linear rate holds for the decay of the error as function of the reciprocal of the number of time-steps. This is in line with the well-known fact that the strong order of the discrete EM scheme is 0.5. Furthermore, for killed diffusion models, the weak error of the discrete EM scheme has been shown to be bounded by a constant multiplied by $N^{-1/2}$ in the number of time-steps N under suitable regularity assumptions on the coefficients and the pay-off function (see Gobet [68, Thms. 2.3, 2.4]).

To increase computational efficiency we used a non-uniform grid for the interpolation of the variance levels and the stock values based on an algorithm from Tavella & Ran-

		Heston		Bates (Kou)		Bates (HEJD)	
	Steps	Midpoint (Error)	Time	Midpoint (Error)	Time	Midpoint (Error)	Time
Barrier option							
Discrete EM	100	12.755 ($\pm$0.0389)	7.9	13.333 ($\pm$0.0407)	9.1	15.358 ($\pm$0.0483)	9.8
Discrete EM	1,000	12.866 ($\pm$0.0388)	79.8	13.432 ($\pm$0.0406)	88.4	15.387 ($\pm$0.0481)	93.9
Discrete EM	10,000	12.935 ($\pm$0.0387)	789.3	13.467 ($\pm$0.0406)	887.7	15.413 ($\pm$0.0482)	958.4
Continuous EM	100	12.948 ($\pm$0.0387)	18.2	13.468 ($\pm$0.0406)	20.0	15.457 ($\pm$0.0482)	82.0
Continuous EM	1,000	12.956 ($\pm$0.0388)	162.7	13.534 ($\pm$0.0408)	165.1	15.478 ($\pm$0.0482)	233.3
Continuous EM†	1,000	12.951 ($\pm$0.0388)	125.1				
Range note							
Discrete EM	100	15.352 ($\pm$0.0373)	8.4	15.374 ($\pm$0.0367)	9.1	15.387 ($\pm$0.0354)	10.2
Discrete EM	1,000	15.288 ($\pm$0.0371)	80.8	15.315 ($\pm$0.0365)	93.1	15.309 ($\pm$0.0352)	97.7
Discrete EM	10,000	15.288 ($\pm$0.0371)	792.9	15.304 ($\pm$0.0365)	928.0	15.286 ($\pm$0.0351)	1079.1
Continuous EM	10	15.177 ($\pm$0.0367)	54.3	15.237 ($\pm$0.0362)	67.7	15.255 ($\pm$0.0350)	132.0
Continuous EM	100	15.288 ($\pm$0.0371)	113.7	15.294 ($\pm$0.0365)	126.3	15.327 ($\pm$0.0352)	364.3
Continuous EM*	100	15.288 ($\pm$0.0371)	1490.5				

Table 3.8: A comparison of different Monte Carlo methods (all ran with antithetic variate reduction and 1 million paths) for (i) an up-and-in call barrier option and (ii) a range note. The market and option parameters are as given in Table 3.7, and the jump parameters as given in Table 3.1. In the column 'Time' the run times are reported in seconds. The continuous EM schemes were run using $n = 7$ recursive steps (for the first-passage time probabilities) and using $n = 5$ recursive steps (for the expected occupation time). †To obtain this value we used the exact Brownian bridge probability. *To obtain this value we used numerical integration of Equation (3.B.1).

dall [129]: Define $c_1 = \text{arcsinh}\left(\frac{a-s}{g_1}\right)$ and $c_2 = \text{arcsinh}\left(\frac{b-s}{g_2}\right)$. Then the lower part of the grid is given by $x_k = s + g_1 \sinh(c_1(1-(k-1)/(A/2-1)))$ and the upper part is given by $x_{k+A/2} = s + g_2 \sinh(c_2 2k/A)$ both for $k \in \{1, ..., A/2\}$. Constants a and b are the minimum and maximum variance levels, which we have set to 0.001 and 0.3 for the variance grid. The midpoint is denoted s, which we have set to V_0, and A is the total number of grid points. Finally, g_1 and g_2 are the uniformity parameters for the lower and upper part of the grid. We have set these to 0.01 and 0.005 respectively in case of the variance grid. These values and the truncation levels of the variance were selected after a rigorous analysis of the distribution function. Less than 0.1% of the paths leave the interval $[0.001, 0.3]$, with most paths staying close to the mean reversion activity rate level ($\delta = 0.1$). Since the upper part of the grid is larger and few variance paths ever get close to the upper bound, we choose a smaller uniformity parameter for this part. For the endpoint, we set $s = \log(S_0)$, $a = \log(0.3 * S_0)$ and $b = \log(H)$. We choose the upper part of the grid to be uniform (*i.e.* $g_2 = 1$) and the lower part to be non-uniform with more spacing close to S_0 (*i.e.* $g_1 = 0.01$).

In Table 3.8 we report the midpoint of the Monte Carlo method and an error based on a 95% confidence interval. To speed up the procedure, we pre-calcuated the path-functionals at 100 endpoints, and 50 variance levels. We use double interpolation during the Monte Carlo simulation. To confirm that this procedure does not introduce noticeable errors, we also evaluate both derivatives without interpolation and using the exact values in case of the Heston model. That is, we used the Brownian bridge probability and the exact value for the occupation time obtained by adaptive quadrature. We report these results in the bottom line for the barrier option and the range note. Note that this also confirms again, that the recursive procedure for the bridges is very accurate. Also here, it can be seen that the bridge based methods are far superior to the discrete EM methods: the values seem to converge much quicker and can be performed more efficiently.

3.7 Summary

We propose a variance reduction technique for a Monte Carlo based bridge sampling method to estimate the expectations of first-passage times and occupation times, under a class of stochastic volatility models with jumps. We utilise Carr's randomisation method and develop a recursive algorithm for these two path-dependent functionals. For the class of mixed-exponential jump-diffusion models, which is dense in the class of all Lévy processes, we determine the explicit form of these recursions. We determine the rate of convergence of the randomisation method and confirm it numerically. By way of illustration it was shown that the recursive algorithm can be evaluated rapidly and that the convergence can be speeded up by Richardson extrapolation. Having a fast algorithm to calculate these bridge quantities efficiently enables us to use these in a Monte Carlo method with only one time step (in the case of a Lévy process). When pre-calculating the bridge quantities to interpolate between these during the Monte Carlo method, exotic derivatives can be evaluated rapidly with small confidence errors. Run times are far superior to the Euler-Maruyama methods with the same confidence errors. In addition, we develop a continuous Euler-Maruyama scheme for a class of stochastic volatility models with jumps. We illustrate numerically the efficiency of the method for pricing barrier options and range accruals in this class of models and investigate its rate of convergence.

Appendix

3.A First-passage time distribution of Brownian motion

For a Brownian motion W, the distributions of the maximum and drawdown at the independent random time $\Gamma_{1,q}$ are given by

$$\mathbb{P}\left[\overline{W}_{\Gamma_{1,q}} \in \mathrm{d}x\right] = \mathbb{P}\left[\overline{W}_{\Gamma_{1,q}} - W_{\Gamma_{1,q}} \in \mathrm{d}x\right] = \sqrt{2q}\mathrm{e}^{-x\sqrt{2q}}\mathrm{d}x,$$

and the Laplace transform of the joint PDF f_t of W_t and $\overline{W}_t$ takes the form

$$\int_0^\infty \mathrm{e}^{-qt} f_t(x,y)\mathrm{d}t = 2\mathrm{e}^{(y-2x)\sqrt{2q}} \quad \text{and hence} \quad f_t(x,y) = \frac{2(2x-y)}{\sqrt{2\pi t^3}}\mathrm{e}^{-(2x-y)^2/(2t)}.$$

Therefore, we obtain the expression

$$\mathbb{P}\left[\overline{W}_t \geq H, W_t \in \mathrm{d}y\right] = \frac{1}{\sqrt{2\pi t}}\mathrm{e}^{-(2H-y)^2/(2t)}\mathrm{d}y,$$

which yields the well-known identity for the first-passage of a Brownian bridge $W^{(t_1,x)\to(t_2,y)}$:

$$\begin{aligned} &\mathbb{P}\left[\sup\{W_s^{(t_1,x)\to(t_2,y)} \,:\, t_1 \leq s \leq t_2\} \geq H\right] \\ &= \exp\left(-\frac{2(x-H)(y-H)}{\Sigma^2(t_1,t_2)}\right), \qquad \Sigma^2(t_1,t_2) = t_2 - t_1, \end{aligned} \tag{3.A.1}$$

for $H > x, y$. More generally, for $X_t = \sigma W_t + \mu t$, a linear Brownian motion with drift μ and volatility $\sigma > 0$, Eqn. (3.A.1) remains valid if $W^{(t_1,x)\to(t_2,y)}$ is replaced by $X^{(t_1,x)\to(t_2,y)}$ and $\Sigma^2(t_1,t_2)$ by $\Sigma^2(t_1,t_2) = \sigma^2(t_2-t_1)$.

3.B Expected occupation time of Brownian motion

Let

$$L_{a_1,a_2} = \int_0^T I_{\left\{W_t^{(0,x)\to(T,y)}\in(a_1,a_2)\right\}}\mathrm{d}t$$

denote the time in the interval $[0,T]$ spent by a Brownian bridge $W^{(0,x)\to(T,y)}$ in the range (a_1,a_2). Note that it holds that

$$\mathbb{P}(W_t \in dz | W_0 = x, W_T = y) = \phi(z;\alpha,\beta^2)\mathrm{d}z$$

with ϕ denoting the Gaussian distribution $\phi(x;\mu,\sigma^2) = \frac{1}{\sqrt{2\pi\sigma^2}}\mathrm{e}^{-(x-\mu)^2/(2\sigma^2)}$,

$$\alpha = x + \frac{t}{T}(y-x) = \frac{(T-t)x+ty}{T}, \quad \beta^2 = \frac{t(T-t)}{T}.$$

We have, by interchanging the order of integration, that

$$\mathbb{E}\left[L_{a_1,a_2}\right] = \int_0^T\int_{a_1}^{a_2}\phi(z;\alpha,\beta^2)\mathrm{d}z\mathrm{d}t, \tag{3.B.1}$$

where α depends on x and y, the start and end point of the Brownian bridge, and both α and β^2 depend on t and T.

For the bridge process corresponding to a linear Brownian motion $X_t = \sigma W_t + \mu t$ with drift μ and volatility σ, the above formulas remain valid when $W^{(0,x)\to(T,y)}$ is replaced by $X^{(0,x)\to(T,y)}$ and β^2 by $\beta^2 = \frac{\sigma^2 t(T-t)}{T}$.

Remark: When considering $X_t = \sigma W_t + \mu t$, a linear Brownian motion with drift μ and volatility $\sigma > 0$, rather than a bridge, it follows that

$$\mathbb{E}\left[\int_0^T 1_{\{X_t\in(a_1,a_2)\}}\mathrm{d}t\right] = \int_{-\infty}^{\infty}\int_0^T\int_{a_1}^{a_2}\frac{1}{\sigma\sqrt{2\pi}}\phi(z;\alpha,\beta^2)\mathrm{e}^{\frac{-(y-\mu)^2}{2\sigma^2}}\mathrm{d}z\mathrm{d}t\mathrm{d}y. \tag{3.B.2}$$

Bibliography

[1] J. Abate, G. Choudhury, and W. Whitt. *An introduction to numerical inversion and its application to probability models.* Printed in Computational Probability, W. Grassman (ed.), Kluger, Boston, 1999.

[2] J. Abate and W. Whitt. Numerical inversion of Laplace transforms of probability distributions. *ORSA Journal on Computing*, 7:36–43, 1995.

[3] M. Abramowitz and I. Stegun. *Handbook of Mathematical Functions.* Dover Publications, 1965.

[4] J. Akahori. Some formulae for a new type of path-dependent options. *Annals of Applied Probability*, 5:383–388, 1995.

[5] K. Amin. Jump-diffusion option valuation in discrete time. *Journal of Finance*, 48:1833–1863, 1993.

[6] L. Andersen. Efficient simulation of the Heston stochastic volatility model. *Journal of Computational Finance*, 11:1–42, 2007.

[7] L. Andersen and J. Andreasen. Jump-diffusion models: Volatility smile fitting and numerical methods for pricing. *Review of Derivatives Research*, 4:231–262, 2000.

[8] L. Andersen and A. Lipton. Asymptotics for exponential Lévy processes and their volatility smile: Survey and new results. *International Journal of Theoretical and Applied Finance*, 16:135001, 2013.

[9] S. Asmussen. *Applied Probability and Queues.* New York: Wiley, 1987.

[10] S. Asmussen, F. Avram, and M. Pistorius. Russian and American put options under exponential phase-type Lévy models. *Stochastic Processes and their Applications*, 109:79–111, 2004.

[11] S. Asmussen and J. Rosiński. Approximations of small jumps of Lévy processes with a view towards simulation. *Journal of Applied Probability*, 38:482–493, 2001.

[12] G. Bakshi and D. Madan. Spanning and derivative-security valuation. *Journal of Financial Economics*, 55:205–238, 2000.

[13] O.E. Barndorff-Nielsen. Normal inverse Gaussian distributions and the modeling of stock returns. *Research Report No. 300, Department of Theoretical Statistics, Aarhus University*, 1995.

[14] O.E. Barndorff-Nielsen. Processes of normal inverse Gaussian type. *Finance and Stochastics*, 2:41–68, 1998.

[15] O.E. Barndorff-Nielsen and N. Shephard. Non-Gaussian Ornstein-Uhlenbeck-based models and some of their uses in economics. *Journal of the Royal Statistical Society: Series B*, 63:167–241, 2001.

[16] D.J. Bartholomew. Sufficient conditions for a mixture of exponentials to be a probability density function. *The Annals of Mathematical Statistics*, 40:2183–2188, 1969.

[17] D. Bates. Jump and stochastic volatility: Exchange rate processes implicit in Deutsche Mark options. *Review of Financial Studies*, 9:69–107, 1996.

[18] J. Bertoin. *Lévy Processes.* Cambride Universtiy Press, Cambridge, 1996.

[19] R.F. Botta and C.M. Harris. Approximation with generalized hyperexponential distributions: Weak convergence results. *Queueing Systems*, 1:169–190, 1986.

[20] M. Boyarchenko. Fast simulation of Lévy processes. Available at SSRN 2138661, 2012.

[21] M. Boyarchenko and S. Levendorskiĭ. Valuation of continuously monitored double barrier options and related securities. *Mathematical Finance*, 22:419–444, 2012.

[22] S. Boyarchenko and S. Levendorskiĭ. On rational pricing of derivative securities for a family of non-Gaussian processes. Institut für Mathematik, Universität Potsdam. Available at http://opus.kobv.de/ubp/volltexte/2008/2519, July 1998.

[23] S. Boyarchenko and S. Levendorskiĭ. Option pricing for truncated Lévy processes. *International Journal of Theoretical and Applied Finance*, 3:549–552, 2000.

[24] S. Boyarchenko and S. Levendorskiĭ. Barrier options and touch-and-out options under regular Lévy processes of exponential type. *Annals of Applied Probability*, 12:1261–1298, 2002.

[25] S. Boyarchenko and S. Levendorskiĭ. *Non-Gaussian Merton-Black-Scholes Theory*. World Scientific: River Edge, NJ, 2002.

[26] S. Boyarchenko and S. Levendorskiĭ. New efficient versions of Fourier transform methods in applications to option pricing. To appear in *Journal of Computational Finance*, 2013.

[27] P.M. Boyle. Options: A Monte Carlo Approach. *Journal of Financial Economics*, 4:328–338, 1977.

[28] P.M. Boyle, M. Broadie, and P. Glasserman. Monte Carlo methods for security pricing. *Journal of Economic Dynamics and Control*, 21:1267–1321, 1997.

[29] M. Brenner and M. Subrahmanyam. A simple formula to compute the implied standard deviation. *Financial Analyst Journal*, 44:80–83, 1988.

[30] D. Brigo and F. Mercurio. *Interest Rate Models - Theory and Practice: With Smile, Inflation and Credit*. Springer Finance, 2006.

[31] M. Broadie, P. Glasserman, and S. Kou. A continuity correction for discrete barrier options. *Mathematical Finance*, 7:325–349, 1997.

[32] M. Broadie and O. Kaya. Exact simulation of stochastic volatility and other affine jump diffusion processes. *Operations Research*, 54:217–231, 2006.

[33] N. Cai, N. Chan, and X. Wan. Occupation times of jump-diffusion processes with double exponential jumps and the pricing of option. *Mathematics of Operations Research*, 35:412–437, 2010.

[34] N. Cai and S. Kou. Option pricing under a mixed-exponential jump diffusion model. *Management Science*, 57:2067–2081, 2011.

[35] P. Carr. Randomization and the American put. *Review of Financial Studies*, 11:597–626, 1998.

[36] P. Carr and A. Chou. Breaking Barriers. *Risk Magazine*, 10:139–144, 1997.

[37] P. Carr and A. Chou. Hedging complex barrier options. *Working Paper, Morgan Stanley and MIT Computer Science*, 1997.

[38] P. Carr, H. Geman, D. Madan, and M. Yor. The fine structure of asset returns: An empirical investigation. *Journal of Business*, 75, 2002.

[39] P. Carr, H. Geman, D. Madan, and M. Yor. Stochastic volatility for Lévy processes. *Mathematical Finance*, 13:345–382, 2003.

[40] P. Carr and D. Madan. Option valuation using the fast Fourier transform. *Journal of Computational Finance*, 2:61–73, 1998.

[41] M. Chesney, M. Jeanblanc-Picqué, and M. Yor. Brownian excursions and Parisian barrier options. *Advances in Applied Probability*, 29:165–184, 1997.

[42] P.K. Clark. A subordinated stochastic process model with finite variance for speculative prices. *Econometrica*, 41:135–155, 1973.

[43] R. Cont and P. Tankov. *Financial Modelling With Jump Processes*. Chapman & Hall/CRC, 2004.

[44] R. Cont and E. Voltchkova. A finite difference scheme for option pricing in jump diffusion and exponential Lévy models. *SIAM Journal on Numerical Analysis*, 43:1596–1626, 2005.

[45] J.W. Cooley and J.W. Tukey. An algorithm for the machine calculation of complex Fourier series. *Mathematics of Computation*, 19:297–301, 1965.

[46] C.J. Corrado and T.W. Miller. A note on a simple, accurate formula to compute implied standard deviations. *Journal of Banking and Finance*, 20:595–603, 1996.

[47] J.C. Cox, J.E. Ingersoll, and S.A. Ross. A theory of the term structure of interest rates. *Econometrica*, 53:385–407, 1985.

[48] J. Crosby, N.L. Saux, and A. Mijatović. Approximating Lévy processes with a view to option pricing. *International Journal of Theoretical and Applied Finance*, 13:63–91, 2010.

[49] J.S. Dagpunar. *Simulation and Monte Carlo: With applications in finance and MCMC*. Wiley, 2007.

[50] D. Davydov and V. Linetsky. Pricing options on scalar diffusions: An eigenfunction expansion approach. *Operations Research*, 51:185–209, 2003.

[51] M. De Innocentis. Fast calculation of prices and sensitivities of European options under Variance Gamma. Available at SSRN 1916020, 2011.

[52] E. Derman, D. Ergener, and I. Kani. Static options replication. *Journal of Derivatives*, 2:78–95, 1995.

[53] K. Detlefsen and W.K. Härdle. Calibration risk for exotic options. *The Journal of Derivatives*, 2007.

[54] E. Eberlein, K. Glau, and A. Papapantoleon. Analysis of Fourier transform valuation formulas and applications. *Applied Mathematical Finance*, 17:211–240, 2010.

[55] E. Eberlein, U. Keller, and K. Prause. New insights into smile, mispricing and value at risk. *The Journal of Business*, 71:371–406, 1998.

[56] W. Feller. *An Introduction to Probability Theory and Its Applications*. Spinger, 1966.

[57] J.E. Figueroa-López and P. Tankov. Small-time asymptotics of stopped Lévy bridges and simulation schemes with controlled bias. *Bernoulli* (to appear), 2013.

[58] F. Fiorani. The Variance-Gamma process for option pricing. Unpublished Research Project, 2003.

[59] G. Fusai. Corridor options and arc-sine law. *Annals of Applied Probability*, 10:634–663, 2000.

[60] G. Fusai and A. Tagliani. Pricing of occupation time derivatives: Continuous and discrete monitoring. *Journal of Computational Finance*, 5:1–37, 2001.

[61] K. Gao and R. Lee. Asymptotics of implied volatility to arbitrary order. Finance and Stochastics, *forthcoming*, 2011.

[62] J. Gatheral. *The Volatility Surface: A Practitioner's Guide*. Wiley Finance, 2006.

[63] H. Geman. Pure jump Lévy processes for asset price modeling. *Journal of Banking and Finance*, 26:1297–1316, 2002.

[64] H. Geman, D. Madan, and M. Yor. Time changes for Lévy processes. *Mathematical Finance*, 11:79–96, 2001.

[65] H. Geman and M. Yor. Pricing and hedging double barrier options: A probabilistic approach. *Mathematical Finance*, 6:365–378, 1996.

[66] P. Glasserman. *Monte Carlo Methods in Financial Engineering*. New York: Springer, 2004.

[67] P. Glasserman and K.K. Kim. Gamma expansion of the Heston stochastic volatility model. *Finance and Stochastics*, Springer Berlin/Heidelberg:1–30, 2009.

[68] E. Gobet. Weak approximation of killed diffusion using Euler schemes. *Stochastic Processes and their Applications*, 87:167–197, 2000.

[69] M. Goldman, H. Sosin, and M. Gatto. Path dependent options: Buy at the low, sell at the high. *Journal of Finance*, 34:111–127, 1979.

[70] P.S. Hagan, D. Kumar, A.S. Lesniewski, and D.E. Woodward. Managing smile risk. *Wilmott Magazine*, 1, 2002.

[71] E.G. Haug. *The Complete Guide to Option Pricing Formulas*. McGraw-Hill, 2006.

[72] S.L. Heston. A closed-form solution for options with stochastic volatility with applications to bonds and currency options. *Review of Financial Studies*, 6:327–343, 1993.

[73] D. J. Higham and X. Mao. Convergence of Monte Carlo simulations involving the mean-reverting square root process. *Journal of Computational Finance*, 8:35 – 61, 2005.

[74] J. Hull and A. White. The pricing of options on assets with stochastic volatilities. *Journal of Finance*, 42:281–300, 1987.

[75] P. Jäckel. *Monte Carlo Methods in Finance*. John Wiley & Sons; Har/Com edition, 2002.

[76] P. Jäckel. By Implication. *Wilmott*, 26:60–66, 2006.

[77] M. Jeannin and M. Pistorius. A transform approach to compute prices and Greeks of barrier options driven by a class of Lévy processes. *Quantitative Finance*, 10:629–644, 2010.

[78] S.G. Kou. A jump-diffusion model for option pricing. *Management Science*, 48:1086–1101, 2002.

[79] S.G. Kou and H. Wang. First passage times for a jump diffusion process. *Advances in Applied Probability*, 35:504–531, 2003.

[80] S.G. Kou and H. Wang. Option pricing under a double exponential jump diffusion model. *Management Science*, 50:1178–1192, 2004.

[81] N. Kunitomo and M. Ikeda. Pricing options with curved boundaries. *Mathematical Finance*, 2:275–298, 1992.

[82] A. Kuznetsov, A.E. Kyprianou, J.C. Pardo, and K. van Schaik. A Wiener-Hopf Monte-Carlo simulation technique for Lévy processes. *The Annals of Applied Probability*, 21:2171–2190, 2011.

[83] A.E. Kyprianou. *Introductory Lectures on Fluctuations of Lévy Processes with Applications*. Springer, 2006.

[84] R.W. Lee. Option pricing by transform methods: extensions, unifications and error control. *Journal of Computational Finance*, 7, 2004.

[85] M. Leippold and L. Wu. Asset pricing under the quadratic class. *Journal of Financial and Quantitative Analysis*, 37(2):271–295, 2002.

[86] S. Levendorskiĭ. American and european options in multi-factor jump-diffusion models, near expiry. *Finance and Stochastics*, 12:541–560, 2008.

[87] S. Levendorskiĭ. Convergence of price and sensitivities in Carr's Randomization approximation globally and near barrier. *SIAM Journal on Financial Mathematics*, 2:79–111, 2011.

[88] S. Levendorskiĭ. Efficient pricing and reliable calibration in the Heston model. *International Journal of Theoretical and Applied Finance*, 15, 2012.

[89] A. Lewis. A simple option formula for general jump-diffusion and other exponential Lévy processes. Working paper, available from http://www.optioncity.net, 2001.

[90] M. Li. Approximate inversion of the Black-Scholes formula using rational functions. *European Journal of Operational Research*, 185:743–759, 2008.

[91] V. Linetsky. Step options: The Feynman-Kac approach to occupation time derivatives. *Mathematical Finance*, 9:55–96, 1999.

[92] A. Lipton. *Mathematical Methods For Foreign Exchange: A Financial Engineer's Approach*. World Scientific, 2001.

[93] A. Lipton. Assets with jumps. *Risk Magazine*, 15:149–153, 2002.

[94] A. Lipton. The vol smile problem. *Risk Magazine*, 15:61–65, 2002.

[95] A. Lipton and W. McGhee. Universal barriers. *Risk Magazine*, 15:81–85, 2002.

[96] A. Lipton and A. Sepp. Filling the gaps. *Risk Magazine*, pages 78–83, 2011.

[97] D. Madan. Financial modeling with discontinuous price processes, Barndorff-Nielsen, O., Mikosch, T., and Resnick, S., eds. In *Lévy Processes - Theory and Applications*. Birkhäuser: Boston, 2001.

[98] D. Madan, P. Carr, and E. Chang. The variance gamma process and option pricing. *European Finance Review*, 2:79–105, 1998.

[99] D. Madan and E. Seneta. The variance gamma (VG) model for share market returns. *The Journal of Business*, 63:511–524, 1990.

[100] D. Madan and M. Yor. Representing the CGMY and Meixner Lévy processes as time changed Brownian motions. *The Journal of Computational Finance*, 12:27–47, 2008.

[101] S. Manaster and G. Koehler. The calculation of implied variances from the Black-Scholes model: A note. *The Journal of Finance*, 37:227–230, 1982.

[102] G. Marchuk and V. Shaidurov. *Difference Methods and Their Extrapolations*. Springer Verlag, New York, 1983.

[103] T. Matache, A.-M. von Petersdorff and C. Schwab. Fast deterministic pricing of options on Lévy driven assets. *ESAIM: Mathematical Modelling and Numerical Analysis*, 38:37–71, 2004.

[104] R. Merton. Theory of rational option pricing. *The Bell Journal of Economics and Management Science*, 4:141–183, 1973.

[105] R. Merton. Option pricing when underlying stock returns are discontinuous. *Journal of Financial Economics*, 3:125–144, 1976.

[106] S. Metwally and A. Atiya. Using Brownian bridge for fast simulation of jump-diffusion processes and barrier options. *Journal of Derivatives*, 10:43–54, 2002.

[107] A. Mijatović, M. Pistorius, and J. Stolte. On a Lévy bridge Monte Carlo method: Pricing of barrier options and range accruals. *Preprint*, 2013.

[108] E. Mordecki. Optimal stopping and perpetual options for Lévy processes. *Finance and Stochastics*, 6:473–493, 2002.

[109] J. Morris. *Computational Methods in Elementary Numerical Analysis*. John Wiley & Sons, 1983.

[110] A. Pelsser. Pricing double barrier options using Laplace transforms. *Finance and Stochastics*, 4:95–104, 2000.

[111] G. Petrella. An extension on the Euler Laplace transform inversion algorithm with applications in option pricing. *Operations Research Letters*, 32:380–389, 2004.

[112] M. Pistorius and J. Stolte. Fast computation of vanilla prices in time-changed models and implied volatilities using rational approximations. *International Journal of Theoretical and Applied Finance*, 15:1250031, 2012.

[113] W. Press, S.A. Teukolsky, W.T. Vetterling, and Flannery B. *Numerical recipes in C++*. Cambridge University Press, 2002.

[114] S. Raible. *Lévy Processes in Finance: Theory, Numerics and Empirical Facts*. PhD thesis, Freiburg University, 2000.

[115] A. Ralston and P. Rabinowitz. *A first course in Numerical Analysis*. Dover Publications, 2001.

[116] A. Ralston and H.S. Wilf. *Mathematical Methods for Digital Computers*. New York: Wiley, 1960.

[117] L.C.G. Rogers. Evaluating first-passage probabilities for spectrally one-sided Lévy processes. *Journal of Applied Probability*, 37:1173–1180, 2000.

[118] B.A. Rogozin. On the distribution of functionals related to boundary problems for processes with independent increments. *Theory of Probability and its applications*, 11:580–591, 1966.

[119] W. Rudin. *Real and complex analysis*. McGraw-Hill, 1987.

[120] J. Ruf and M. Scherer. Pricing corporate bonds in an arbitrary jump-diffusion model based on an improved Brownian-bridge algorithm. *Journal of Computational Finance*, 14, 2011.

[121] K. Sato. *Lévy Processes and Infinitely Divisible Distributions*. Cambridge University Press, 1999.

[122] J. Schiff. *The Laplace Transfrom: Theory and Applications*. Springer Verlag, New York, 1999.

[123] W. Schoutens. *Lévy processes in finance*. Wiley, 2003.

[124] L. Scott. Pricing stock options in a jump-diffusion model with stochastic volatility and interest rates: Applications of Fourier inversion methods. *Mathematical Finance*, 7:413–426, 1997.

[125] A. Sepp. Analytical pricing of double-barrier options under a double-exponential jump diffusion process: Applications of Laplace transform. *International Journal of Theoretical and Applied Finance*, 7:151–175, 2004.

[126] A. Sidi. *Practical Extrapolation Methods: Theory and Applications.* Cambridge University Press, Cambridge, 2003.

[127] E.M. Stein and J.C. Stein. Stock price distributions with stochastic volatility: An analytic approach. *Review of Financial Studies*, 4:727–752, 1991.

[128] J. Stolte. *Implementing Static Hedges for Reverse Barrier Options: Under the Consideration of Market Frictions.* Lambert Academic Publishing, *Published Master's Thesis*, 2011.

[129] D. Tavella and C. Randall. *Pricing Financial Instruments: The Finite Difference Method.* Wiley, 2000.

[130] N. Wiener and E. Hopf. Über eine Klasse singulärer Integralgleichungen. *Sitzungsberichte der Königlich Preußischen Akademie der Wissenschaften zu Berlin*, pages 696–706, 1931.